Renewable and Sustainable Energy Reviews 41 (2015) 1080–1118

Contents lists available at ScienceDirect

Renewable and Sustainable Energy Reviews

journal homepage: www.elsevier.com/locate/rser

A review of solar energy driven desalination technologies

H. Sharon, K.S. Reddy *

Heat Transfer and Thermal Power Laboratory, Department of Mechanical Engineering, Indian Institute of Technology Madras, Chennai 600036, India

ARTICLE INFO

Article history:
Received 15 February 2013
Received in revised form
5 August 2014
Accepted 3 September 2014

Keywords:
Desalination
Solar energy
Environment
Membrane process
Thermal process

ABSTRACT

Water plays an important role in all our day to day activities and its consumption is increasing day by day because of increased living standards of mankind. Some regions of the globe are under severe stress due to water scarcity and pollution. The fresh water needs of mankind can be only satisfied if saline water which is available in plenty is converted to potable water by desalination. Desalination industry has shown increased threats of CO_2 emissions and severe environmental impacts. Desalination industry can be made sustainable if they are integrated with renewable energy and if proper brine disposal methods are followed. In this review different desalination units integrated with renewable energy with special emphasis given to solar energy is discussed. The problems associated with desalination units and their remedies have been presented. Apart from this some novel methods of desalination process has also been explained. This review will allow the researchers to choose appropriate desalination technology for further development.

Contents

* Corresponding author. Tel.: +91 44 22574702; fax: +91 44 22574652.
E-mail address: ksreddy@iitm.ac.in (K.S. Reddy).

http://dx.doi.org/10.1016/j.rser.2014.09.002
1364-0321/

1. Introduction

Fresh water demands are increasing day by day because of industrialization, motorization and increased life standards of mankind. Naturally available fresh water reserves are not capable of meeting the fresh water demands because of their less availability [1]. It has been estimated by United Nations Organization that by 2025, nearly 1800 million people around the globe will be under severe water scarcity [2]. This situation can be tackled only if mankind finds some other ways to produce fresh water. Luckily, desalination technology developed long back resembling natural hydrological cycle has the capacity to tackle this problem but it consumes more energy and also has some negative impacts on environment.

Desalination is widely adopted in Middle east, Arab countries, North America, Asia, Europe, Africa, Central America, South America and Australia to meet their fresh water and process water demands [3]. Nearly 10,000 tons of oil is required every year to produce 1000 m^3/d of desalinated water [4]. The brine discharged from desalination plants has posed severe threats to marine aquatic life [5]. The most common desalination plants are multi-stage flash (MSF), multi-effect distillation (MED), vapor compression (VC), reverse osmosis (RO) and electro-dialysis (ED) [6]. Conventional desalination plants operated by fossil fuel has also contributed to green house gas (GHG) emissions. This has forced researchers to look for alternate way of powering desalination units by renewable energy [7].

Renewable energy commonly considered for desalination are solar, wind and geothermal and among these solar energy occupies nearly 57% of renewable energy based desalination market [8]. Fossil fuel rich countries like Middle East and Arab Nations have turned their attention towards solar energy with the aim to provide desalinated water in an sustainable way [9]. Renewable energy based desalination units are highly suitable for arid, semi-arid and remote regions where no other mode of power supply is possible [10]. Most of the desalination systems require thermal and/or electrical input that can be provided by Solar energy and hence much focus has been given to solar based systems. The solar thermal collectors are very well developed [11] and now attention has been paid towards solar PV cells to reduce its cost and increase its efficiency there by considerable reduction in water production cost could be achieved. The classification of solar desalination systems is shown in Fig. 1.

In this paper different types of solar energy operated desalination units; their operating principle; advantages and limitations has been extensively reviewed. Novel desalination methods like natural vacuum desalination, forward osmosis (FO), freezing and adsorption desalination has been discussed. the problems with desalination units and steps to overcome has been identified from literature and has been presented briefly.

2. Direct desalination systems

2.1. Solar still

Solar still consists of a blackened basin filled with brackish or saline water up to a certain depth and covered by an inclined glass to facilitate transmission of solar radiation and condensation. The solar radiation entering the basin heats up the blackened liner which in turn heats up the water causing evaporation, because of partial pressure difference and temperature difference the water vapor gets condensed along the inclined glass cover and it is collected by suitable provision at the bottom. The condensate obtained will be of high quality and low quantity in the range of 2–3 l/m^2/d [12]. The condensate yield of solar still has been increased by coupling solar stills with flat plate collector [13], evacuated tube collector [14], concentrating dish type collector [15], solar ponds [16], wind turbine [17], booster mirrors [18] and air conditioning unit [19]. Addition of phase change material (PCM) and re-use of latent heat of condensation by using multiple effects has also resulted in increased condensate yield [20]. Coating the basin liner with photo catalyst like CuO, PbO_2 and MnO_2 and incorporation of heat generating media like bromine and iodine containers has shown reasonable increase in yield [21,22]. Condensing cover material and its inclination, water depth and absorber coating also has significant effect on distillate yield [23–26]. The better yield was found to be obtained by using glass cover as condensing surface at an inclination equal to the latitude of the location for minimum water depth [27]. Single slope and pyramid shaped solar still are found to give best average and maximum daily distillate yield at a water production cost of 0.0135 and 0.031 USD/l [28]. The working principle of wick type solar still, inverted absorber solar still and solar still integrated with compound parabolic concentrator (CPC) can be found in [29,30]. The schematic representation of simple solar still is shown in Fig. 2.

The distillate yield from the basin type solar still is given [31] by

$$\dot{m_d} = \frac{\dot{q_{ew}} \times A_w}{h_{fg}} \tag{1}$$

$$\dot{q_{ew}} = h_{ew} \times (T_w - T_g) \tag{2}$$

$$h_{ew} = 16.273 \times 10^{-3} \times h_{cw} \times \left(\frac{p_w - p_g}{T_w - T_g}\right) \tag{3}$$

The convective heat transfer coefficient is given by Dunkle's relation as

$$h_{cw} = 0.884 \times \left[T_w - T_g + \frac{(p_w - p_g)(T_w - T_g)}{268.9 \times 10^3 - p_w}\right]^{1/3} \tag{4}$$

The effect of solar radiation, brine depth, cover tilt angle and dyes on distillate yield of basin type solar still has been given in the form of correlation in [32].

2.2. Solar humidification–dehumidification–desalination

The main idea behind the solar humidification–dehumidification process is that the moisture carrying capacity of the air increases with the increase in temperature. When hot air heated by solar collector circulated in natural or forced mode comes in contact with saline water which is sprayed in the evaporator, a certain quantity of vapor is extracted by the air which could be recovered by condenser where saline feed water is pre-heated [33]. The four types of humidification–dehumidification desalination configurations are closed air, open water cycle; closed air, closed water cycle; open air, open water cycle and open air, closed water cycle

Nomenclature

$\dot{m}_d$	distillate output (kg/s)
$\dot{q}_{ew}$	rate of evaporative heat transfer (W/m^2)
T_w	water temperature (K)
T_g	glass temperature (K)
h_{ew}	evaporative heat transfer coefficient (W/m^2 K)
h_{cw}	convective heat transfer coefficient (W/m^2 K)
p_w	partial saturated vapor pressure at water temperature (N/m^2)
p_g	partial saturated vapor pressure at glass temperature (N/m^2)
G	mass flow rate of dry air (kg/s)
W_{ia}	absolute humidity of inlet airstream to the condenser (kg H_2O/kg dry air)
W_{oa}	absolute humidity of outlet airstream to the condenser (kg H_2O/kg dry air)
h_{fg}	latent heat of evaporation (J/kg)
C_p	specific heat capacity of water (J/kg K)
T_{in}	temperature of water at the top of evaporator tower (K)
T_{out}	temperature of water at the bottom of evaporator tower (K)
$\dot{m}_h$	mass flow rate of water in evaporator (kg/s)
$\dot{Q}_{in}$	heat input to evaporator (W)
W_c	compressor power (W)
η_{th}	thermal efficiency (%)
h	height of water column (cm)
$\dot{m}_a$	air flow rate (kg/s)
P_{out}	electrical power output of solar chimney (W)
η_{coll}	collector efficiency (%)
g	acceleration due to gravity (m/s^2)
C_{pa}	specific heat capacity of air (J/kg K)
T_a	ambient temperature (K)
H_{ch}	chimney height (m)
A_{coll}	collector area (m^2)
I	solar radiation (W/m^2)
D_{coll}	diameter of collector (m)
D_{xu}	diameter of storage unit (m)
P_e	total power output (W)
$P_{e,ai}$	power output from air turbine (W)
$P_{e,wa}$	power output from water generator (W)
η_c	total conversion efficiency (%)
n_f	factor of pressure drop at the turbine
η_t	turbine efficiency (%)
A_{ch}	area of chimney (m^2)
u	velocity in vertical direction (m/s)
Δp	total pressure difference in the chimney (Pa)
η_{wa}	efficiency of water generator (%)
$\Delta\dot{m}_w$	mass flow rate of water vapor condensed to water in high-efficiency condenser (kg/s)
$\dot{m}_f$	feed water flow rate (kg/s)
$\dot{m}_b$	brine flow rate (kg/s)
T_o	top brine temperature (°C)
T_n	brine temperature at 'n' stage (°C)
t_1	temperature of feed water entering the brine heater (°C)
t_2	temperature of feed water leaving the first stage (°C)
X_f	salinity of feed (ppm)
X_b	salinity of brine (ppm)
ΔT	temperature drop in stage
n	number of stages
i	stage number
A_b	brine heater surface area (m^2)
U_b	overall heat transfer coefficient of brine heater (W/m^2 K)
$(\mathrm{LMTD})_b$	log mean temperature difference in brine heater
U_c	overall heat transfer coefficient of condenser (W/m^2 K)
$(\mathrm{LMTD})_c$	log mean temperature difference in condenser
Π	power required by MVC/freeze desalination compressor (kW)
$\dot{m}_v$	mass flow rate of vapor to compressor (kg/h)
η_{co}	compressor efficiency (%)
M_{wt}	molecular weight of water (kg/kg mol)
Υ	heat capacity ratio
P_1	vapor pressure at compressor suction point (kPa)
P_2	vapor pressure at compressor exit (kPa)
T_1	water vapor temperature at compressor inlet (°C)
T_2	water vapor temperature at compressor outlet (°C)
R	universal gas constant (kJ/kg mol K)
Q_1	volumetric flow rate of vapor (m^3/s)
P_{wc}	fresh water productivity of freeze desalination unit (kg)
e	bed porosity
ρ_{ice}	density of ice (kg/m^3)
ρ_l	density of liquid (kg/m^3)
B_o	bed permeability
μ_l	dynamic viscosity of liquid (N s/m^2)
W	wind function
U	wind velocity (m/s)
E_v	rate of evaporation (kg/s)
P_s	vapor pressure at temperature equal to that of water surface (Pa)
P_a	vapor pressure at temperature equal to air above water surface (Pa)
m_{sg}	mass of silica gel (kg)
m_{water}	mass of fresh water generated (kg)
X_i	fraction of amount adsorbate adsorbed by the adsorbent at equilibrium condition in different location of adsorption cycle (kg/kg dry adsorbent), $i=1, 2, 3, 4$
T_i	temperature at different locations of adsorption cycle (K), $i=1, 2, 3, 4$
C_{sg}	specific heat capacity of silica gel (J/kg K)
h_{fg1}	specific enthalpy of phase change at condenser pressure (J/kg)
h_{fg2}	specific enthalpy of phase change at evaporator pressure (J/kg)
$Q_{heating(bed)}$	heat supplied to the bed (J)
$Q_{cooling(bed)}$	heat removed from the bed (J)
$Q_{cooling(cond)}$	heat removed from condenser (J)
Q_{evap}	cooling effect in evaporator (J)
Q_{des}	heat of desorption (J/kg)
Q_{abs}	heat of adsorption (J/kg)
N_A	mass flux of RO unit (l/m^2)
L	permeability coefficient of RO membrane
ΔP	transmembrane pressure difference
$\Delta\pi$	osmotic pressure difference between the feed and product
π	osmotic pressure (Pa)
C	ion concentration (molar units)
T	operating temperature of RO/MD unit (K)
D	water diffusivity (m^2/s)
S	water solubility
V	water partial molar volume (m^3/mol)
l	RO membrane thickness (m)

R_W	recovery in RO unit
Q_p	permeate volumetric flow rate (m^3/s)
Q_f	feed volumetric flow rate (m^3/s)
Q	product flow rate (m^3/s)
η	current efficiency (%)
I_c	current (A)
CP	number of cell pairs
F	Faraday's constant
ΔN	change in normality between feed and product
SR	salt removal (%)
C_f	concentration of feed (mol/m^3)
C_p	concentration of product (mol/m^3)
ε	membrane porosity
ρ_m	density of membrane (kg/m^3)
ρ_{pol}	density of polymer material (kg/m^3)
τ	tortuosity
J_w	mass flux in MD/FO units (l/s)
D	diffusion coefficient (m^2/s)
P	total pressure in pore (Pa)
P_{air}	air pressure within membrane pore (Pa)
M_w	molecular weight of water vapor (kg/kg mol)
δ	MD membrane thickness (m)
r	pore radius (m)
μ	dynamic viscosity of water vapor ($N\,s/m^2$)
P^*	partial pressure of water (Pa)
P_{avg}	average pressure in pore (Pa)
ε_T	thermal efficiency of MD unit (%)
A	membrane area (m^2)
Q_m	heat transfer in the feed channel (W)
ε_E	energy efficiency of MD unit (%)
E_{in}	global energy input (W)
$\Delta T_{MD,\,\mathrm{mod}\,ule}$	axial temperature drop along membrane module
ΔT_{MD}	temperature difference across the membrane
ΔT_{HE}	temperature difference across the heat exchanger
σ_D	reflection coefficient of draw solution
π_D	osmotic pressure of draw solution (Pa)
σ_F	reflection coefficient of feed solution
π_F	osmotic pressure of feed solution (Pa)
SWR	swelling ratio
W_s	weight of swollen polymer hydrogel (g)
W_d	weight of dry polymer hydrogel (g)
F	water flux (l/m^2h)
V	volume of water permeated through the membrane (l)
t	time (h)

In closed water cycle, the brine discharged from the evaporator would be mixed with the feed water while in case of open water cycle the brine would be discharged in every stage of operation. The schematic representation of the closed air system and open air system is shown in Fig. 3. The components used in solar humidification–dehumidification process solar air heaters, humidifier and dehumidifier were extensively reviewed in [34]. Closed air open water, water heated type humidification–dehumidification–desalination is more effective and the cost of water produced by this unit is about 3–7 USD/m^3 [34]. There always exists an optimum mass flow rate ratio of water to dry air for maximum thermal energy recovery rate for a given spray water temperature and condenser water temperature and the thermal energy recovery rate could be increased by increasing the number of stages [35,36]. The fresh water production rate of humidification–dehumidification unit depends mainly on mass flow rate and temperature of feed water, inlet air and incident heat flux and it could be increased by pre-heating both air and water [37,38]. Recycling of discarded brine could reduce the specific thermal energy consumption and increase the fresh water production [39].The exergy efficiency of humidification–dehumidification process is low because of lower exergy efficiency of solar collectors and loss of exergy through discarded brine [40]. Economic analysis of the system showed that the system would be more suitable and competitive when operated in smaller capacity range [41]. Different configurations of solar humidification–dehumidification plants have been tried by lot researchers their salient features, visible outcomes, distillate yield and water production cost is shown in Table 1.

The distillate yield of the humidification–dehumidification unit is given by [62]

$$\dot{m}_d = G \times (W_{ia} - W_{oa}) \tag{5}$$

Gained output ratio (GOR) is defined as the ratio of total latent heat of evaporation of the distillate to the thermal energy input. It can be mathematically expressed as [63]

$$\mathrm{GOR} = \frac{\dot{m}_d \times h_{fg}}{\dot{m}_h \times C_p \times (T_{in} - T_{out})} \tag{6}$$

Desalination of sea water by passing compressed air bubbles through heated sea water was studied by El-Agouz and Abugderah [64]. The distillate yield of the unit depends on the temperature of the water and mass flow rate of air. The average production cost of distillate was 0.095 USD/m^3. The high cost is due to the cost associated with the use of compressor [65].

The thermal efficiency of the desalination unit is given by [66]

$$\eta_{th} = \frac{\dot{m}_d \times h_{fg}}{Q_{in} + \dot{W}_c} \times 100 \tag{7}$$

The distillate yield is given by the following correlation [66]:

$$\dot{m}_d = \frac{1.597 \times 10^{-7} (T_w)^{3.971} \times \left(0.127 + 2352 \times 10^{-7} h\right) \times \left(0.87231 - 0.02473 \times \dot{m}_a\right)}{60} \tag{8}$$

valid for $50 \le T_w \le 87$ °C; $20 \le h \le 60$ cm; $4.2 \le \dot{m}_a \le 14$ kg/h.

2.3. Solar chimney

Solar chimney converts solar thermal energy into kinetic energy which in turn is converted into electrical energy using turbo-generator. The main components of solar chimney are large diameter solar collectors, turbine, generator and long chimney. Collectors used are mainly glass or plastic sheet which act as greenhouse, trapping heat and causes the earth below the collector to get warmed up resulting in temperature difference between the ambient air and the air inside the system causing heated air to flow through the chimney. The kinetic energy of the moving air causes rotation of turbine mounted below the chimney to produce power [67]. Compared to conventional solar chimney power plant, sloped solar chimney power plants are more efficient and can give smoother power output [68].

The power output of the conventional solar chimney power plant [67] is given by

$$P_{out} = \frac{2}{3} \times \eta_t \times \eta_{coll} \times \frac{g}{C_{pa} \times T_a} \times H_{ch} \times A_{coll} \times I \tag{9}$$

Integration of desalination system with solar chimney power plants has been studied by Zuo et al. [69] using mathematical models. The integrated system consists of rock bed energy

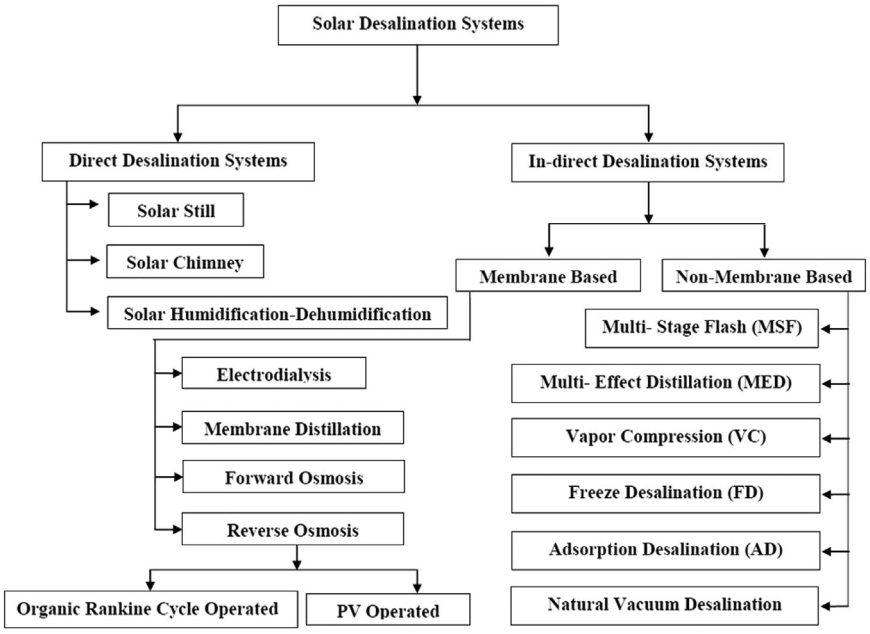

Fig. 1. Classification of solar desalination systems [6].

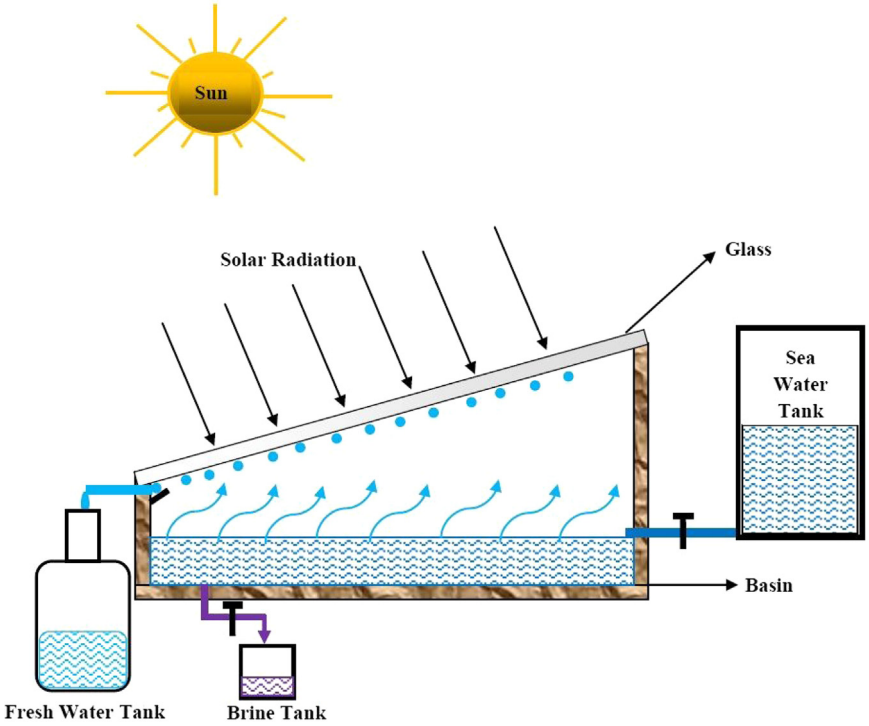

Fig. 2. Simple solar still [31].

storage unit and annular type blackened basin containing saline water covered with inclined glass cover placed below the solar chimney collector cover. Solar radiation heats up the water and air, causing evaporation of water to produce distillate and movement of air through chimney to produce power. If the plant is operated for 8 h a day, the cost of water production would be 2.23 USD/m^3 which is lower than the cost of water produced by any other systems. The variation of temperature at different layers, power output and water output of similar kind of small scale unit is given in [70]. The schematic representation of the system is shown in Fig. 4a.

The daily utilization efficiency of solar energy of the integrated system [69] is given by

$$\eta = \frac{(1/4)\pi \times \left(D_{coll}^2 - D_{xu}^2\right) \times \dot{q_{ew}} + P_{out}}{(1/4)\pi \times \left(D_{coll}^2 - D_{ch}^2\right) \times I} \tag{10}$$

The hourly distillate yield is given by [69]

$$\dot{m_d} = \frac{\dot{q_{ew}} \times 3600}{h_{fg}} \tag{11}$$

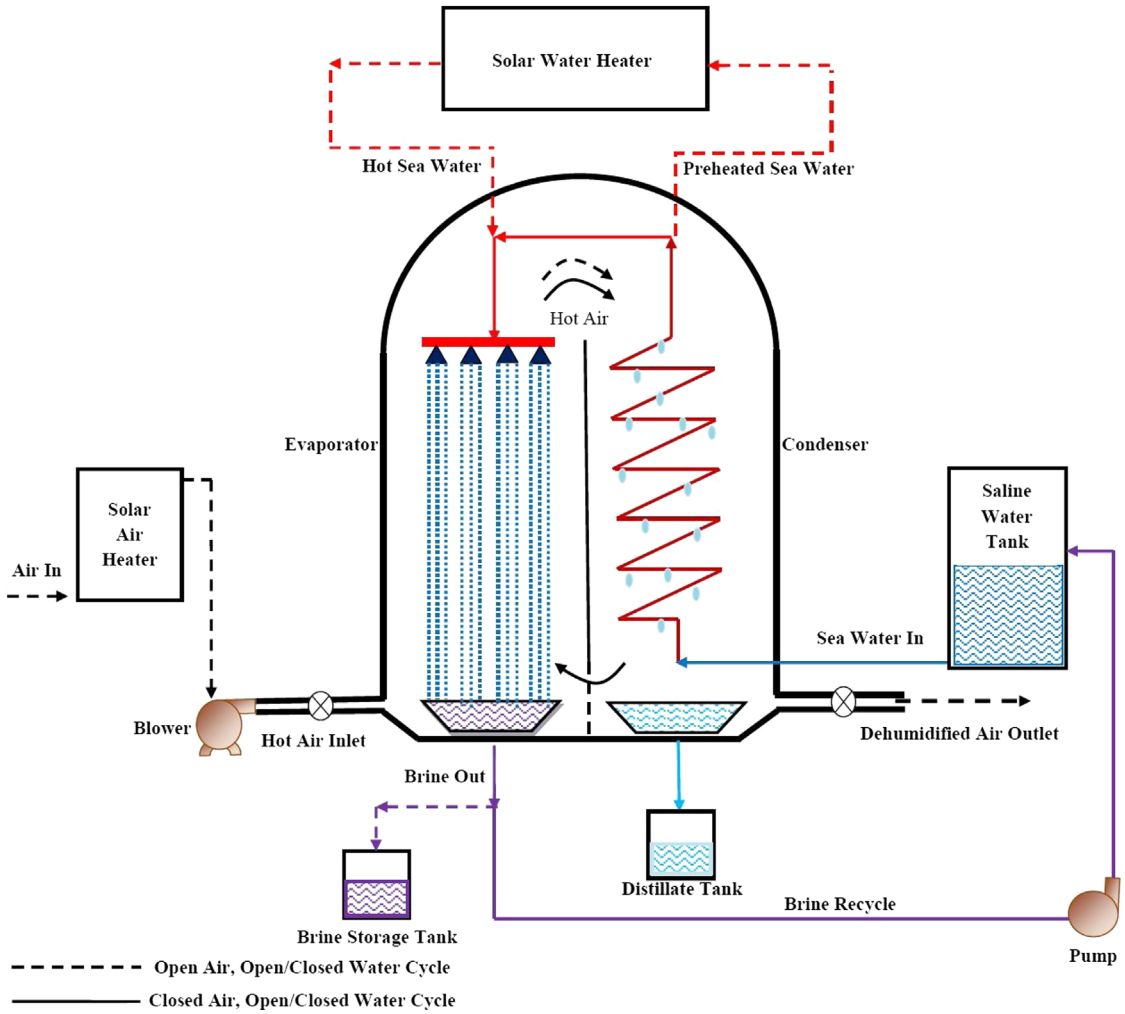

Fig. 3. Solar humidification–dehumidification desalination system [33].

Solar chimney system for power generation and sea water desalination proposed by Zhou et al. [71] consists of solar collector, solar chimney, turbine, generator and high efficiency condenser. The entire system was constructed above the saline water basin which acts as an absorber bed. In this system humid air moves through the chimney resulting in reduced power output due to the decrease in driving force of air because of the presence of moisture in it. The system was found to be economical when compared to classical solar chimney if the chimney height and solar collector diameter was 445 m and 6000 m respectively. The schematic representation of the system is shown in Fig. 4b.

The total conversion efficiency of the system is given by [71]

$$\eta_c = \frac{P_e}{A_{coll} \times I} \tag{12}$$

$$P_e = P_{e,ai} + P_{e,wa} \tag{13}$$

$$P_{e,ai} = \eta_t \times n_f \times A_{ch} \times u \times \Delta p \tag{14}$$

$$P_{e,wa} = \eta_{wa} \times \Delta \dot{m}_w \times g \times H_{ch} \tag{15}$$

The advantages and limitations of various direct solar desalination systems are shown in Table 2.

3. Indirect desalination systems

3.1. Non-membrane processes

In non-membrane desalination process, the heated feed water is allowed to evaporate in distillation units to produce water vapors which are condensed using condenser to produce distillate. The distillate produced is of high quality and the rate of distillation can be enhanced by incorporating vacuum. In this process temperature of feed water, condensing surface and pressure plays an important role in distillate yield [4,6]. The different types of non-membrane process employed for desalination is explained below.

3.1.1. Solar multi stage flash desalination

In multi-stage flash desalination system, the feed saline water is heated above the saturation temperature in brine heater and is made to flash in the vessel where low pressure is maintained using vacuum pump. The brine discharged from the previous stage is allowed to flash in successive stages and the vapors formed in each stage is condensed using condenser where inlet saline water is preheated. A 10 m^3/d capacity solar powered multi-stage flash desalination plant with brine recirculation was developed by Mexico and Federal Republic of Germany in 1974. The plant consists of double tube flat plate collector, parabolic trough collectors (water as heating fluid), storage tanks (capable of supplying thermal energy for 24 h) and desalination unit [72].

Table 1
Comparison of solar powered humidification–dehumidification desalination systems.

Desalination plant	Components of the plant	Visible outcome
Direct contact, open water cycle, closed air cycle. Farid et al. [42]	• Solar flat plate collector for heating water • Humidifier • Condenser • Air blower • Water pump	Best performance at an • Optimum flow rate of water 70 kg/h • Optimum flow rate of air 50 kg/h • Water production – 12 l/m^2/d
Direct contact, open water cycle, closed air cycle. Nawayseh et al. [43]	• Solar flat plate collector • Humidifier – surface area varied from 2 to 23 m^2 • Condenser – surface area varied from 1 to 40 m^2	Best performance at an • Optimum flow rate of water 0.48 kg/min • Optimum flow rate of air 0.24 kg/min • Optimum humidifier surface area 10 m^2 • Optimum condenser surface area 12 m^2. Further increase in surface areas has only little effect on water production • Water production – 6.8–9.8 kg/d
Direct contact, open water cycle, closed air cycle. Al-Hallaj et al. [44]	• Solar flat plate collector was simulated using electric heater • Evaporator • Condenser • The unit was built using Plexiglas sheets	• Higher the feed water inlet temperature higher the yield • Flow rate of air has less effect on yield • Water Production-0.65 kg/m^2.h
Direct contact, open air cycle. Dai et al. [45,46]	• Solar flat plate collector • Honey comb type humidifier • Condenser • Fan	• Mass flow rate and inlet feed temperature affects water production rate • Higher flow rate of air was necessary at lower temperature of feed water • Thermal efficiency 0.68 • Water Production – 6.2 kg/m^2/d
Direct contact, closed air cycle. Garg et al. [47]	• Solar flat plate collectors • Hot water storage tank • Distillation chamber (humidifier and condensation) • Movement of air by natural convection	• Higher the temperature of feed water entering the humidifier higher the humidity of air and higher the water production • Water production – 8.28 kg/h
Direct contact, closed air cycle. Fath et al. [48]	• Solar air heater • Humidifier – falling film type • Dehumidifier – an air cooled heat exchanger • Fan	• Higher the solar intensity, ambient temperature, humidifier and dehumidifier effectiveness higher the water production • Water production – 3.5 kg/m^2/d
Humidification–dehumidification solar still, closed air cycle. Fath et al. [49]	• Rectangular box with top glass cover acts as still • Central stepped absorber carry saline water in basin • Regions above and below the absorber acts as evaporator and condenser • Natural convection of air takes place above and below the absorber	• Higher the saline water temperature, solar intensity and ambient temperature higher the water production. • Material properties, saline water mass, area of condenser and evaporator surface has only little effect • Water production – 5.2–5.3 l/m^2
Humidification–dehumidification seawater greenhouse. Goosen et al. [50]	• Two evaporators free falling type • Condenser (air/water heat exchanger) • Transparent planting area roof	• Maximum distillate was obtained for optimum dimension 200 m × 50 m • Evaporator height 2 m • Roof transparency 0.4% • Water production – 125.5 m^3/d
Humidification–dehumidification. Nafey et al. [51]	• Solar parabolic trough collector • Solar flat plate air heater • Humidifier – canvas as packing material • Dehumidifier – water cooled heat exchanger	• Higher the feed water inlet temperature, solar intensity and inlet air temperature higher the water production • Higher the cooling water temperature and feed water flow rate lower the water production • Water production – 2.75–17 kg/d
Multi stage heating/humidifying technique. Chafik [52]	• Solar air heater made of polycarbonate plate inserted with aluminum strips • Humidifier • Heat recovery and dehumidification unit	• Optimum number of heating/humidifying stages was found to be 5 • Lower the air flow rate higher the plant efficiency • By Stepwise heating/humidifying technique humidity of air at 80 °C was found to be equivalent to humidity of air that be achieved using air heated to 230 °C • Water production – 10 m^3/d • Water production cost –63.65 USD/m^3
Closed air multiple effect humidification plant. Houcine et al. [53]	• Solar air heater made of polycarbonate plate inserted with aluminum strips • Heat recovery unit • Condensation unit • Blower	• Deformation of polycarbonate plate of collectors • No technical problems • Corrosion of pumps and heat exchanger • Feed sea water was preheated by more than 35 °C by passing through condenser

Table 1 (*continued*)

Desalination plant	Components of the plant	Visible outcome
	• Pumps Mass flow rate of air 1500 kg/h Mass flow rate of water 1000 l/h	• Water production – 140–355 kg/d • Water production cost – 53.29 USD/m^3 for 18 stage plant, 47.972 USD/m^3 for 12 stage plant, 72.092 USD/m^3 for 9 stage plant
Closed/open air cycle humidification–dehumidification plant. Orfi et al. [54]	• Solar collector for heating water • Solar collector for heating air • Evaporation chamber • Condenser	• Performance of open air cycle was found to be better than closed air cycle • Annual water production – 5791 l/m^2 for closed system and 6170 l/m^2 for open system
Closed circulation humidification–dehumidification plant. Yuan et al. [55]	• Two compartments each compartment has honey comb evaporator and water cooled condenser are placed side by side • Solar flat plate water heater	• Fresh water production depends mainly on collector area rather than humidifier length • Water production – 27–52 kg/d
Solar multiple condensation–evaporation system. Zhani et al. [56]	• Solar flat plate air heater • Solar flat plate water heater • Humidifier – packing material textile (viscose) • Distillation module – evaporator and condenser in same compartment • Fan	• Outlet and inlet temperatures at various compartments and follows the same trend as solar radiation. • Performance of the system depends on solar radiation • Water production – 16–21.75 kg/d • Water Production cost – 0.1072 USD/l
Open air cycle solar humidification–dehumidification system. Mohamed et al. [57]	• Solar parabolic trough collector • Heat exchanger • Air pre-heater • Humidifier and dehumidifier	• Distilled water production depends on season • Water production – 0.22 kg/kg of air in winter, 0.35 kg/kg of air in spring, 0.50 kg/kg of air in summer, 0.37 kg/kg of air in autumn
Open air cycle solar humidification–dehumidification system. Yuan et al. [58]	• Solar evacuated tube air heater • Solar evacuated tube water heater • Humidifier–dehumidifier unit • Hot water storage tank • Pre treatment and post treatment units	• Gained output ratio of the system is 2.0–2.3 • Relative humidity of the air at the outlet of humidifier is 80–90% • Solar collector field occupies 67.7% of the total capital cost • Water production – 1 m^3/d • Water production cost – 6.58 USD/m^3
PV powered humidification–dehumidification unit with free and forced circulation of air. Wang et al. [59]	• Electric heater and pump powered by solar PV panel • Evaporation chamber • Condensation chamber	• Higher distillate yield at higher brackish water inlet temperature to the evaporator and lower cooling water temperature to the condenser • Distillate yield was found to be more for forced circulation mode • Water production – maximum 0.873 kg/m^2 d for forced circulation • Water production cost – 21.8 USD/m^3 for forced circulation, 2.3 USD/m^3 for free circulation
Solar diffusion driven desalination system. Alnaimat et al. [60]	• Solar flat plate water collector • Air blower • Evaporator • Condenser	• Delayed operation of the plant after the saline water reaches sufficient temperature increases yield and reduced electric consumption • Water production – 6.3 l/m^2 d • Energy consumption – 3.6 kWh/m^3 • Water production cost – 4 USD/m^3
Multi effect condensation–evaporation distillation system. Dayem [61]	• Solar flat plate collector • Storage tank • Distillation chamber • 4 kW auxiliary heater	• Optimum solar collector area was found to be 6 m^2 for which the life cycle saving was maximum for a solar fraction of 77% • Water production – 24 l/d

The operation status of similar kind of desalination unit developed by Swiss Federal Institute of Technology and Atlantis Energy Ltd., and tested in Kuwait was found to be satisfactory [73]. It is worth to note that the water production cost of the multi stage flash desalination unit could be brought down by increasing the plant capacity and by coupling the desalination unit with solar pond where both collection and storage of solar energy is possible [74]. Compared to conventional solar still, the performance ratio of solar multi stage flash desalination unit was found to be 3–10 times higher and for the same plant capacity the water production cost and capital investment of multi stage flash plant is lower than solar still [75].

The distillate yield of the plant could be increased by increasing the temperature difference between hot brine and inlet seawater temperature [76]. Transient analysis of solar multi stage flash desalination unit carried out by Hanafi [77] confirmed that the production of water could be increased by using water as heat transfer fluid in solar collectors and by increasing the number of storage tanks and its volume.

Laboratory prototype experiments have proved that nearly 15 m^3/d of water could be produced by coupling 10 flash desalination units of 1 m^2 area operating at 0.9 bar with solar pond of 70 °C [78]. The gained output ratio of solar multi stage flash desalination unit could be increased by operating the plant at wide temperature range and by discharging the condensate at last stage [79].The distillate yield from the MSF desalination unit depends on the top brine temperature, number of stages, feed water salinity and fouling resistance of brine heater [80–82]. Provision of feed water cooler to reduce

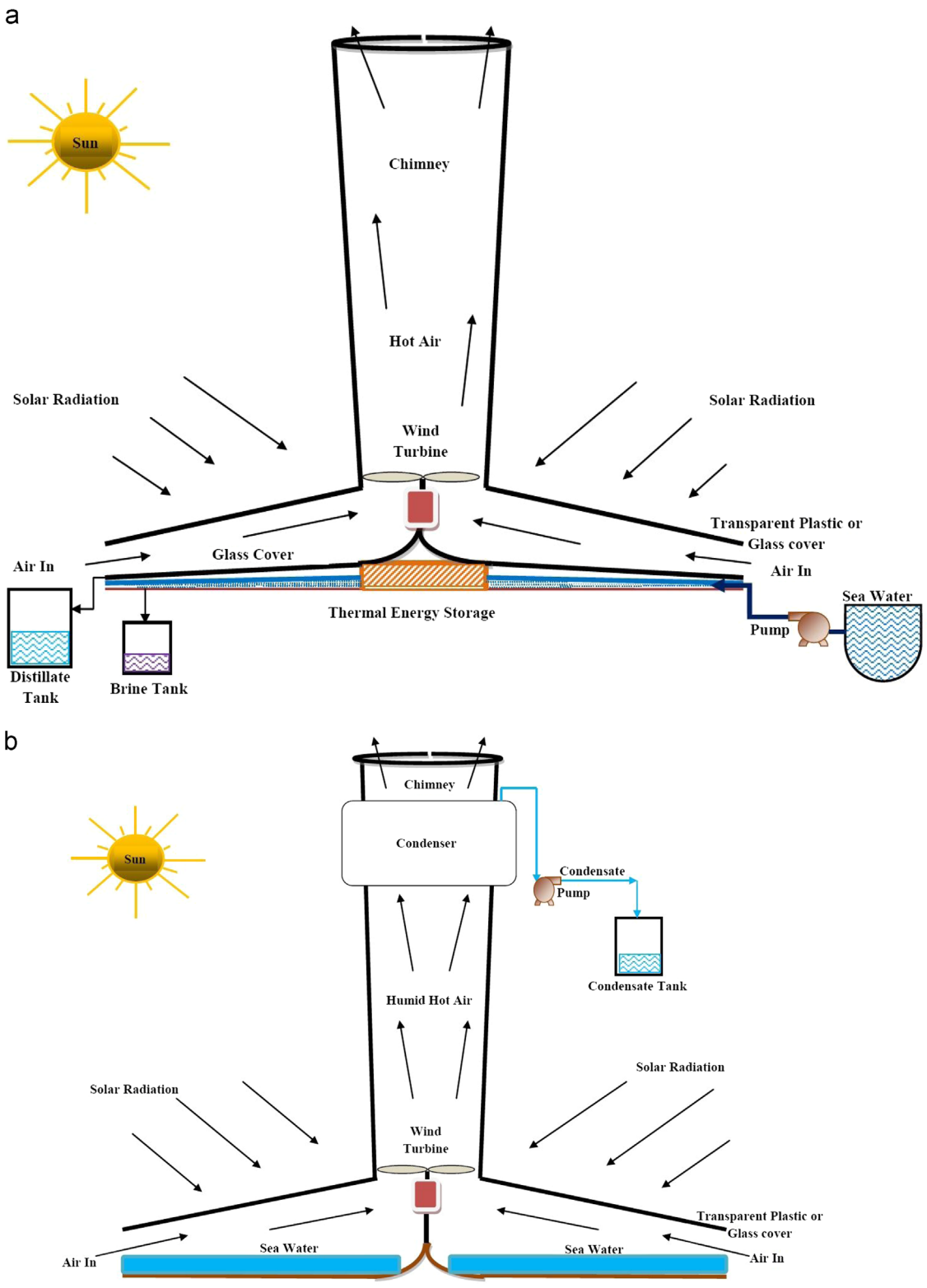

Fig. 4. (a) Basin type desalination system integrated with solar chimney [69] and (b) combined solar chimney system for power generation and sea water desalination [71].

the inlet feed water temperature will make the plant to operate at wide temperature range without any increase in top brine temperature and this type is highly possible in power plant integrated desalination units [83,84]. The exergy efficiency of the MSF desalination unit can be increased by utilizing the heat from the hot distillate at early stages for other thermal systems [85]. The schematic representation of the solar powered multi stage flash desalination system is shown in Fig. 5a.

Mass balance in MSF desalination unit is given by [82]

$$\dot{m}_f = \dot{m}_d + \dot{m}_b \tag{16}$$

Table 2
Advantages and limitations of direct solar desalination systems.

Solar still [17]	**Solar humidification–dehumidification** [33,34]	**Solar chimney** [69]
Solar stills can be constructed with locally available materials	The system is more flexible	Combined power and water can be produced under one roof
Minimum maintenance and operation cost	Low installation and operation costs	Byproducts like salt would be obtained
Eco-friendly	Any kind of low grade energy can be utilized	Ecological benefits
Product water is of High quality	Suitable for decentralized operation	Waste barren land can be utilized
Low distillate yield per m^2	Requires large number of stages for efficient operation	Any kind of waste water can be treated
Requires large area	Capital cost is higher	Low water production cost
Low overall performance	Water production cost is higher	Large area requirement
Low efficiency		Structure is heavy and requires lot of engineering expertise and materials
		Very high capital cost

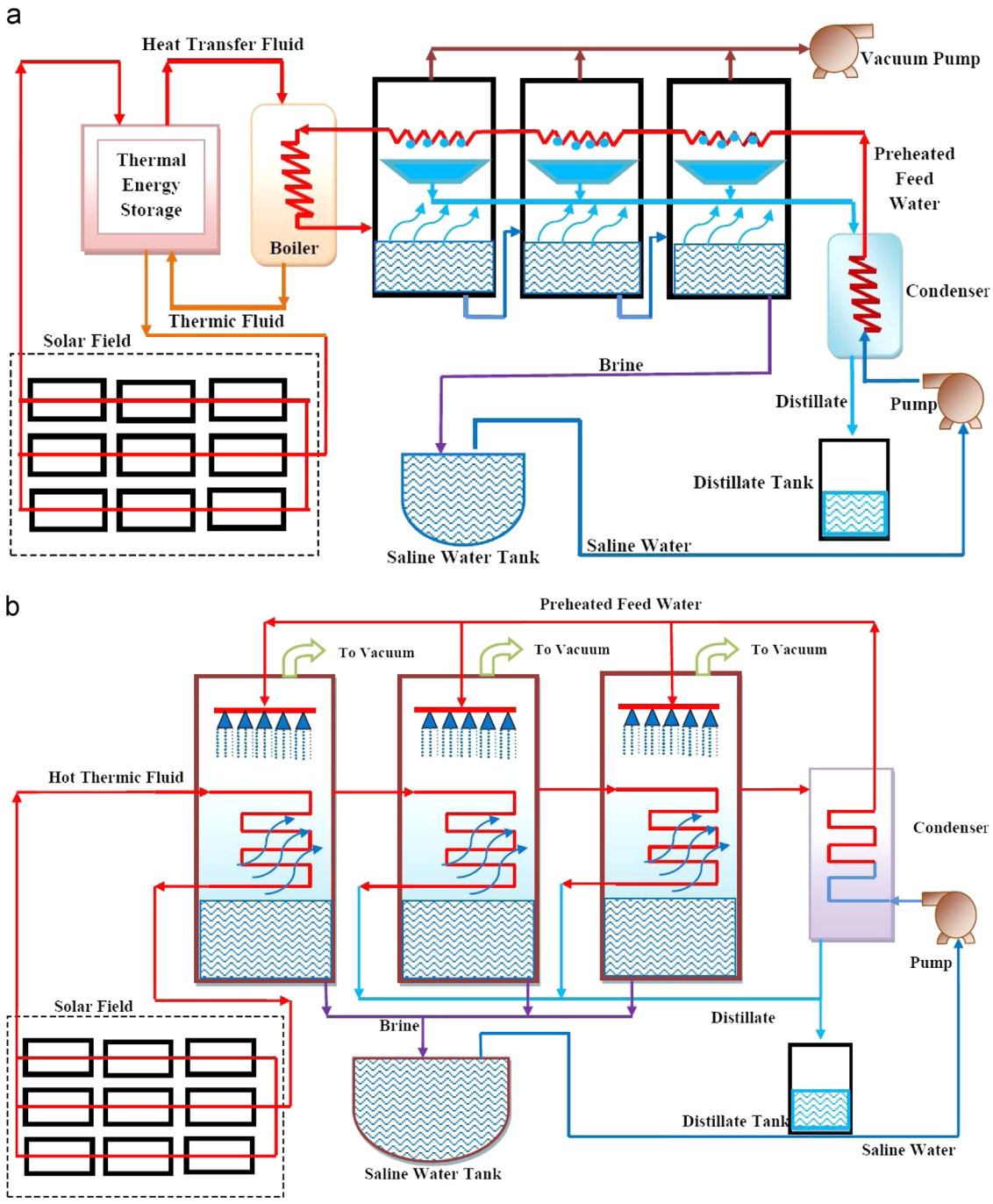

Fig. 5. (a) Solar powered multi-stage flash desalination system [76] and (b) solar powered multi-effect distillation system [95].

Salinity balance in each stage of MSF desalination unit assuming distillate is free from salt is given by

$$\dot{m}_f X_f = \dot{m}_b X_b \tag{17}$$

The temperature drop in each stage is given by

$$\Delta T = \frac{(T_o - T_n)}{n} \tag{18}$$

The stage temperature and condenser temperature in each stage is given by

$$T_i = T_o - i\Delta T \tag{19}$$

$$t_i = T_f + [n-(i-1)]\Delta T \tag{20}$$

The distillate yield at each stage is given by

$$\dot{m}_d = \dot{m}_f \left[1-(1-y)^n\right] \tag{21}$$

y is a constant given by

$$y = \frac{C_p \Delta T}{h_{fg}} \tag{22}$$

The brine heater heat transfer area is given by

$$A_b = \frac{\dot{m}_f C_p (T_o - t_1)}{U_b (\mathrm{LMTD})_b} \tag{23}$$

The condenser heat transfer area is given by

$$A_c = \frac{\dot{m}_f C_p (t_1 - t_2)}{U_c (\mathrm{LMTD})_c} \tag{24}$$

In future the fossil fuel cost would be increasing and cost of parabolic trough collector would be decreasing as a result solar operated MSF unit would be more economical than conventional multi stage flash desalination if more solar fraction was utilized [86]. Zero discharge desalination could be achieved by integrating MSF desalination unit with solar pond and brine concentration recovery system (BCRS) such that the brine rejected could be converted into salt and could be used for maintaining salinity of solar pond [87]. MSF desalination plant integrated with solar pond and partially powered by commercial electricity is more economical than any other solar powered desalination technologies [88].

3.1.2. Solar multi effect distillation

Multi-effect distillation (MED) unit consists of vessels which are generally called effects maintained successively at low pressure where saline water is sprayed. The heat required to cause evaporation in first effect is supplied by solar energy or by combustion of fossil fuel and the vapors thus formed are used to heat the feed in the next effect. Thus, the latent heat of the produced vapors in the previous effects are successfully utilized for the next effect in MED. MED systems are gaining more market share because of its better compatibility with solar thermal desalination [80]. The MED unit coupled to solar pond of area 30,000–40,000 m^2 is capable of producing 1,00,000 tons of distilled water per year at a cost comparable to conventional methods of desalination and the water production cost is mainly dependent on the cost of the salt and it decreases with the increases in solar pond area [89].

Double effect Li–Br absorption heat pump powered by solar collector field and coupled to MED is more attractive in which the heat pump uses the heat from the solar field and the MED unit uses the heat rejected by the condenser and absorber of the heat pump. The water vapor generated in the desalination unit is condensed using the evaporator of the absorption heat pump thereby the circulation of external cooling water is eliminated. The thermal energy consumption and solar field requirement for this unit is nearly 50% lower than conventional MED systems. The system can be operated in a hybrid solar/gas mode, solar mode or gas mode with an performance ratio between 10 and 20 [90–92].

The feasibility of low temperature MED (LT-MED) unit integrated with flash chamber and solar collector was studied by Jiang et al. [93]. The water heated in the solar collector was allowed to flash in the flash chamber and the vapors produced were used as heating source for first stage of MED and the water discharged from flash chamber was used as feed for MED unit. The flash chamber pressure and temperature of feed water has more effect on distillate yield compared to MED stage pressure. LT-MED unit replacing the condenser of solar operated power plant is more efficient than the LT-MED fed by the exhaust steam of solar operated power plant compressed by thermal vapor compressing unit [94]. Integrating solar powered organic Rankine cycle (SORC) with MED to produce both power and water is more attractive but it requires large collector field area. Different configurations like multi effect distillation-backward feed (MED-BF), multi effect distillation-parallel feed (MED-PF), multi effect distillation-forward feed with heater (MED-FFH) and multi effect distillation-forward feed (MED-FF) are available and among these MED-FFH and MED-PF are found to be more efficient [95]. The SORC-Ejector-MED unit is capable of treating high saline water with an exergy efficiency of 40% [96]. Gain output ratio (GOR) of the MED unit depends mainly on the evaporator temperature of last effect and it is very much less affected by the temperature of the feed stream [97]. Solar operated MED unit of 3 m^3/d capacity with a performance ratio of 2.0 is developed by Joo and Kwak [98]. The schematic representation of the MED system is shown in Fig. 5b.

3.1.3. Vapor compression desalination

In vapor compression desalination, the feed saline water heated by external heat source is allowed to flash, the vapors thus produced are compressed using mechanical vapor compressor (MVC) or thermo vapor compressor (TVC) to raise the condensation pressure and temperature of the vapor and the compressed vapor is used to heat the same stage or feed water of other stages. The schematic representation of mechanical vapor compression desalination unit is shown in Fig. 6.

Mechanical vapor compression desalination unit of 120 m^3/d capacity powered by battery less hybrid PV/diesel with heat recovery was developed by Helal and Al-Malek [99]. The hybrid system is capable of reducing 179 tons of CO_2 emissions per year but the water production cost is higher than the conventional methods however it can be reduced by increasing the capacity of the plant.

Mechanical vapor compressor (MVC) desalination unit driven by wind/PV hybrid system consists of MVC, PV module, wind turbine and storage tank. The power required for the desalination system is supplied by the hybrid unit and in case of deficient power supply electricity is supplied from external electrical network. At the times of excess power generation, part of the energy is stored and the remaining is supplied to external electrical network. The system was theoretically studied for three different locations in Morocco and the cost of water production by this method is comparable to the conventional water production methods if the capacity is more than 120 m^3/d [100].

Specific power consumption, steam flow rate and total water production cost of multi effect distillation-parallel feed-thermo vapor compressor (MED-PF-TVC) unit is lower than multi effect distillation-parallel feed-mechanical vapor compressor (MED-PF-MVC) unit. The gain output ratio (GOR) of MED-PF-TVC unit is higher even at less number of stages because of the presence of steam ejector. MED-PF-MVC is competitive if the number of stages are increased beyond 12 effects [101]. The schematic representation of MED integrated with mechanical

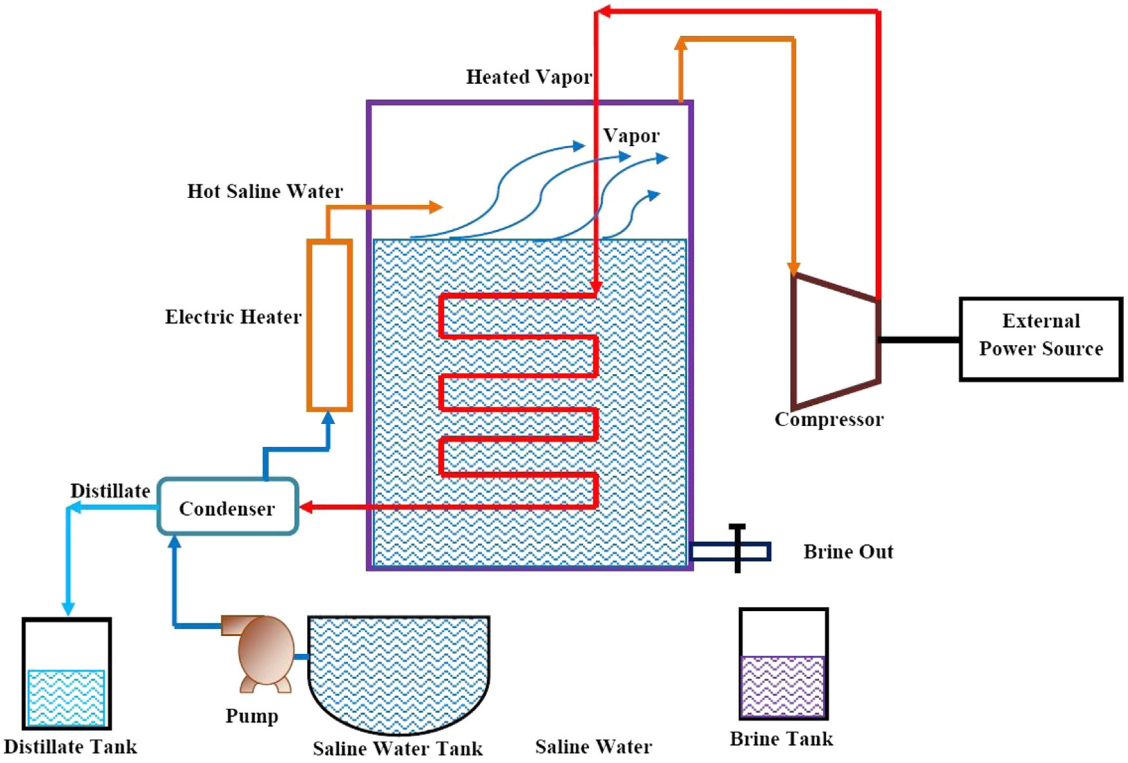

Fig. 6. Mechanical vapor compression desalination system [99].

vapor compressor and thermo vapor compressor is shown in Fig. 7a and b respectively.

The energy balance of MVC is shown in Fig. 7c. The power required by the MVC is given by [99]

$$\Pi = \left(\frac{\dot{m}_v}{3600 \times \eta_{co} \times M_{wt}}\right)\left(\frac{\Upsilon \times R \times (T_1+273.15)}{\Upsilon - 1}\right)\left(\left(\frac{P_2}{P_1}\right)^{(\Upsilon-1)/\Upsilon} - 1\right) \tag{25}$$

$$\frac{(T_2+273.15)}{(T_1+273.15)} = \left[\frac{P_2}{P_1}\right]^{(\Upsilon-1)/\Upsilon}. \tag{26}$$

3.1.4. Compact solar thermal desalination systems

Zhang et al. [102] experimentally investigated the performance of horizontal tube falling film evaporation desalination system integrated with solar collector which supplies hot water to the horizontal evaporator tube over which saline water is sprayed. The water vapor thus formed is carried by air pump and condensed using incoming feed water thereby nearly 100% heat is recovered. The optimum start temperature of the unit is 70 °C and the distillate yield of the system is around 13.5–18.308 kg/d and it increases with the increase in temperature. Solar desalination system with falling film evaporation and condensation process which uses both multi stage flash evaporation and multi effect regeneration units has a performance ratio of 2.35 and distillate yield of 135 kg/h for a feed temperature of 90 °C at an operating pressure of 15 kPa. Increased distillate yield can be obtained at reduced pressures and at high inlet feed water temperature [103].

Reddy et al. [104] carried out theoretical and experimental studies with evacuated multi stage solar desalination system which consists of inclined trays representing evaporator–condenser unit maintained at reduced pressure using vacuum pump. The evaporator trays are provided with silk cloth to enhance evaporation over which the feed water heated by solar collectors is allowed to flow as thin film. The optimum number of stages, the optimum gap between the stages and the optimum operating pressure was found to be 4, 100 mm and 0.03 bar respectively under which maximum yield of 53.2 kg/m^2/d was obtained. The schematic representation of the system is shown in Fig. 8.

Nafey et al. [105] carried out experimental and theoretical studies with solar desalination unit consisting of solar flat plate collectors and flash vessel integrated with the condenser. The performance ratio of the system was about 0.7–0.9 and the maximum and minimum productivity of the system was found to be 7 kg/d/m^2 and 1.04 kg/d/m^2 respectively and it depends mainly on solar radiation. A similar kind of unit with production capacity of 3 l/d was designed by Wessley and Mathews [106].

Multi-stage stacked type desalination unit capable of producing 9 l/d designed and fabricated by Shatat and Mahkamov consists of four rectangular shaped stacks filled with water kept one above the other [107]. The heat energy to the bottom water stack was supplied by solar collectors using heat exchanger and the latent heat of condensation of water vapors are used by the other stages to produce distillate. A three stage multi effect desalination system with enhanced condenser surface integrated with evacuated tube collectors is capable of producing 43 kg/d of distillate [108].

3.1.5. Natural vacuum desalination systems

In desalination systems, the fresh water vapors can be produced from saline water at low operating temperatures if the required vacuum is provided by vacuum pump, but it consumes more power. This electrical energy consumption can be reduced or eliminated by creating vacuum by natural means using the force of gravity by allowing fall of water under gravity thereby producing vacuum at the head space maintained above [109].

Natural vacuum desalination systems are suitable for small scale applications. Al-Karabsheh and Goswami [110] carried out theoretical studies with evacuated desalination system in which vacuum in the evaporator was created using natural process by allowing water to fall under gravity and the heat required for the

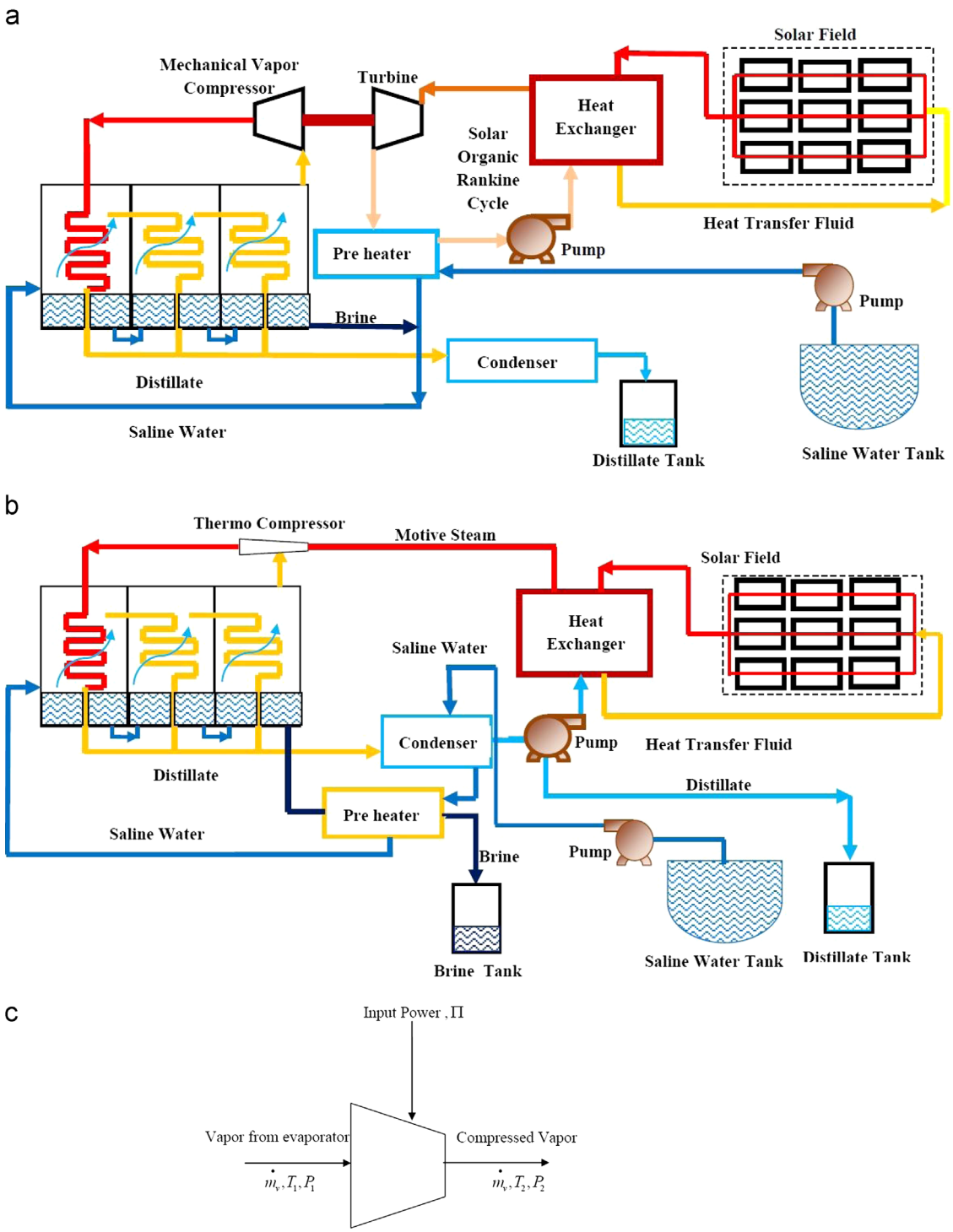

Fig. 7. (a) Solar powered mechanical vapor compression unit coupled with MED [101], (b) solar powered thermo vapor compression unit coupled with MED [101] and (c) energy balance in mechanical vapor compressor [99].

process was supplied by solar flat plate collectors. The system was flushed at regular intervals to remove the trapped non-condensable gases and the distillate yield from the system was found to be 6.5 kg/d m^2 of evaporator area. The schematic representation of the system is shown in Fig. 9. This system was able to produce a distillate of 100 l/d by incorporating thermal energy storage of capacity 3 m^3 and solar collector of area 18 m^2 [111]. The schematic representation of the system is shown in Fig. 10a. Cooling capacity of 3.25 kW and distillate yield of 4.5 kg/h was obtained by coupling natural vacuum desalination system with absorption refrigeration system and thermal storage [112]. The schematic representation of the system is shown in Fig. 10b.

Thermal analysis of natural vacuum solar driven flash desalination system operation in single stage mode and two stage mode was carried out by Maroo and Goswami [109]. In single stage operation the feed water heated in solar collectors was allowed to flash in the evaporator and the vapors formed are subsequently condensed in the condenser. In case of two stage operation the brine left behind in first stage was allowed to flash in second stage evaporator there by generating additional distillate. For a solar

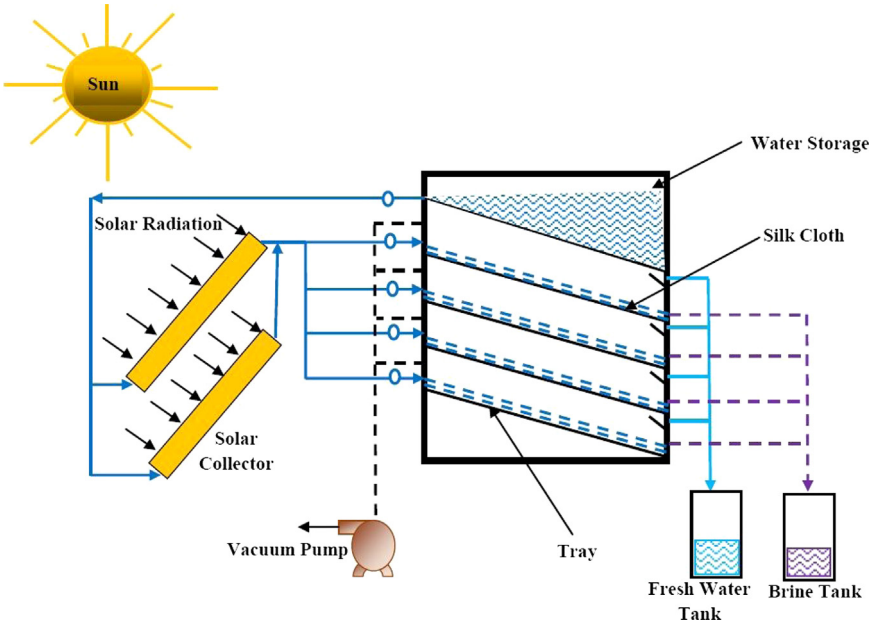

Fig. 8. Evacuated multi-stage solar water desalination system [104].

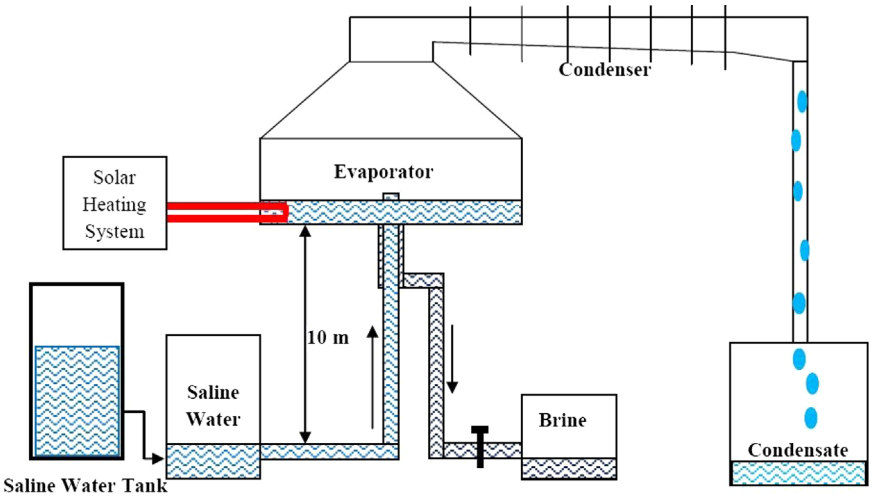

Fig. 9. Natural vacuum desalination system proposed by Al-Karabsheh and Goswami [110].

collector of 1 m^2 area, the proposed system produces nearly 5.54 kg and 8.66 kg of distillate while operating in single stage and two stage mode with an performance ratio of 0.748 and 1.350 respectively. The schematic representation of the system is shown in Fig. 11a.

In two stage low temperature natural vacuum desalination process the vapor formed in the first stage was condensed in the heat exchanger incorporated in the second stage there by rejecting heat to second stage causing vaporization of saline water in the second stage, the vapors thus formed in the second stage were condensed using external condenser. The cost of water production by this method was found to be 3 USD/m^3. The specific thermal energy consumption and mechanical energy consumption was about 1500 MJ/m^3 and 1 kWh/m^3 respectively [113].

The natural vacuum desalination proposed by Ayhan and Al Madani [114] consists of evaporator column exposed to solar radiation and shaded condenser column. The schematic representation of the system is shown in Fig. 11b. The vapors generated in the evaporator were moved to the condenser column by forced mass transfer (using fan). Zhao and Liu [115] proposed an innovative solar multi effect evaporator–condenser desalination system in which the vacuum required by the system was maintained by tides. The theoretical study indicates that the stable operation of the unit can be achieved for areas with tides of range 2 m.

3.1.6. *Freeze desalination*

Freeze desalination is a technique in which sea water is allowed to cool below its freezing point, thereby the ice crystals of pure water are formed on the surface. The three types of freeze desalination are direct contact freeze desalination, indirect contact freeze desalination and vacuum operated freeze desalination [116].

3.1.6.1. Direct contact freeze desalination. In direct contact freeze desalination process liquid refrigerant (usually n-butane) is mixed

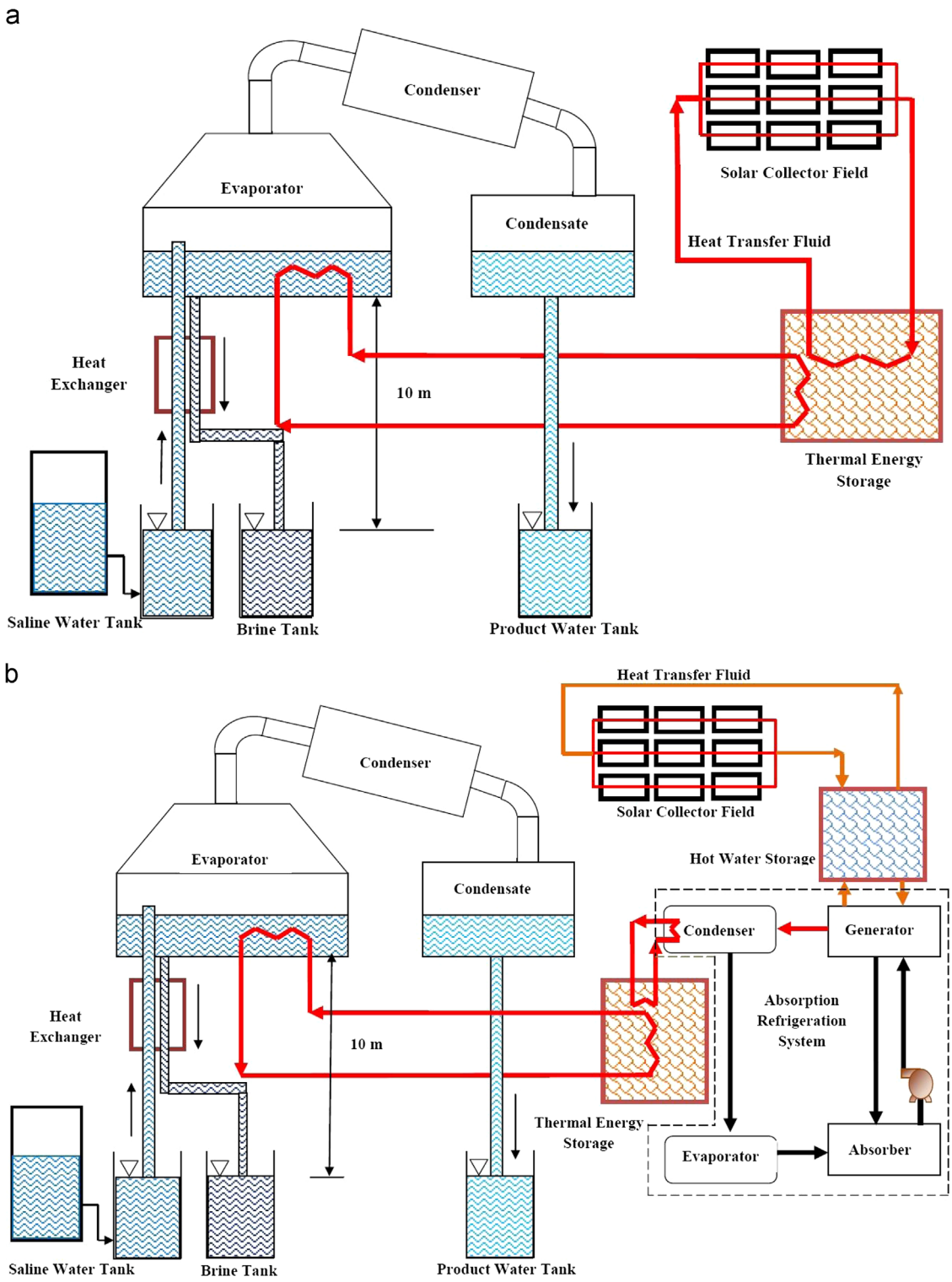

Fig. 10. (a) Natural vacuum desalination system with thermal energy storage [111] and (b) natural vacuum desalination system with thermal energy storage and absorption refrigeration [112].

directly with feed saline water in a freezer such that the heat from saline water will be absorbed by the refrigerant resulting in the formation of ice crystals which are then separated and purified to obtain potable water. This kind of freeze desalination process requires less pressure ratio, achieving this pressure ratio with conventional compressors is not economical and this has lead to the development of hydraulic refrigerant compressor. The hydraulic refrigerant compressors do not use lubrication oil as a result contamination of ice crystals by lubrication oil is avoided. The size of the freeze desalination plant melter and washer could be reduced by accepting some amount of salt in the water as a result cost and size of the system could be reduced and the product water could be used for irrigation purposes in water scarce areas [117].

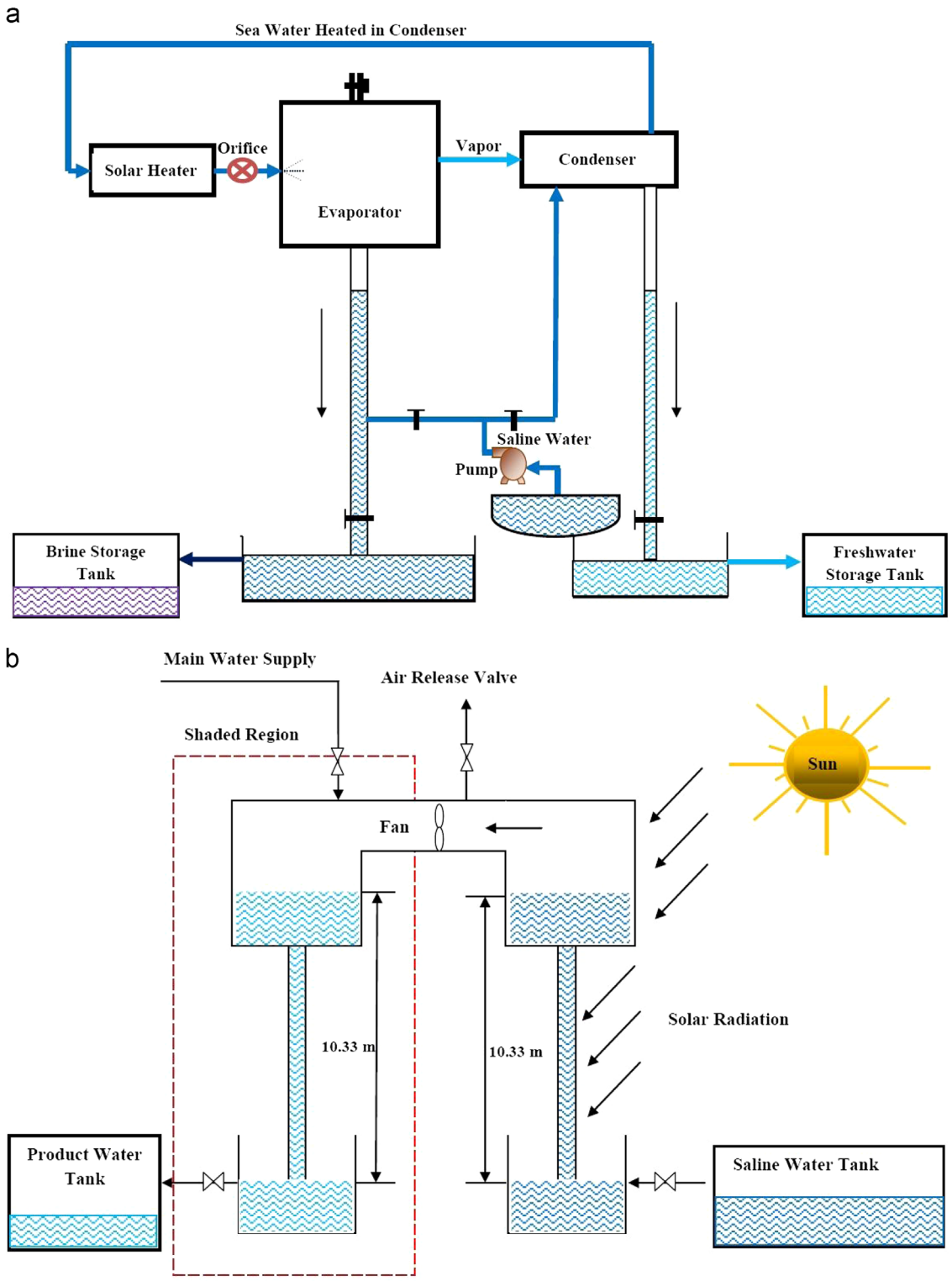

Fig. 11. (a) Single stage flash solar natural vacuum desalination system [109] and (b) solar natural vacuum desalination system proposed by Ayhan and Al Madani [114].

In two stage direct contact freezing/solar evaporator system salts like sodium, potassium and magnesium are recovered from the rejected brine of direct contact freezing system using solar evaporators. At high conversion ratio, two stage direct contact freezing system is more efficient than single stage direct contact freezing system. The two stage direct contact freezing plant of capacity similar to the capacity of entire Arabian Gulf desalination plants requires less evaporator area compared to other desalination plants of same capacity [118].

The power requirements of compressors used in freeze desalination plant is given by [118]

$$\Pi = \left(2.78 \times 10^{-4} \times \frac{\gamma}{\gamma - 1}\right) \times Q_1 \times P_1 \times \left(\left(\frac{P_2}{P_1}\right)^{(\gamma-1)/\gamma} - 1\right) \tag{27}$$

The fresh water productivity is given by

$$P_{wc} = -\upsilon_G(1-e)\rho_{ice} \tag{28}$$

$$-\upsilon_G = \frac{(B_o \rho_1 g)}{(e\mu_1)} \tag{29}$$

The area of solar evaporator required to treat the discharged brine can be found from rate of evaporation of water which is given by

$$E_v = W[P_s - P_a] \tag{30}$$

$$W = \left(2.7 \times 10^{-2}\right) + \left(7.5 \times 10^{-5}\right) U \tag{31}$$

Lloyd [119] proposed an integral design for direct contact freeze desalination plants in which processes like crystallization, washing, melting and decanting takes place in a single cylindrical vessel thereby the losses due to transport of the working fluid is reduced. The capital cost of the proposed system containing two integral vessels was found to be 20% lower than the previous design. The cost of water production was found to be 3.461×10^{-4} USD/l.

Fresh water production from sea ice uses gravity induced desalination in which the sea ice when exposed to sunlight melts because of pore expansion resulting in gravity induced brine drainage due to increase in temperature. Sea ice desalination is limited for two reasons: (a) collection and transportation of sea ice requires special equipments and (b) collection of sea ice affects marine ecosystem, sea water salinity and coastal climate [120].

3.1.6.2. Indirect contact freeze desalination. In indirect contact freeze desalination, the refrigerant and the saline water are not mixed with each other, they are separated in crystallizer by heat transfer surfaces and the ice formed is in the system is then scraped off from the heat transfer surfaces [116]. Removal of produced ice in freeze desalination process is a big problem, Attia et al. [121] proposed a new method of freeze desalination process using auto reversed vapor compression heat pump working with R-22 as refrigerant. The system consists of two tanks (A and B), solenoids (for filling the tank with saline water and for draining brine and produced fresh water) and heat pump arrangement. During the first cycle tank A is filled with saline water, the saline water in tank A acts as heat source and saline water flowing inside tank B acts as heat sink, the saline water in tank A is converted into slurry of ice and brine, the brine is drained out by opening the valves. During the second cycle the heat pump system uses saline water in tank B as heat source and ice in tank A as heat sink, as a result slurry of ice and brine is formed in tank B, and the ice formed in tank A gets melted and it is removed and the cycle is again repeated. The schematic representation of the system is shown in Fig. 12. Major advantages of freeze desalination using auto reversed vapor compression heat pump includes (1) elimination of complex mechanical systems for removal of ice and (2) higher efficiency and low maintenance.

In hybrid process of freeze desalination integrated with membrane distillation system (FD–MD), the brine discarded from freeze desalination process is used as feed for membrane distillation process. The optimum freezing duration was found to be two hours and if freezing of brine solution was carried out for more than two hours, trapping of brine inside ice crystals was noticed. For 8 kg of feed water, freeze desalination produces 1.46 kg of fresh water with 0.146 g/l salinity and MD produces 4.26 kg of fresh water with 0.062 g/l salinity. The total water recovery and specific energy consumption of the system was found to be 71.5% and 2.343 kWh/m^3 respectively, if heating alone is considered [122]. The block diagram of the system is shown in Fig. 13.

3.1.6.3. Vacuum operated freeze desalination. In vacuum operated freeze desalination system, the feed saline water is cooled below its triple point at reduce pressure to produce both ice and vapor. The ice formed is collected and the vapor generated is compressed and condensed in frozen chamber. This method requires compressors of large size due to high specific volume of water

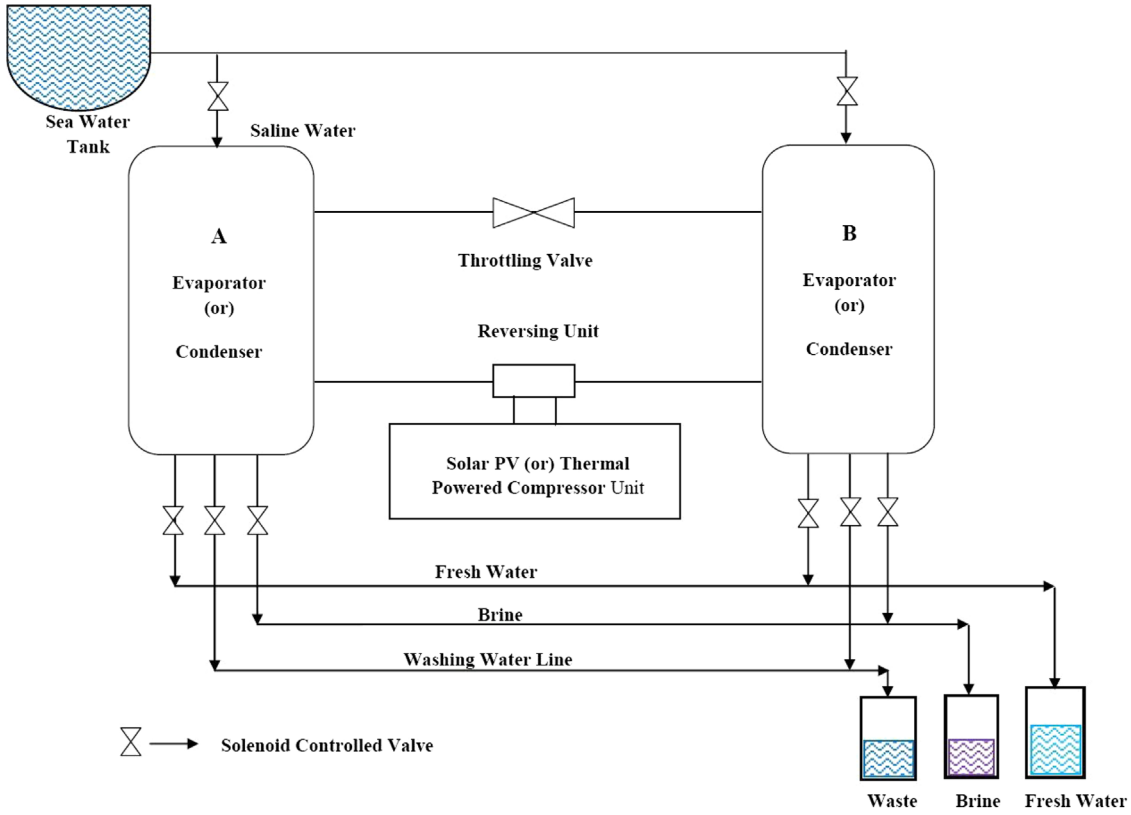

Fig. 12. Freeze desalination using auto reversed vapor compression heat pump [121].

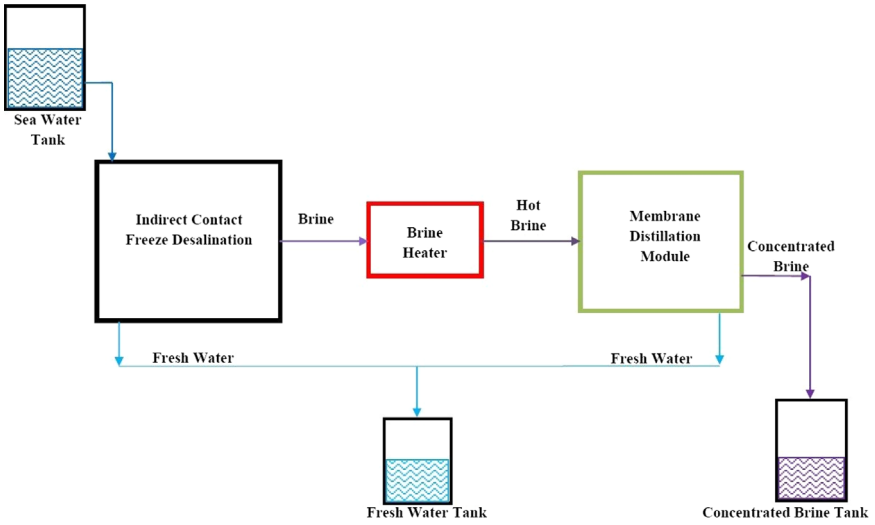

Fig. 13. Block diagram of hybrid indirect contact freeze desalination–membrane distillation [122].

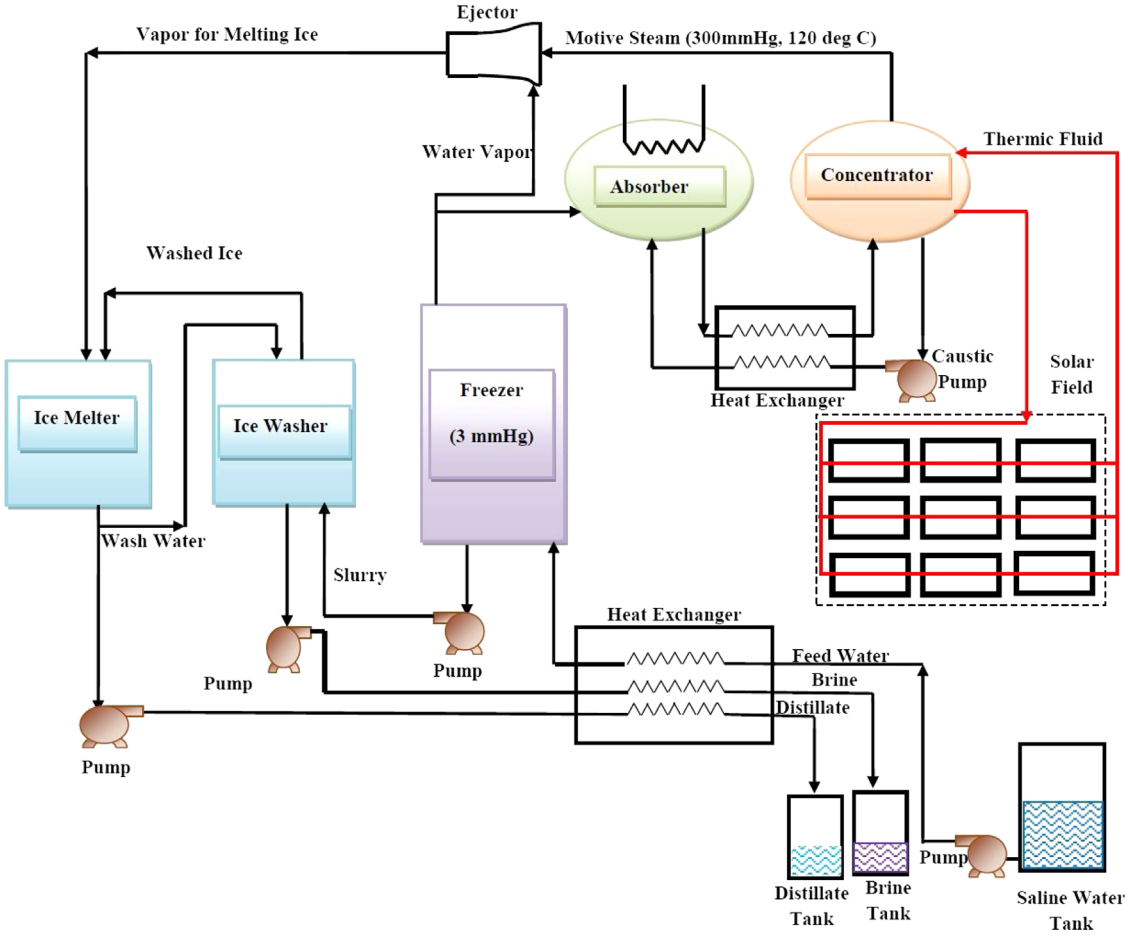

Fig. 14. Solar operated vacuum freezing ejector absorption (VFEA) desalination system [123].

vapor and is called vacuum vapor compression freeze desalination. This difficulty can be overcome by using vacuum absorption freeze desalination process [116]. Performance and economic analysis of 4500 m^3/d capacity solar desalination plant using vacuum freezing ejector absorption (VFEA) process was studied by El-Nashar [123]. In vacuum freezing ejector absorption process formation of both vapor and ice takes place simultaneously. The ice formed is washed and melted in ice washer and melter. The vapor formed is passed through absorber which contains NaOH solution which absorbs the vapor and the vapor is released by heating the solution using solar assisted heating system. The vapor thus released is used as motive steam for ejector system which is further used for melting ice in the melter. The sea water salinity and temperature plays an important role in deciding the cost of the plant. Capital cost of the plant can be reduced by using evacuated tube solar collectors instead of flat plate collectors. The schematic representation of the system is shown in Fig. 14. A commercial freeze desalination plant (200 m^3/d) integrated with power plant

powered by Fresnel type solar collectors in Yanbu, Saudi Arabia was shut down after one year due to leakage of steam into storage medium [124].

Freeze desalination process is also capable of concentrating the reverse osmosis brine, such that the yield from RO unit can be increased and the quantity of brine discharged can be reduced [125].

3.1.7. Adsorption desalination

The adsorption desalination system mainly consists of evaporator, adsorption beds (silica or zirconia) and condenser. The adsorption bed is supplied with hot or cooling water as per requirement. The saline water evaporated in the evaporator is adsorbed by the bed maintained at low temperature by circulating cooling water. The water vapor trapped in the bed is recovered by circulating hot water, the recovered water vapor is condensed in the condenser and is of high quality because of double distillation. For a two bed system, adsorption takes place in one bed and desorption takes place in other bed simultaneously [126]. The schematic representation of two bed adsorption desalination system is shown in Fig. 15a. The cooling water inlet temperature, hot water inlet temperature and silica gel adsorption constant play an important role in determining the water production rate and

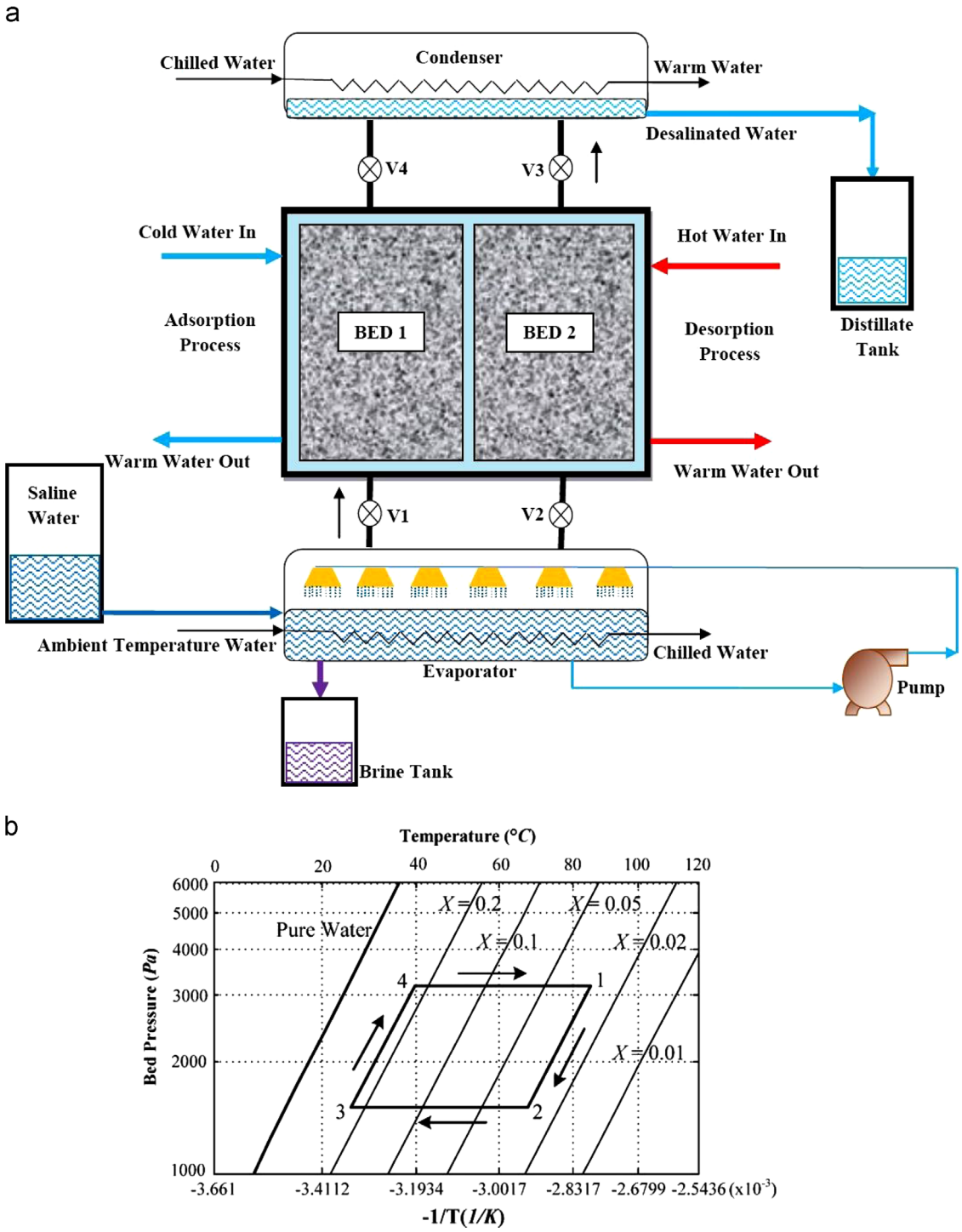

Fig. 15. (a) Adsorption desalination system [126] and (b) thermodynamic cycle of adsorption desalination cycle [126].

energy consumption of the system. High water production rate with less energy consumption can be attained only if the plant is operated under optimum conditions [126].

The thermodynamic cycle of adsorption-based desalination unit [126] is shown in Fig. 15b.

Process 1 to 2: Circulation of cooling water through the adsorption bed to reduce the bed temperature to facilitate adsorption of water vapor.
Process 2 to 3: Opening of valve between adsorption bed and evaporator and charging of the adsorption bed with water vapor from evaporator until maximum concentration is reached.
Process 3 to 4: Closing of valve between adsorption bed and evaporator followed by circulation of hot water through the bed to increase the bed temperature
Process 4 to 1: Opening of valve between bed and condenser and desorption of water vapor from the bed followed by condensation in condenser to produce potable water.

The total heat required for single cycle is given by

$$Q_{heating(bed)} = (X_3 m_{sg} C_p + m_{sg} C_{sg})(T_4 - T_3) + \left[m_{sg} C_{sg} + \left(\frac{X_4 + X_1}{2} \right) m_{sg} C_p \right] (T_1 - T_4) + (X_4 - X_1) m_{sg} Q_{des} \quad (32)$$

The cooling requirement for single cycle is given by

$$Q_{coolin(bed)} = (X_1 m_{sg} C_p + m_{sg} C_{sg})(T_1 - T_2) + \left[m_{sg} C_{sg} + \left(\frac{X_2 + X_3}{2} \right) m_{sg} C_p \right] (T_2 - T_3) + (X_3 - X_2) m_{sg} Q_{ads} \quad (33)$$

The cooling requirement of the condenser is given by

$$Q_{cooling(cond)} = m_{sg}(X_4 - X_1) h_{fg1} \quad (34)$$

The cooling effect in the evaporator is given by

$$Q_{evap} = m_{sg}(X_3 - X_2) h_{fg2} \quad (35)$$

The mass of fresh water generated in single cycle is by

$$m_{water} = (X_4 - X_1) m_{sg} \quad (36)$$

The concept of solar adsorption desalination system in combination with multi effect distillation system was studied by Zejli et al. [127] using theoretical models. The proposed system consists of two adsorption beds containing zeolite as adsorbent placed between the evaporator operating in cyclic mode and the heat required for the process was supplied by solar parabolic trough collectors. The vapors leaving the adsorption system were used as heat source for three effect distillation system. The saline sea water entering the condenser of three effect distillation unit was preheated and its temperature was raised to 70 °C by the heat transfer fluid and it was allowed to flash inside the evaporator to produce vapors. At the mean time, during the first cycle one adsorbent bed would be at a temperature of 120 °C and other would be at high temperature of 195 °C, during the second cycle the adsorbent bed temperature would be reversed by changing the direction of flow of hot fluid. The produced vapors would be adsorped by the low temperature zeolite bed and the adsorped water vapor would be released by passing hot heat transfer fluid through the bed. The vapors were used as heat source for three effect distillation system to cause evaporation of brine water disposed by the evaporator and the vapors thus formed were condensed using condenser.

Wu et al. [128] analyzed different possible thermodynamic cycles for adsorption desalination system by assuming temperature of the evaporator less than or equal to or greater than the cooling water inlet temperature. The maximum water production with minimum energy consumption was obtained if the evaporator temperature was kept equal to or higher than the cooling water used to cool the adsorption bed because this would make the adsorption system to produce potable water rather than chilling effect. The proposed models for thermodynamic models were verified by experiments and the results were found to be closer to the predicted values [129]. The daily water productivity of four bed adsorption desalination plant operating with low temperature waste heat was found to be 4.7 kg/kg of silica gel. The water productivity can be enhanced by increasing the chilled water temperature supplied to evaporator and by reducing the temperature of cooling water temperature circulated around the adsorption bed for the constant hot water inlet to the adsorption bed [130]. The water productivity for the four two bed system was higher than the two bed system under similar operating conditions [131]. The optimum cycle time for the two systems for which maximum distillate production was obtained at different hot water inlet temperature is graphically represented in Fig. 16a.

Ng et al. [132] studied the performance of waste heat driven four bed adsorption desalination cycle producing potable water and refrigeration using mathematical models and by experiments for different operating parameters. They noticed that the system can operate even at hot water inlet temperature of 65 °C. The specific water production and specific cooling effect produced by the system at varying chilled water inlet temperatures to evaporator with a fixed desorper hot water inlet temperature of 65 °C is shown in Fig. 16b. It could be seen that both the distilled water and cooling effect produced were found to be maximum at higher chilled water inlet temperature to the evaporator. Thu et al. [133] developed an advanced adsorption desalination system utilizing heat rejected by the condenser for evaporating saline water from the evaporator. Better yield was obtained at high hot water inlet temperature, low cooling water temperature and by maintaining high flow rates. The optimum cycle time of this advanced adsorption desalination system was found to be lower than the conventional adsorption desalination system. The advantages and limitations of various indirect solar desalination systems (non-membrane process) are shown in Tables 3 and 4.

3.2. Membrane processes

In membrane process, fresh water is produced from saline water by allowing passage of water molecules (in case of reverse osmosis) or ions (in case of electrodialysis) through membranes by applying high pressure (above osmotic pressure) or electrical potential. The salinity of feed water plays an important role in determining the yield of the unit [6]. The different types of solar powered membrane process is described below.

3.2.1. Solar powered reverse osmosis desalination

Reverse osmosis (RO) is a pressure driven desalination process in which pressurized feed water is allowed to pass through the cross flow membrane module. If the applied pressure is higher than the osmotic pressure, fresh water permeates across the membrane and it is collected through the permeate tube and the brine is drained out [137,138].

The mass flux that is transported through the RO membrane is given by [137]

$$N_A = L(\Delta P - \Delta \pi) \quad (37)$$

Osmotic pressure is given by

$$\pi = \mathrm{CRT} \quad (38)$$

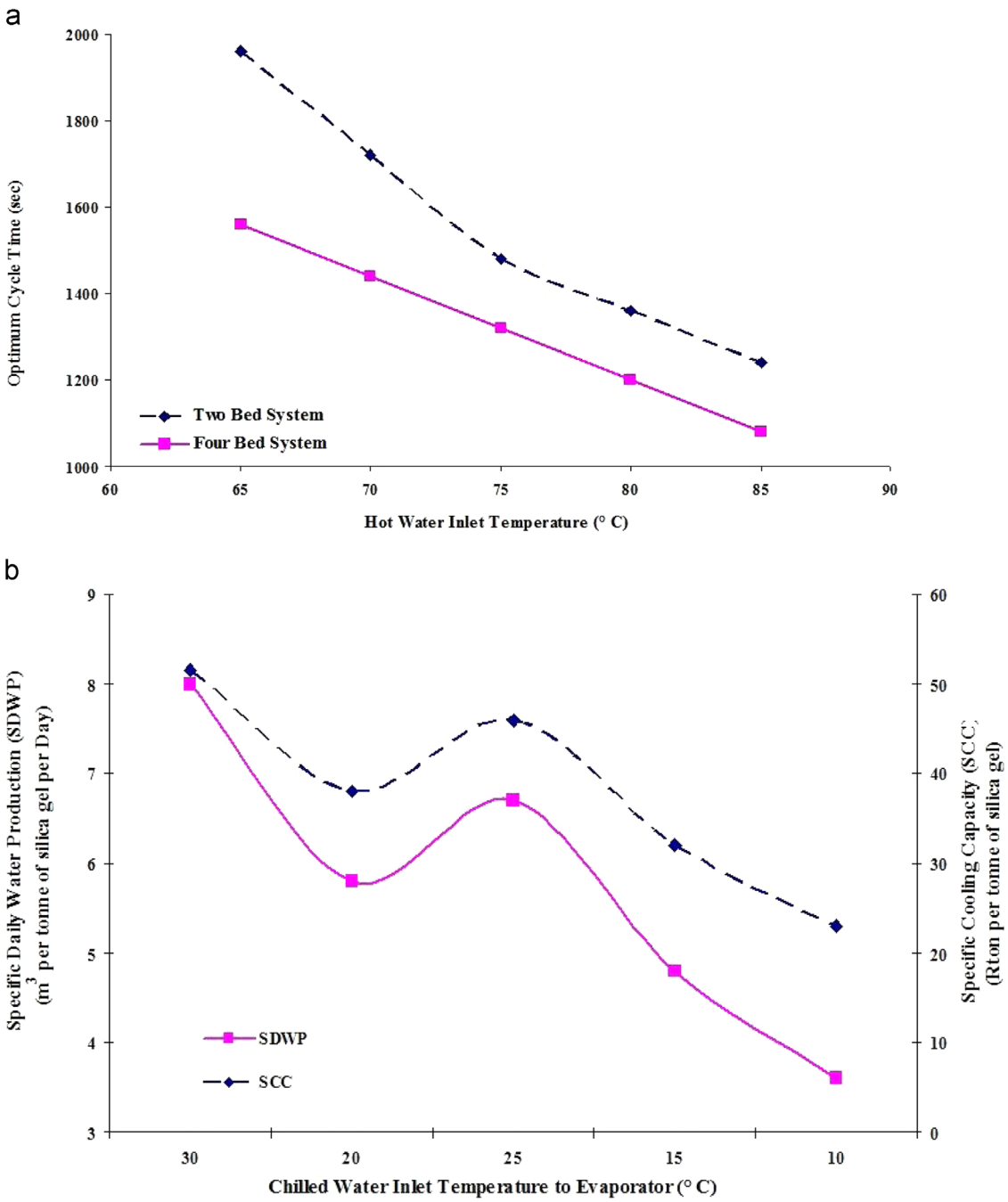

Fig. 16. (a) Effect of hot water inlet temperature on optimum cycle time [131] and (b) effect of chilled water inlet temperature to evaporator on water production and cooling effect [132].

Permeability coefficient of the membrane is given by

$$L = \frac{\mathrm{DSV}}{\mathrm{RTI}} \tag{39}$$

Recovery of membrane in RO unit is given by

$$R_W = \frac{Q_p}{Q_f} \tag{40}$$

Water recovery for RO plant is in the range of 25–45% for sea water and 90% for brackish water. Energy requirement for RO process depends on the membrane properties and salinity of the feed water [137,138]. The RO modules can be connected in series or parallel configurations and it is schematically represented shown in Fig. 17. The major components of RO system are [138] membrane modules, high pressure pumps, energy source and energy recovery systems.

3.2.1.1. Solar PV powered RO desalination. In solar PV powered RO unit, the power required for the desalination process is supplied by photovoltaic panels and the system can be operated with (or) without batteries. Solar PV operated reverse osmosis unit has better socio-economic and environment benefits compared to diesel generator operated reverse osmosis unit [139]. In 1979, Petersen et al. [140] demonstrated the performance of solar PV powered RO plant of capacity 1.5 m^3/d in northern part of Mexico

Table 3
Advantages and limitations of in-direct solar desalination systems (non-membrane processes).

Multi stage flash desalination [80]	**Multi effect distillation** [80]	**Vapor compression desalination** [80,134,135]
Suitable for large scale production of distilled water	Low thermal energy consumption	High efficiency
The plant is more reliable	System could be operated even at temperature below 70 °C	Does not require additional cooling medium
Plant can tolerate feed water of any quality	The system is reliable	Low energy consumption
High quality distillate is produced	The produced distillate is of high quality	Suitable for low capacity applications
Minimal or no feed water pre treatment is required	Feed water does not need pre treatment	Feed requires less pre-treatment
High energy consumption	CO_2 emissions are lower than MSF desalination system	Product water is of high quality
Corrosion takes place due to high temperature operation	It consumes electrical power for vacuum pump	Size of the plant is limited by the size of compressor
The plant is heavy and costly	The system is heavy and costly	Corrosion of compressor
	Suffers by corrosion problem	High initial cost
		Higher water production cost
		Low environmental impact

Table 4
Advantages and limitations of in-direct solar desalination systems (non-membrane processes).

Natural vacuum desalination [136]	**Freeze desalination** [12]	**Adsorption desalination** [128]
Feed water like waste water, sewerage and seawater can be used	Theoretically energy required for the process is low	Solar or waste heat can be used
Reduced water production cost	Reduced corrosion and scaling	No possibility of bio-fouling
Low temperature heat source is sufficient	Handling of ice and water mixture are complex	Evaporator operates at low temperature hence less fouling and corrosion
Destruction of organic matter in the product is prevented	Equipments are costlier	Requires less maintenance due to the presence of less movable part
Can be integrated with tall buildings	Complicated refrigeration system	Chilled water can also be produced
High structures of height above 10 m is required	Freshwater is needed for washing produced ice before melting	Distillate of high quality can be produced
Requires removal of non-condensable gases formed during evaporation of water		

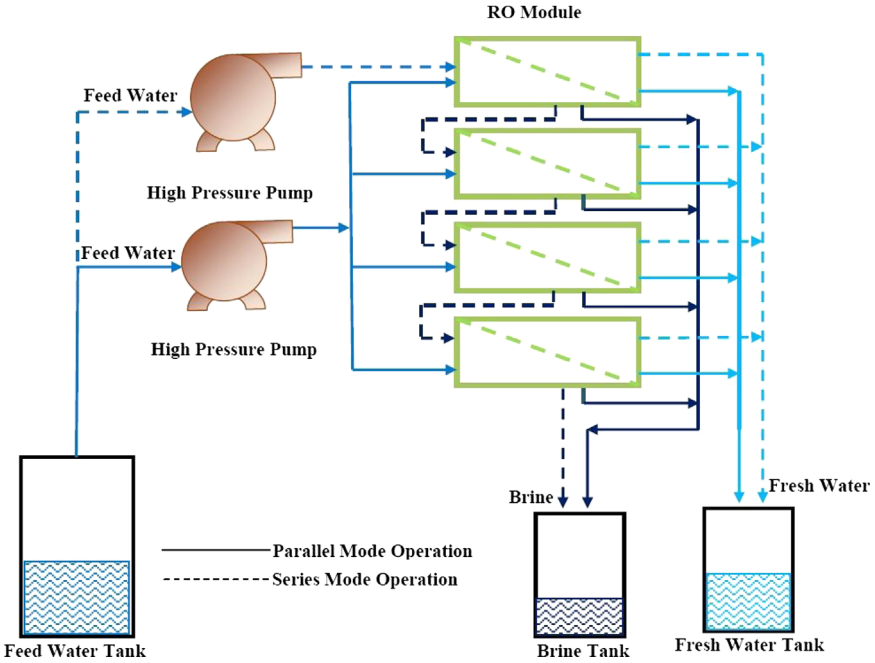

Fig. 17. Series and parallel arrangement of RO modules [137].

and Wind powered RO plant of capacity 9 m^3/d in north sea, German coast.

Standalone solar PV powered RO desalination plant of capacity 1.2 gal/min at Jeddah, Saudi Arabia is capable of meeting the drinking water demands of 250 inhabitants [141]. The permeate yield, recovery % and salinity of the product can be improved by increasing the operating pressure of solar PV powered RO plants. It has been estimated that nearly 55 million m^3 of natural gas can be saved per year, if conventional fossil fueled multi stage flash desalination systems used in Bahrain were replaced by solar PV powered RO plants [142].

Computer simulation of solar PV operated RO unit carried out by Hrayshat [143] for 10 locations in Jordan indicates that the climatic conditions and feed water salinity plays an important role in permeate yield. Colangelo et al. [144] proposed mathematical models for different configurations of solar PV operated RO units

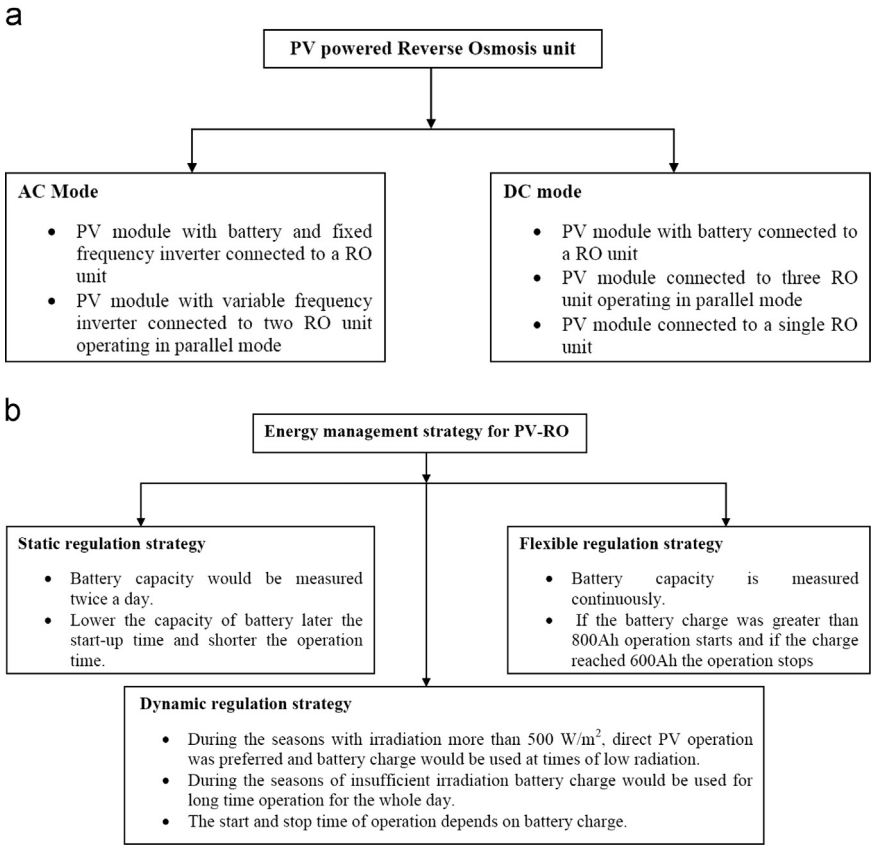

Fig. 18. (a) Configurations of PV powered RO unit [144] and (b) energy management strategy for PV powered RO unit [146].

and are shown in Fig. 18a. For remote locations, Al-Suleimani and Nair [145] found that the solar PV powered RO unit of capacity 5 m^3/d with a lifetime of 20 years was found be more economical than the diesel operated RO unit of same capacity. The cost of water production/m^3 was found to be 8.68 USD and 6.52 USD for diesel and solar powered RO system respectively. Herold et al. [146] proposed three energy management strategies for PV–RO system and are shown in Fig. 18b.

Battery less PV powered sea water RO desalination system simulated by Thomson et al. [147] consists of photovoltaic array, multi power point tracker (MPPT), inverter, induction motor, progressive cavity pump, plunger pump, Clark pump (operated by the concentrate leaving the RO modules) and RO modules. The system operation was mainly affected due to passing of clouds and because of this intermittent operation the salinity level of permeate was found to be higher than the value set by the World Health Organization (WHO). The cost of water production by this system at 8% discount rate was found to be 2.64 USD/m^3 but its reliability was not reported [148]. The battery less PV powered RO unit with tracking produced 15% more distillate and 25% more power than the system with no tracking [138].

Simulation of stand-alone wind–solar PV powered hybrid RO unit was carried out by Mohamed et al. [149]. The cost of water production by this hybrid system was found to be lower than the system operating with autonomous PV system due to higher cost of PV. The energy recovery with pressure exchanger caused reduction in energy consumption from 12 kWh/m^3 to 6.3 kWh/m^3. Steady state and dynamic simulations of large scale hybrid PV-wind powered stand alone battery less RO desalination plant was carried out by Cherif et al. [150] using ROSA software and BG environment of 20 sim software. Solar PV and Wind turbine produced nearly 30.8 kW and 2.8 kW respectively. The simulation results showed that the system could meet the freshwater demands of high environmental quality (HEQ) hotels in Djerba Island.

Khayet et al. [151] developed a solar thermal and PV powered RO desalination unit which consists of low pressure pump, high pressure pump, spiral wound polyamide thin film composite membrane (1.2 m^2), and spherical thermal collector to preheat the feed water. The optimum feed pressure, flow rate and temperature for a feed concentration of 6 g/l were 7.7 bar, 252.8 l/h, and 33 °C respectively. The RO unit is capable of producing permeate of at least 0.2 m^3/d with an energy consumption less than 1.3 kWh/m^3. Peterson and Gray [152] evaluated the performance of PV-powered RO unit at Brisbane botanic garden, Australia which consists of two solar PV-array of capacity 1.44 kW each with tracking arrangement, two pumps and a RO unit. The treated water was used for the botanic garden and the concentrate was treated using terrace ponds where marine plants were grown to make fodder for animals. The system shows better performance during dry seasons and during rainy season its performance was affected. The system produces nearly 3.36 million l of permeate for 484 days with maximum production rate of 10.27 kl/d during the month of August 2009.

Battery less solar energy operated RO unit of 1 m^3/d capacity developed by Soric et al. [153] consists of 5 photovoltaic modules, RO unit, pumps and electric regulator (to provide stable voltage to the pumps). Continuous operation of the plant was noticed during summer and the system is capable of producing permeate in the range of 275–373 m^3/year.

The power consumption and water productivity cost of RO desalination unit mainly depends on the membrane configurations, efficiency of the system and total dissolved salts in feed water [154]. The efficiency of the solar PV powered RO unit depends on all the individual components efficiency. The water

production cost and energy consumption of the PV operated systems can be brought down by using high efficiency PV cells, novel tracking systems and novel long life membranes. Even though the cost of PV panels has considerably decreased, the main hindrances to this system are higher initial cost and land availability. Solar PV powered RO units are highly suited for small scale desalination and it is not suitable for medium or large scale desalination [155].

3.2.1.2. Solar thermal powered RO desalination. In solar thermal powered RO desalination, the mechanical energy produced by the solar organic cycles is directly used to run the high pressure pumps of RO unit [155]. The schematic representation of solar organic Rankine cycle RO desalination unit is shown in Fig. 19. The solar thermal driven RO desalination unit is a more promising technology, any development in RO technology would be useful for developing RO technology based on solar thermal systems [156]. The unit cost of water produced by RO plant could be reduced by using hybrid solar assisted steam cycle for supplying required shaft power for RO high pressure pump [157]. Integrating RO unit with solar operated Rankine cycle could cut off CO_2 emissions and lead to environmental savings with little additional increment in capital cost [158].

Manolakos et al. [159] proposed a low temperature solar Rankine cycle which uses HFC-134a as working fluid in which the mechanical power derived from expander was used to run the pumps of RO system. From basic mass and energy balance it was found that the fresh water production of the system would be around 1012 m^3/year with an specific energy consumption of 2.5 kWh/m^3. The laboratory scale experiments with reverse running scroll compressor as expander and 100 kW electric heater confirmed that the power output was sufficient to operate RO unit with a capacity of 280 l/h [160].

Delgado-Torres et al. [161] proposed and carried out theoretical studies with solar thermal powered RO system equipped with pressure exchanger in which condensing organic fluid was used to preheat the feed water of the RO unit. Preheating of feed water has only little effect on distillate yield and the fresh water production rate with toluene as working fluid in organic Rankine cycle was higher than the yield obtained by using octamethylcyclotetrasiloxane and hexamethyldisiloxane as working fluid.

The performance of solar operated double cascade organic Rankine cycle integrated with RO unit was studied by Delgado-Torres and Garcia-Rodriguez [162]. The plant was analyzed with toluene and hexamethyldisiloxane as working fluid for topping cycle and iso-pentane as working fluid for bottom cycle. The power output from top cycle was used to run the high pressure pump of RO unit and the power generated by the bottom cycle was used to operate the auxiliaries. The heat rejected from bottom cycle was used to preheat the feedwater to RO unit. The performance of the system was found to be higher than the conventional system driven by PV cells. For standalone system operation the use of hexamethyldisiloxane as working was found to be more suitable than toluene. Bruno et al. [163] carried out simulation of solar operated Rankine cycle for RO desalination unit with different working fluids and different types of solar collectors. Highest organic Rankine cycle efficiency was obtained for fluids with high critical temperature. Among the collectors studied, parabolic trough collectors gave best results. The cost of electricity produced by the PV system to drive RO desalination system was found to higher than the cost of electricity produced by solar operated Rankine cycle.

Thermo-economic analysis of solar organic Rankine cycle-RO unit revealed that for the system with energy recovery unit like pelton wheel turbine and pressure exchanger, the unit water production cost was found to be 24% and 24.2% less than the system with no energy recovery [164]. Only 2% increase in distillate production was noticed by preheating the feed water with rejected heat from condenser of solar organic Rankine cycle [165]. RO unit powered by solar organic Rankine cycle and PV panel for supplying fresh water to Chalki Island was studied by Karellas et al. [166]. The system uses parabolic trough collectors and R134a as working fluid. The PV system was used to supply power to cooling pump and working fluid pump. The power produced by turbine was used for RO high pressure pump and the system is able to generate fresh water of 83,000 m^3/year. The cost of water production is about 13.63 USD/m^3 and it can be reduced to 8.74 USD/m^3 if 40% subsidy was included.

Exergy, energy and cost evaluation of solar organic Rankine cycle was carried out by Nafey and Sharaf [167]. The working fluids considered were butane, hexane and toluene for flat plate collector, compound parabolic collector and parabolic trough collector.

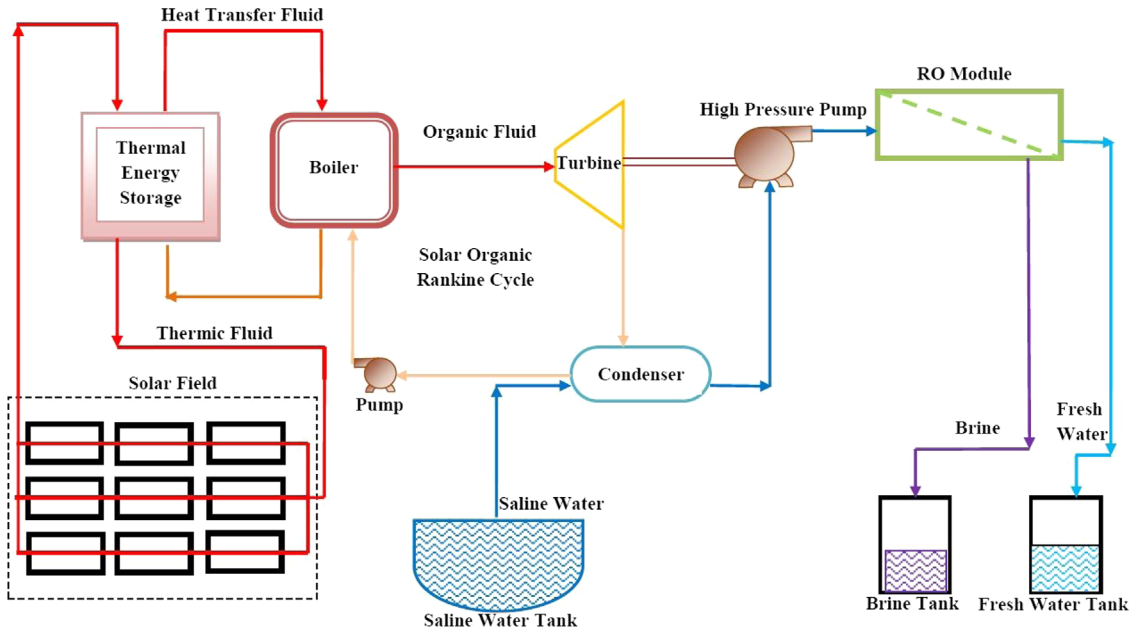

Fig. 19. Solar organic Rankine cycle powered RO unit [164].

The cycle was simulated under saturated and superheated conditions and was compared with the results obtained with water as working fluid. Parabolic trough collectors were found to be more suitable for organic Rankine cycle. Best power output from the system could be was obtained with water and toluene at reduced cost and reduced exergy destruction. Penate and Garcia-Rodriguez [168] compared RO desalination unit powered by solar operated Rankine cycle (with regeneration and superheating) with double cascade solar operated Rankine cycle. Solar field requirement for double cascade system was 23% higher than the solar operated Rankine cycle with regeneration and superheating. This technology was found to be more superior than solar parabolic trough operated multi effect distillation unit which requires additional electricity for the operation of accessories.

Davies [169] proposed a new solar operated steam Rankine cycle which uses two pistons connected by crank mechanism. The steam generated by the collector was used to push the power piston which in turn pushes the pump piston containing feed water against the RO membrane. For feed water with salinity 5000 ppm, the fresh water production was found to be 620 l/d/m^2 and 350 l/d/m^2 for the system operating with parabolic trough collector and linear Fresnel reflector. Attia [170] proposed solar desalination system consisting of solar parabolic dish concentrator with spherical tank at its focal point coupled to a pressure tank which in turn coupled to RO unit. High temperature due to reflection of sun rays by the concentrator causes evaporation of working fluid in the spherical tank which increases the pressure on one side of the pressure tank. This pushes the piston of the pressure tank containing sea water to the other side against the RO membrane as a result fresh water was produced. The fresh water production would be reduced if the required pressure for RO membrane or the salinity of the feed water was increased. The schematic representation of the system is shown in Fig. 20. It could be seen that solar organic Rankine cycle powered RO desalination with parabolic trough collectors unit is more attractive and can be used for standalone large scale operation. Toluene is an attractive working fluid for this system, but safety measures needs to be taken before using it. Finally, solar organic Rankine cycle powered RO desalination unit has the capacity to replace solar powered MED desalination unit.

3.2.2. Solar powered electrodialysis (ED)

Electrodialysis (ED) is the process of removal of salts from saline water and the ED unit consists of large number of compartments filled with saline water and separated by cation and anion exchange membranes. When DC polarity is applied across the cathode and anode, the negative ions passes through the anion exchange membrane and positive ions passes through the cation exchange membranes and these ions gets accumulated in a particular compartment and is discharged out as brine. Reversal of polarity is usually followed every 20 min to prevent deposition of salts in the membranes [171,172]. The operating principle of ED system is shown in Fig. 21a. ED systems are capable of treating the brine disposed from RO plants [173]

The product flow rate from the ED unit is given by [172]

$$Q = \frac{\eta \times I_c \times \mathrm{CP}}{F \times \Delta N} \tag{41}$$

The salt removal % in ED unit is given by,

$$\mathrm{SR} = \frac{(C_f - C_p)}{C_f} \times 100 \tag{42}$$

The salt removal factor for ED unit was found to be 95% and 99% for groundwater and NaCl solution respectively [172].

Lundstrom [174] proposed a ED desalination system which uses the cooling water preheated by concentrated PV system as its feed. The ED system was designed in such a manner that its load can be varied according to the power output from the PV unit thereby the size of the battery was considerably reduced. The water production cost/m^3 for the plant with a PV array cost of 5 USD/W and 10 USD/W was found to be 3.248 USD and 3.6415 USD respectively. The water production cost of gasoline operated ED plant of same capacity was found to be 3.038 USD/m^3. The solar powered ED desalination system is suitable for (a) areas having less or no electric power, (b) areas with no access to low cost fuel supply and (c) areas with abundant sunshine.

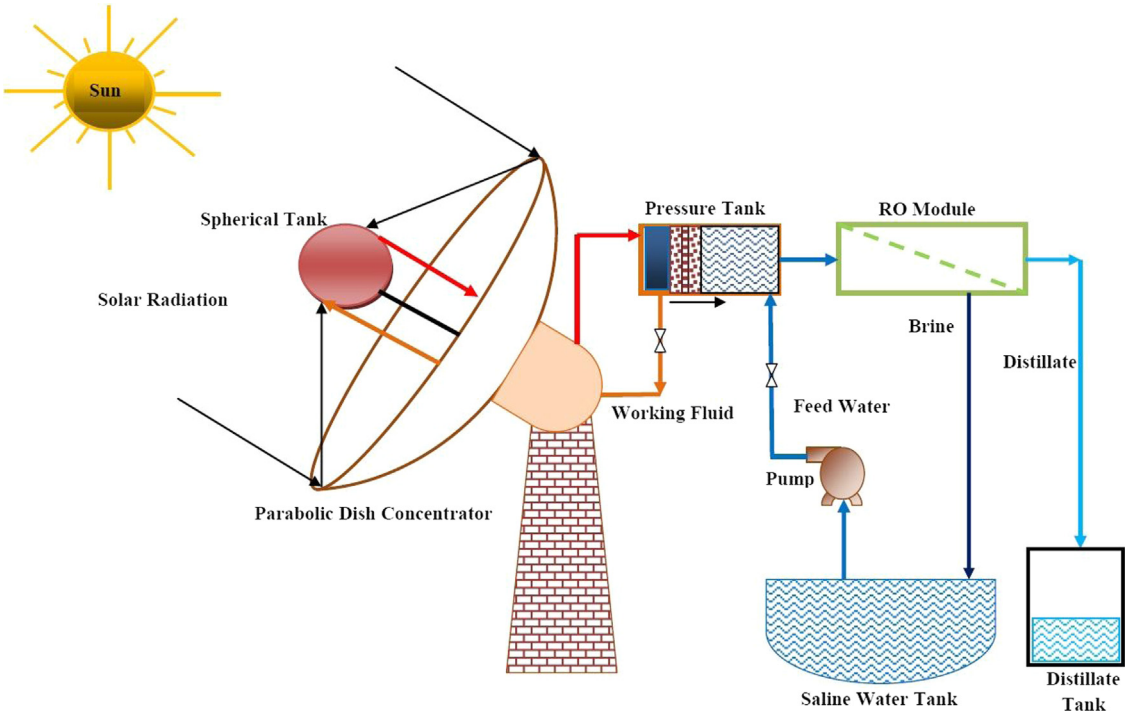

Fig. 20. RO unit using solar energy as pressure source [170].

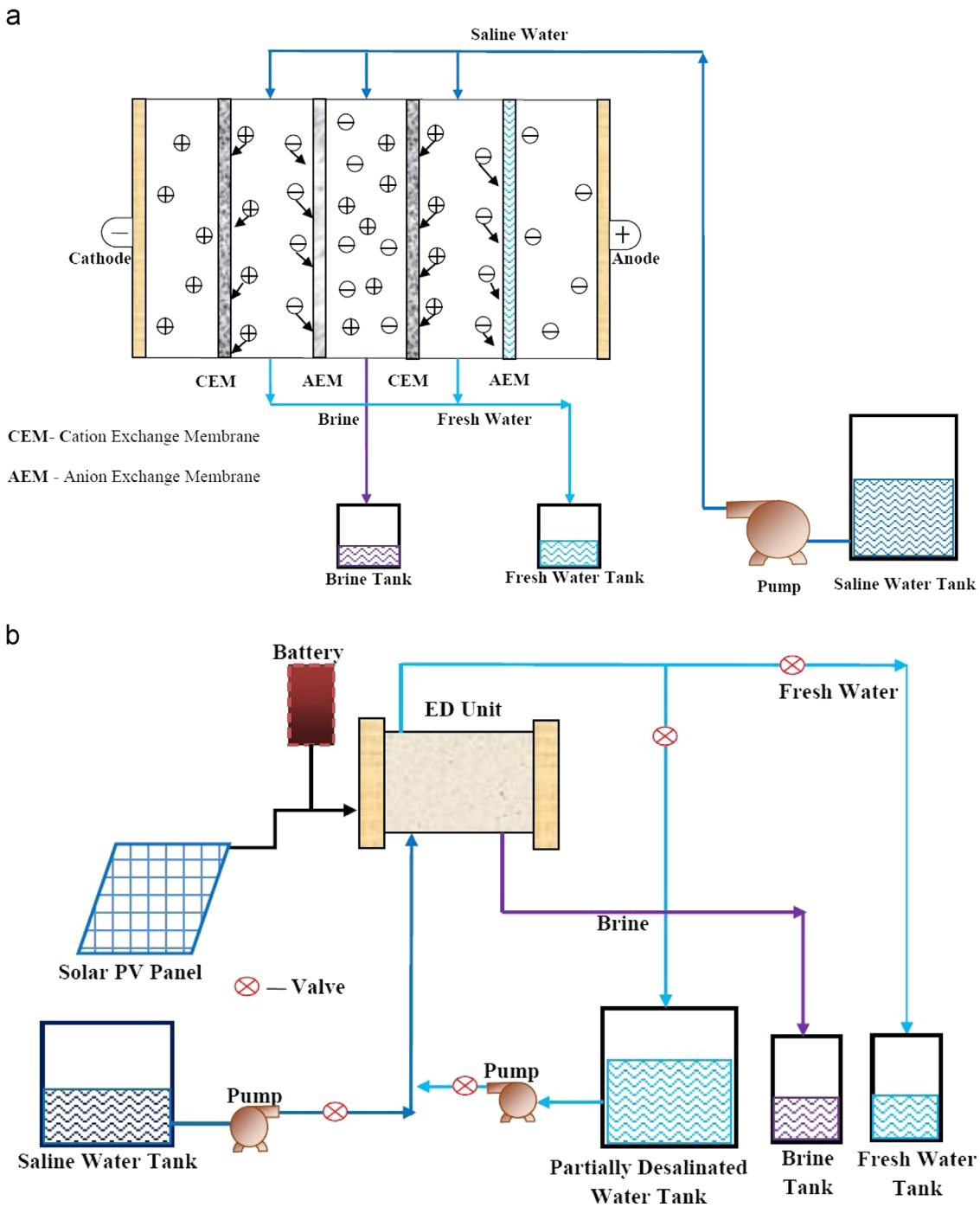

Fig. 21. (a) Operation principle of electrodialysis unit [171] and (b) solar PV powered electrodialysis unit with partially desalinated water storage tank [175].

Kuroda et al. [175] proposed and demonstrated a novel solar PV powered ED sea water desalination plant. The schematic representation of the system is shown in Fig. 21b. During the times of strong solar radiation the large PV power output was used to partially desalinate the feed sea water. The partially desalinated water was desalinated to fresh water during the times of low solar radiation thereby the capacity of battery was reduced.

Batteryless PV powered ED desalination system of capacity 1000 l/d installed at Tanote, Thar Desert, India showed satisfactory performance during one year field test and was found to be reliable for rural and remote locations. The system consists of PV array (450 W) which was manually tracked three times a day (south-east, south, south-west) and one time a month(north–south tilt). The plant was operated every day from 8:30 am to 4:30 pm supplying drinking water to Border Security Forces and local inhabitants [176]. Ishimaru [177] carried out experimental studies with solar PV powered ED desalination unit at Fukue city, Nagasaki. The PV system efficiency and overall system efficiency was found to vary between 6.8–10.5% and 6.0–8.2% respectively. The water production was found to vary between 200 m^3/d and 375 m^3/d and the electric power consumption/m^3 of water produced was found to be lower than the designed value of 1.92 kWh/m^3.

Mathematical modeling of battery less solar PV operated ED unit was studied by Ortiz et al. [178]. The proposed model was capable of predicting the number of PV modules, volume of brackish water needed and variation of concentration for input variables like climatic conditions, stream flow rates and required

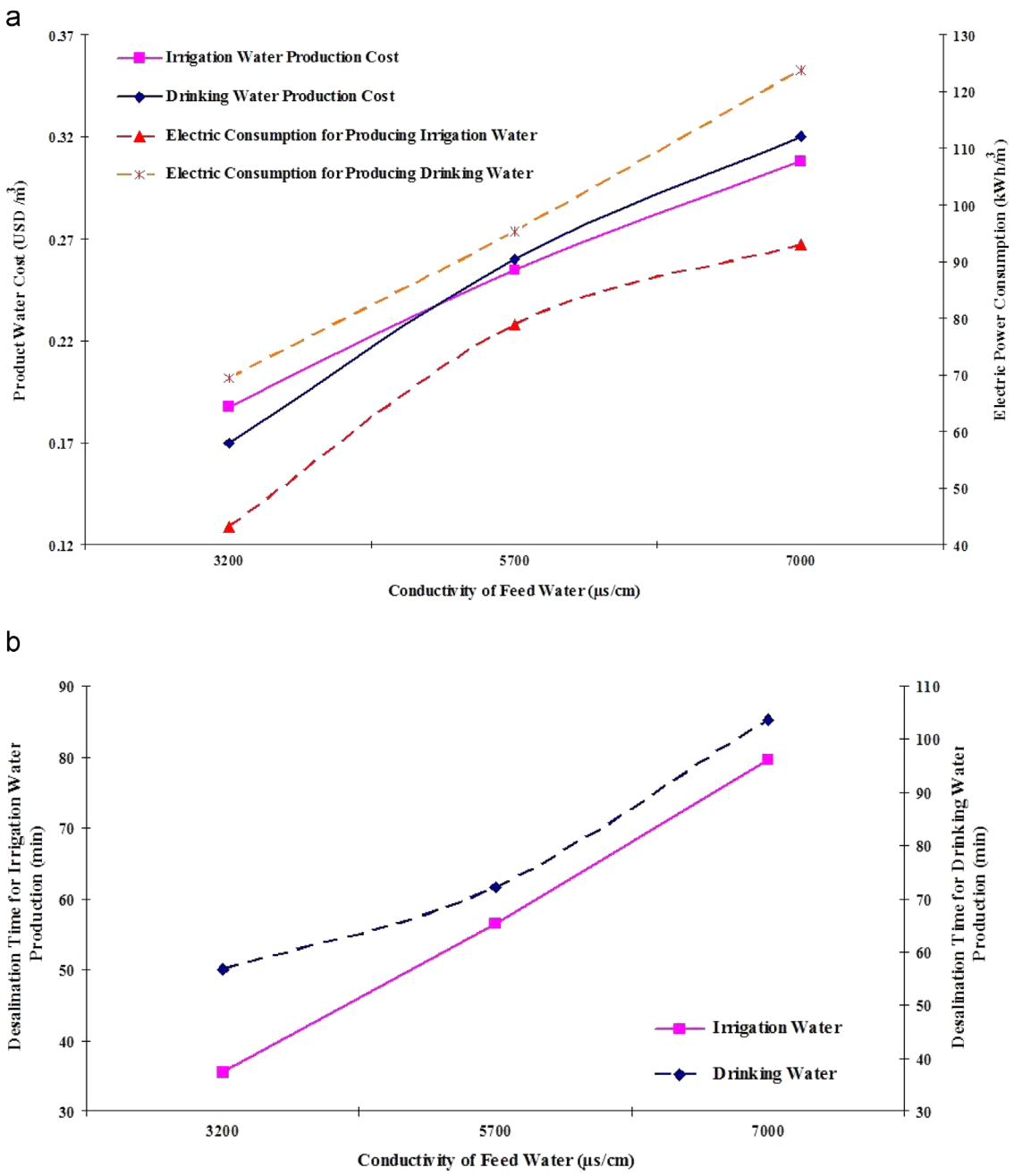

Fig. 22. (a) Effect of feed water salinity on water production and electric power consumption of solar PV powered electrodialysis [179] and (b) effect of feed water salinity on desalination time required by solar PV powered electrodialysis [179].

fresh water. The results of mathematical model were compared with experimental results and were found to be closer [179]. The power consumption, water production cost and desalination time for feed waters of different salinity level is shown in Fig. 22a and b respectively. It could be seen as the conductivity (salinity) of feed increases desalination time, water production cost and power consumption also increases.

3.2.3. *Solar powered membrane distillation (MD)*

Membrane distillation is a separation process in which only vapors are allowed to pass through a porous hydrophobic membrane. The separation is achieved because of the vapor pressure differences between the membrane surfaces. There are mainly four types of membrane distillation processes namely air gap membrane distillation, sweeping gas distillation, direct contact membrane distillation and vacuum membrane distillation [180]. In all these processes the hot feed solution is in direct contact with the membrane surface. The salient features of each membrane distillation process are shown in Fig. 23. A typical solar powered membrane distillation unit is shown in Fig. 24.

The membranes used for membrane distillation process must be highly hydrophobic, highly porous and must have low thermal conductivity. The permeate flux increases with the increase in pore size and reduction in membrane thickness. The operating parameters like feed water temperature, flow rate, thickness of air gap, thickness of membrane, thermal conductivity of membrane, porosity, tortuosity and long term operations have effects on distillate yield [181]. The comparison between different membrane modules is shown in Table 5.

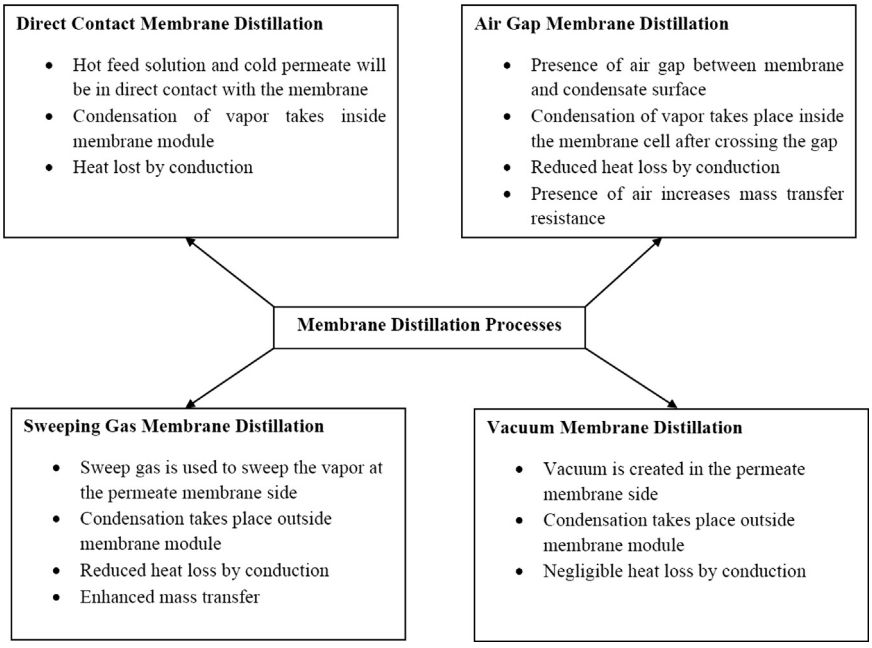

Fig. 23. Types of membrane distillation processes [180].

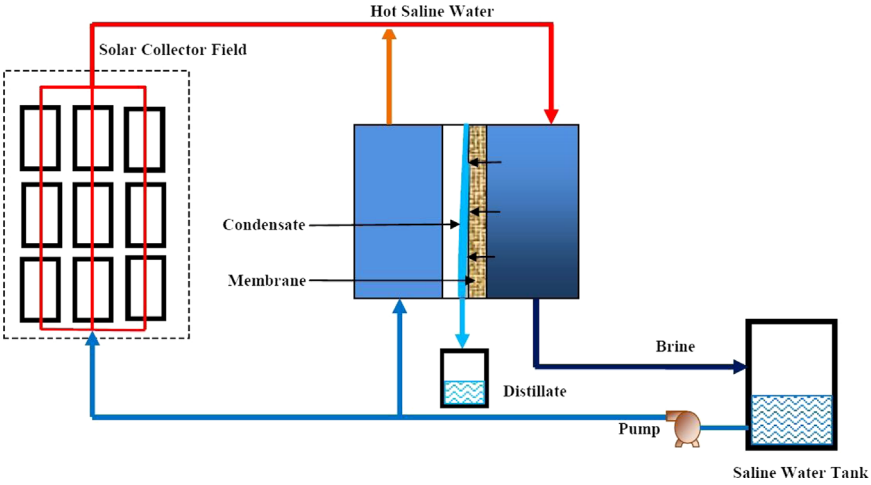

Fig. 24. Solar powered membrane distillation unit [180].

Membrane porosity is given by [181]

$$\varepsilon = 1 - \frac{\rho_m}{\rho_{pol}} \tag{43}$$

Membrane tortusity is given by

$$\tau = \frac{(2-\varepsilon)^2}{\varepsilon} \tag{44}$$

Mass flux transport in DCMD is given by

$$J_W = \frac{1}{P_{air}} \frac{\varepsilon}{\tau\delta} \frac{\mathrm{DPM}_w}{\mathrm{RT}} \Delta P \tag{45}$$

Mass flux transport in AGMD is given by

$$J_W = \frac{\mathrm{PM}_w}{\mathrm{RTP}^*} \left(\frac{D}{((\delta)/(\varepsilon^{3.6}))+1} \right) \Delta P \tag{46}$$

Mass flux transport in VMD is given by

$$J_W = \frac{\pi}{\mathrm{RT}\delta\tau} \left[\frac{2}{3} \left(\frac{8\mathrm{RT}}{\pi M_w} \right)^{1/2} r^3 + \frac{r^4}{8\mu} P_{avg} \right] \Delta P \tag{47}$$

Mass flux transport in SGMD can be calculated from the formula used for DCMD.

Experimental and numerical studies were carried out by different researchers around the globe for evaluating the feasibility of carrying out membrane distillation process using solar energy for producing potable water.

Hogan et al. [182] carried out both simulation and experimental studies on solar powered membrane distillation system producing domestic drinking water in arid rural regions of Australia. The models created using mass and energy balances were coded using FORTRAN and simulated using TRNSYS. Increasing effective membrane area for a constant flow rate and feed temperature increased distillate production rate and maximum heat recovery rate. Comparison of water production costs for different solar powered membrane distillation systems were carried out by Saffarini et al. [183]. For a recovery ratio of 4.4%, the water production cost for direct contact membrane distillation, air gap membrane distillation and vacuum membrane distillation were found to be 12.7 USD/m^3, 18.26 USD/m^3 and 16.02 USD/m^3 respectively. Multi-staging of distillation process, increasing effective

membrane length, decreasing the air gap width and feed channel depth would reduce the water production cost of air gap membrane distillation process.

Summers et al. [184] used theoretical models to compare the energy efficiency of different membrane distillation desalination systems. The comparison was made on the basis of gained output ratio (GOR) which is defined as the ratio of latent heat of evaporation of a unit mass of product water to the amount of energy used by the desalination system to produce unit mass of product. Increased GOR was noticed for direct contact membrane distillation and air gap membrane distillation system by increasing the effective membrane length and feed water inlet temperature. GOR of the vacuum membrane distillation was found to be lower than all other systems and the GOR of the multistage vacuum membrane distillation could be achieved by single stage air gap membrane distillation system and direct contact membrane distillation without the use of additional energy for vacuum pumps. GOR of air gap membrane distillation would be increased if the air gap width is increased. Chang et al. [185] carried out experiments with fully automated solar membrane distillation desalination system which consists of hot and cold fluid thermostat, thermal storage tank, air gap membrane distillation, pumps and energy recovery unit. The hot thermostat simulates the solar absorber using the predefined values for solar radiation. Distillate yield of the system was found to be 0.258 kg/d for sunny day and 0.142 kg/d for cloudy day.

Asadi et al. [186] used membrane distillation process to treat saline oily waste water from Sarkhon gas refinery, Iran. The membrane used was hydrophilic and was made from nonporous polymeric material. Six nonporous black hydrophilic membrane bags (pore size 5–10 Å) filled with saline oily waste water and covered with ethylene tetrafluoroethylene foil were exposed to solar radiation. The water gets heated up and it permeates through the membrane wall and evaporates on the outer surface of the black membrane due to pervaporation which is a combination of membrane permeation and evaporation. The distillate was collected along the sides of the cover foil and was found to be 1.3 l/d/m^2 of membrane area. The process was not found to be economical but the product water quality was found to be better than the quality set by the Iranian Irrigation Board. The properties of Sarkhon gas refinery oily waste saline water and purified water is shown in Table 6. Zwijnenberg et al. [187] studied the solar driven desalination process using membrane pervaporation. The experiments were carried out with sea water from North Sea, de-oiled formation water from Oman oil-well and artificial sea water. The distillate was found to be of high quality and the distillate flux was not affected by feed concentration and fouling.

Five year performance of solar membrane distillation demonstration plant installed in Pozo Izquierdo-Gran Canaria Island (Spain), was found to be satisfactory. Enhanced version of direct contact membrane distillation unit was used for the plant and during the five year operation, three times the membrane modules were replaced. The distillate production was found to vary between 5 and 120 l/d and is of high quality, the specific thermal energy consumption of the plant was in the range of 140–350 kWh/m^3 [188].

Performance of large scale solar MD desalination system using numerical simulation was studied by Kim et al. [189]. The performance ratio and total distillate yield were affected by the fiber length, packing density, feed and permeate inlet temperature and flow rate. The specific thermal energy consumption could be reduced by increasing solar collector area and sea water storage volume but increased specific electric energy consumption was noticed with the increase in solar collector area because of the requirement of high pumping power.

Performance of vacuum membrane distillation coupled with salt gradient solar pond and solar collector was simulated by

Table 5
Comparison of membrane modules [181].

Membrane module	Arrangement	Packing density	Maintenance	Tendency to fouling	Energy consumption
Plate and frame membrane	Membranes and spacers are layered together between two plates	Low	Easy to clean and replace	–	–
Hollow fiber membrane	Bundled hollow fibers are sealed inside shell tube	Very high	Difficult to clean and maintain	High	Low
Tubular membrane	Tube shaped membrane inserted between two cylindrical chambers	Low	Easy to clean	Low	High
Spiral wound membrane	Flat sheet membrane and spacers rolled around a central collector tube	High	–	Average	Medium

Table 6
Properties of the feed oily saline water and the purified water obtained by membrane pervaporation process [186].

	Total dissolved solids (mg/l)	Conductivity (μs/cm)	Chloride (mg/l)	Oil grease (mg/l)
Sarkhon gas refinery waste water	1991	3342	1565	31.1
Purified water	91	150	6.6	1.12

Table 7
Performance of large and small solar powered membrane distillation systems [191,192].

System type	Recover ratio (%)	Gained output ratio	Thermal recovery ratio	Energy consumption (kWh/m^3)	Distillate yield (l/d/m^2)	Conductivity of distillate (μs/cm)
Large scale	Between 2 and 5	0.4–0.7	0.4–1	200–300	2–11	20–250
Small scale	Between 1 and 4	0.3–0.9	1–2	200–300	19	5

Mericq et al. [190]. Four options were considered: (a) membrane distillation unit fed by water from solar pond; (b) membrane distillation unit directly immersed in solar pond; (c) membrane distillation unit fed by water heated using solar collectors and (d) membrane distillation unit fed by water heated by solar collector integrated with membrane distillation unit. The distillate yield obtained by supplying water preheated by solar collectors was found to be high and this technology was found to be simple when compared to others. Even though the cost of water production using solar pond was low the technology was more complex.

Banat et al. [191,192] reported the performance of large autonomous solar driven membrane distillation plant in Aqaba, Jordan and small scale compact solar driven membrane distillation plant in Irbid, Jordan. The performance of the systems is shown in Table 7. The water production cost largely depends on membrane life time and plant life time. The cost of water production by compact unit and large unit was found to be 15 USD/m^3 and 18 USD/m^3 respectively [193]. Exergy efficiency of the compact unit and large unit was found to be 0.01% and 0.05% if the exergy collected by the solar collector is about 0.3% and 0.5% for compact and large unit respectively [194]. Wang et al. [195] studied the potential of solar heated hollow fiber vacuum membrane distillation system for potable water production from underground water in Hangzhou, China. Increased distillate yield was noticed by increasing feed flow rate and feed inlet temperature and reduced energy consumption was noticed by incorporating heat recovery unit.

Banat et al. [196] studied the possibility of producing potable water by integrating solar still with shell and tube type membrane distillation module in which heated brine from solar still was used as feed for membrane distillation unit. The distillate yield increased as brine temperature and flow rate increased. The distillate produced by solar still and membrane distillation unit was found to be 20% and 80% of the total output. Removal of arsenic from contaminated ground water using solar energy driven direct contact membrane distillation horizontal module was studied by Manna et al. [197]. The gained output ratio, thermal recovery ratio and the water flux were found to be 0.9, 0.4 and 90 kg/m^2 h at a feed temperature of 60 °C, feed flow rate of 120 kg/h, permeate flow rate of 150 l/h and arsenic concentration of 396 ppb. The distillate yield decreased with the increase in arsenic content in the feed water.

Numerical modeling and indoor simulation of immediate assisted solar direct contact membrane distillation system in which the feed water would be heated by the absorber attached to the membrane module was done by Chen and Ho [198]. The proposed system consists of a blackened absorber plate between glass and polytetrafluoroethylene membrane and parallel flow was maintained between hot stream and cold stream. Their numerical study was good in agreement with the experimental results and the maximum distillate yield was found to be 4.1 kg/m^2 h. Guillen-Burrieza et al. [199] experimentally evaluated the performance of an air gap membrane distillation solar desalination pilot system developed under MEDESOL project. The temperature of the feed water and its flow rate was found to have more effect on system performance than the temperature and flow rate of cold fluid. The performance ratio of the system was below 1 and it was noticed that multistage three module system was capable of reducing thermal energy consumption.

Guillen-Burrieza et al. [200] experimentally evaluated the performance of two types of air gap membrane distillation module (prototype A and prototype B) having same configurations. In prototype A feed flow occurs through six parallel channels. In prototype B feed flow occurs through two parallel channel and three series channel. Increasing the feed flow rate has positive impact on performance ratio for prototype A and it has negative effect on prototype B. The distillate flux for prototype A and prototype B increased with the increase in inlet feed water temperature and flow rate and the effect of salinity was less pronounced in both the systems. Increasing the number of modules from 1 to 3 reduced external heat input and increased recovery ratio and performance ratio of the system.

Energy consumption and water production cost for different membrane distillation systems was found to vary between 1 and 9000 kWh/m^3 and 0.3 USD/m^3 and 130 USD/m^3 respectively. The cost related with pre-treatment, optimum flow conditions, fouling and membrane life were not available to a satisfactory level. Water production cost using membrane distillation technologies could be reduced by using renewable energy technologies and brine management technologies [201]. Specific energy consumption was found be higher and gained output ratio (GOR) was found to be lower for solar powered membrane distillation systems. Solar powered membrane distillation systems could not compete with other thermal desalination technologies and it could be used in combination with other thermal desalination systems to desalinate hot brine [202]. Ong et al. [203] proposed the concept of integrating multi effect membrane distillation unit with high concentration photovoltaic system to produce potable water by

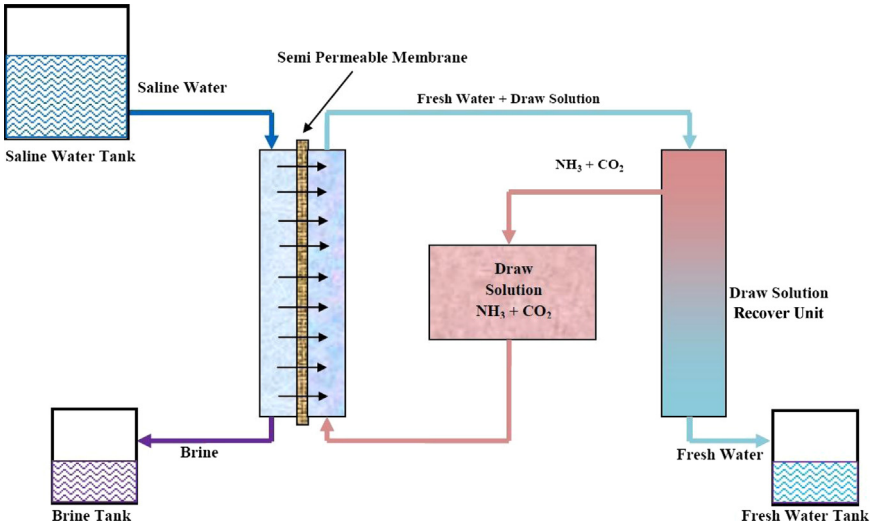

Fig. 25. Forward osmosis unit using NH_3–CO_2 as draw solution. [211].

utilizing the heat carried by the cooling water of concentrated photovoltaic system. Economical operation of solar powered membrane distillation unit could be achieved by heat recovery using external heat exchangers and the yield could be increased by increasing the effective surface area of membrane or by decreasing the flow rate of both feed and permeate [204].

Thermal efficiency of MD unit is given by [201]

$$\varepsilon_T = \frac{J_W A h_{fg}}{Q_m} \tag{48}$$

Energy efficiency of MD unit is given by

$$\varepsilon_E = \frac{J_W A h_{fg}}{E_{in}} \tag{49}$$

Gained output ratio (GOR) is given by

$$\mathrm{GOR} = \varepsilon_T \frac{\Delta T_{MD,module}}{\Delta T_{MD} + \Delta T_{HE}}. \tag{50}$$

3.2.4. Forward osmosis (FO)

Forward osmosis is a process in which the water molecules from saline water moves through the semi-permeable membrane towards the draw solution which is maintained at higher concentration than the feed solution. FO mainly uses osmotic pressure gradient and not the hydraulic pressure gradient [205]. Forward osmosis is being widely studied for desalination, the recent technologies and challenges associated with this can be found in [206].

The water flux transport in FO process is given by [207]

$$J_w = A(\sigma_D \pi_D - \sigma_F \pi_F) \tag{51}$$

Desalination of sea water by direct osmosis using hypertonic glucose solution as draw solution to produce potable water in lifeboats during emergency purposes was carried out successfully by Kravath and Davis [208]. Novel process of using ammonia-carbon dioxide as draw solution for FO was studied by McCutcheon et al. [209]. High water flux was obtained and it was concluded that the conventional RO membrane was not suitable for FO because of higher internal concentration polarization caused by higher concentration of draw solution. The performance of the FO unit can be further improved by improving the membrane to withstand higher internal concentration polarization [210]. The schematic representation of the FO system [211] is shown in Fig. 25.

Zhao et al. [212] compared the desalination of brackish water with salinity 3970 mg/l using forward osmosis–nanofiltration (FO–NF), nano-filtration (NF) and reverse osmosis (RO). The membranes used were flat sheet cellulose triacetate FO membrane NF270 (polyamide TFC) and BW30LE (polyamide TFC) for nanofiltration (NF) and reverse osmosis (RO). Direct NF was not suitable for treating brackish water and RO process requires high pressure of 30 bar. Treating brackish water with FO unit is found to be a better option which uses 1.5 M Na_2SO_4 solution as draw solution. Due to osmotic pressure difference the water molecules from brackish water diffuses into the draw solution resulting in the dilution of Na_2SO_4 solution which was further desalted using nano-filtration to get fresh water.

Phuntsho et al. [213] studied the effect of draw solution and feed solution on water flux in forward osmosis. The draw solution was KCL solution of concentration varying from 0.5 to 3.0 M. The feed solution of NaCl solution (5 g/l NaCl) prepared in deionised water resembled brackish water. The experiments were carried out by varying the temperature of feed and draw solution between 25 °C and 45 °C. The membrane used was cellulose triacetate forward osmosis membrane. It was noted that the water flux increases with the increase in draw solution concentration and temperature. The effect of heating the draw solution from 25 °C to 45 °C caused 21% increase in flux while heating of feed solution caused only 15% increase in flux. The effect of draw solution concentration and feed water and draw solution temperature on water flux is shown in Table 8.

Li et al. [214] carried out investigation of composite polymer hydrogel as draw agent for forward osmosis. Composite polymer hydrogel was prepared by incorporating carbon particles and the size of the prepared hydrogels varies between 100–200 μm and 500–700 μm. The prepared hydrogel was placed on the active side of the semi-permeable membrane and NaCl solution was used as feed solution. The water from feed solution passes through the membrane and it gets adsorbed by the polymer hydrogel which makes it to swell and the water can be recovered by external

Table 8
Effect of temperature of draw solution and brackish water on water flux for different draw solution concentration [213].

Draw solution concentration (M)	Water flux (μm/s)			
	DS25 °C–BW25 °C	DS35 °C–BW25 °C	DS25 °C–BW35 °C	DS45 °C–BW45 °C
1.0	2.4	2.6	2.4	3.4
3.0	4.5	4.8	4.7	7

DS – draw solution and BW – brackish water.

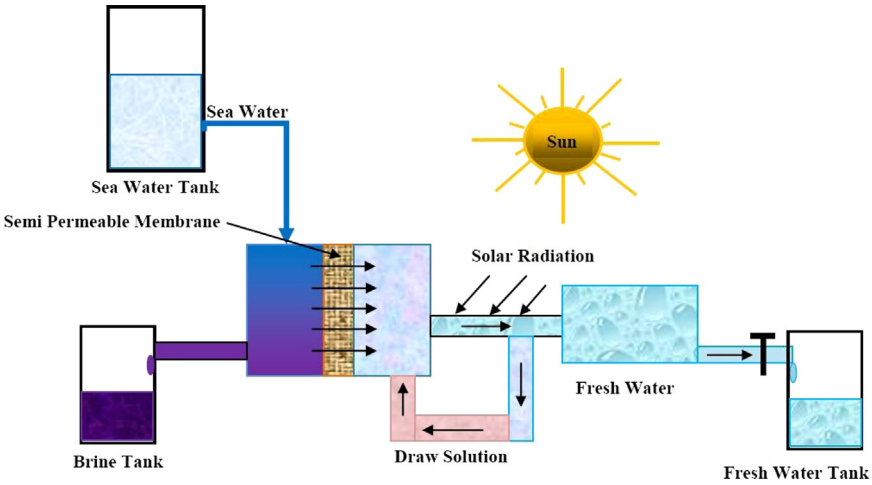

Fig. 26. Forward osmosis unit proposed by Trevi systems [217].

Table 9
Distinct features of in-direct solar desalination systems (membrane processes).

Solar PV powered RO [144,146,155]	**Solar thermal powered RO** [159]	**Electrodialysis** [219]
Ease of operation	Low temperature energy is used	High water recovery
Flexibility in capacity expansion	Mechanical work is directly used to run RO pump with no loss in efficiency	Membranes have longer life because of better stability
Operation in ambient temperature	Low operating and maintenance cost	Reduced membrane fouling or scaling
Can be built as portable or compact unit	Environmental friendly due to absence of batteries	Less raw water pre-treatment is required
Highly suitable for treating brackish water and ground water	Non-skilled labor can be employed	Easy start up and shut down of the plant
Low power consumption	Flexible operation	Can be operated with DC mode hence no inverter is needed hence reduced losses
Membranes usually have short life time	System is safe, since no electricity is involved	Operation at low pressures
Pre-treatment of feed water is required		Non-ionic substances and micro-organisms remain in the product water
Biological fouling of membrane is possible		Reversal of polarity is needed for every 20 min to prevent salt deposition on the membranes
		Energy consumption and product water cost increases with salinity of feedwater

Table 10
Distinct features of in-direct solar desalination systems (membrane processes).

Membrane distillation [180,181,220,221]	**Forward osmosis** [205]
Pipe lines are thinner due to the absence of high pressure	Operation under low or no hydraulic pressure
Reduced leakage compared to RO	High salt rejection
Highly saline feed can be treated	Less membrane fouling
Operation is simpler compared to RO	Equipment is simple
Feed water pre-treatment is not necessary	Membrane needs less support
System efficiency is independent of feedwater salinity	Low energy use and low operating temperature
Low temperature operation	Lack of efficient draw solution recovery process
Membrane wetting	Lack of high performance membrane
Large membrane surface area is required because of low driving force	
Membranes are expensive	

stimuli like solar radiation etc. The water flux decreased with the increase in size of polymer hydrogel and with the increase in feed solution concentration. The performance of cellulose triacetate membrane (FO) was better than thin film polyamide RO membrane because of hydrophobicity of RO membrane and increased thickness of RO membrane.

The swelling ratio of polymer hydrogels is given by [214]

$$\mathrm{SWR} = \frac{W_s - W_d}{W_d} \tag{52}$$

The water flux obtained is given by

$$F = \frac{V}{A \times t} \tag{53}$$

Khaydarov et al. [215] developed a direct osmosis desalination system of capacity 1 m^3/h which uses diethyl ether solution (100 ml/l) as draw solution, RE-1812-LP reverse osmotic membrane and water from Aral sea region as feed solution in which solar energy was used to heat the dilute draw solution to separate the water from diethyl ether. The energy consumption of this unit is 0.5 kWh/m^3 in comparison with 2–5 kWh/m^3 for RO and 2–4 kWh/m^3 for MSF and MED. The system showed shorter life time due to the damage of the membrane caused by diethyl ether. Commercial solar FO system has been developed by Trevi systems uses a novel draw solution (RTS-2300). The osmotic driving force of draw solution was over 5000 psi and as a result membrane of less surface area is sufficient for treating feed waters [216]. The schematic representation of their system [217] is shown in Fig. 26. The energy consumption of forward osmosis system is lower than the reverse osmosis system of same capacity [218]. The distinct features of various in-direct solar desalination systems (membrane process) are shown in Tables 9 and 10.

4. Discussion

In previous sections, different types of solar based desalination systems, their advantages and disadvantages have been discussed. The review on desalination systems will be incomplete if the problems associated with desalination units and its solutions are not discussed. This section deals with the discussion on problems associated with desalination units and its solution.

4.1. Corrosion and scaling in desalination units

In solar based desalination systems the cost of materials and its maintenance occupy a major part of the capital cost and variable cost. Hence, proper selection of corrosion free materials will result in increased system reliability and life time which is highly needed for remote and rural applications. The non-condensable gases released during flashing or evaporation in thermal desalination systems causes corrosion of heat transfer surfaces resulting in contamination of distillate with Cu and Ni ions. Carbon steel replaced by copper–nickel alloys (10% Ni–90% Cu and 30% Ni–70% Cu) for heat transfer surfaces in distillation units has prevented the contamination of distillate by metal ions and has reduced the weight of the units. Occurrence of corrosion in RO units will cause blockage of membrane passages and these problems can be avoided if high grade stainless steel or duplex steel materials are used [222]. The life time of thermal desalination units can be increased to 50 years if corrosion free materials like stainless steel, duplex steel and titanium are used [223]. The corrosion occurring in saline water intake, discharge and distillate water discharge units can be avoided by using fiber glass pipes which can withstand high pressure and temperature of 50 bar and 110 °C [224].

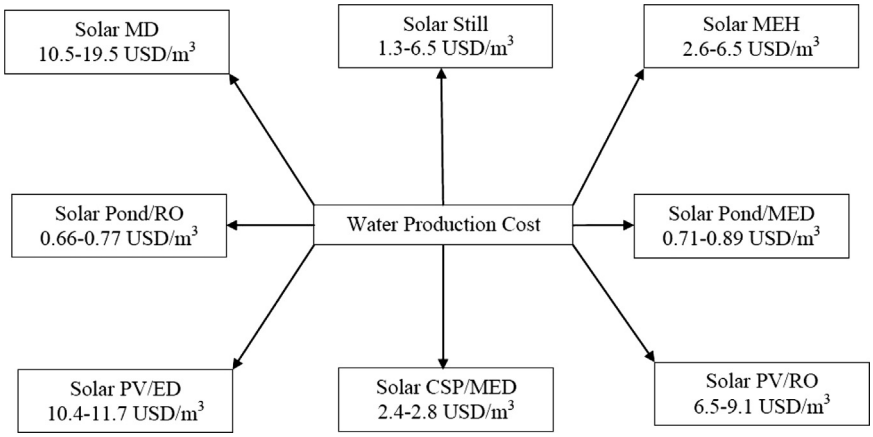

Fig. 27. Water production cost of solar powered desalination units [233].

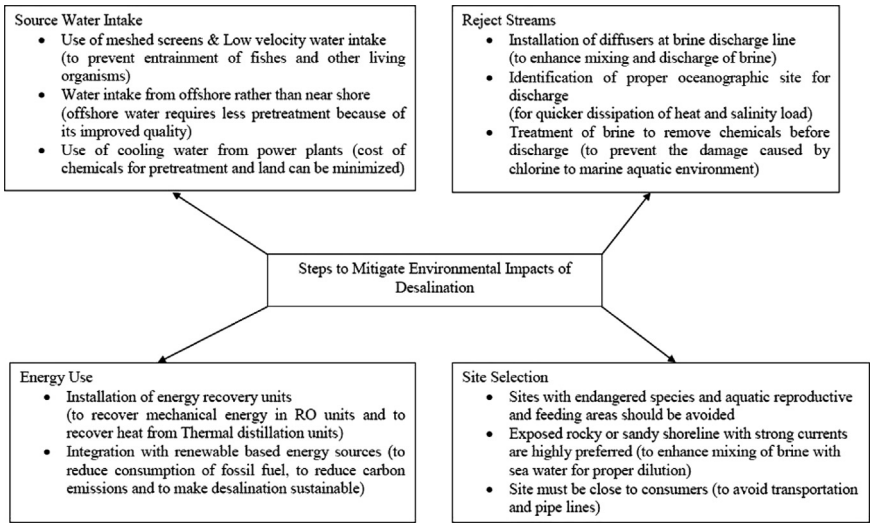

Fig. 28. Mitigation of environmental impacts of desalination units [236].

Scaling is caused due to the deposition of $CaCO_3$ and $Mg(OH)_2$ present in sea water over the tube surfaces of evaporator and condenser. The scales are multilayered and are of varying composition. The condenser units are generally affected by pitting corrosion, fatigue corrosion and circumferential cracks [225]. The HCO_3^- ion in water plays an important role in scale formation.At moderate temperature decomposition of HCO_3^- ion occurs as per Eq. (54)

$$2HCO_3^- = CO_3^{2-} + CO_2 + H_2O \quad (54)$$

to cause precipitation of $CaCO_3$At high temperatures CO_3^{2-} ion hydrolyzes as per Eq. (55)

$$CO_3^{2-} + H_2O = 2OH^- + CO_2 \quad (55)$$

causing precipitation of $Mg(OH)_2$.

4.2. Fouling of desalination membranes

Fouling of RO membranes is caused due to concentration polarization which is defined as the presence of rejected species along the membrane surface at a concentration higher than the concentration of bulk feed solution. Fouling results in reduced flux output and permeate of very poor quality. Fouling in RO membrane is caused by (1) inorganic compounds, (2) particulate matter and (3) organic compounds (bacterial growth). The tendency of membrane fouling can be reduced by (1) direct method (promoting turbulence, periodic depressurization, flow reversal, precoating of membrane surface and modification of membrane polymer structure), (2) modification of membrane configuration and operating conditions, (3) regular membrane cleaning and (4) pretreatment of feed [226].

Fouling of MD membranes are mainly caused due to deposition of $CaCO_3$ and $CaSO_4$ which causes 50% reduction in process efficiency. Fouling rate in MD membranes can be reduced by (1) increasing the feed flow rate, (2) lowering feed temperature, (3) partial cleaning of fouling layer (complete removal of the layer may cause wettability of hydrophobic membrane and may result in scaling in membrane pores). The fouling layer in MD membrane is of porous type (causes reduced mass transfer because of increased temperature resistance) and non-porous type (increased mass transfer resistance leading to zero permeate flux) [227]. Because of reduced pressure operation of FO compared to RO the scale layers are loosely packed and can be easily cleaned. The fouling in FO membranes can be reduced by (1) selection of proper draw solution and (2) increasing cross flow velocity [228,229].

4.3. Water production cost

The water production cost of desalination units depends on (1) *capital cost*: cost of land, cost of equipments and installation cost

Table 11
Performance comparison of desalination technologies.

Desalination technology	Plant capacity (m^3/d)	Specific energy consumption (kWh/m^3)	Gain output ratio/performance ratio (GOR/PR)	Efficiency (%)	Recovery ratio (%)
Direct desalination					
Solar still [7,201,233]	< 100	640	< 1	30–40	NA
Solar humidification–dehumidification [63,233]	1–100	31.1	0.5–2.75 (GOR)	40–58	
Solar chimney integrated desalination [69,71]	69,462–92,616 tons/a	NA	NA	55.35	NA
	3807.1 kg/s	NA	NA	46.0	NA
Indirect desalination thermal process					
Solar multi-stage flash [4,6,76,105]	0.009–10	< 144	6.5–8.0 (GOR,12 stages) 1.7–3.3 (PR,4 stage) 0.7–0.9 (PR, single stage)	NA	0.6–6
Solar multi effect distillation [6]	20–3000	2.5–8.0 (electric) 50–194 (thermal)	9.3–10.7 (GOR, 14 effect) 12.4 (GOR, 18 effect) 11.0 (PR, 14 stage + adsorption heat pump)	NA	6–38
Solar mechanical vapor compression [99]	120	14–25	NA	NA	44
Freeze desalination [6]	48–178	108.0	NA	NA	NA
Adsorption desalination [127,131]	NA	38.01–63.95	10.16–17.10 (PR)	NA	NA
	10	NA	0.61 (PR)	NA	NA
Natural vacuum desalination [109]	13.9 kg/d	416.0	1.42 (PR)	NA	NA
Multi effect regeneration system [103]	135 kg/h	NA	2.35 (PR)	NA	NA
Multi stage evacuated system [104]	53.2 kg/d	NA	NA	53.9	NA
Membrane processes					
Solar electrodialysis [171,172,177]	1–200	0.8–1.0	NA	8.5	20–95
Solar reverse osmosis (organic Rankine cycle based) [156,159,168]	1000–5000	2.1–3.0	NA	20–25	20
Solar reverse osmosis (PV based) [6,233]	< 100	1.5–6.0	NA	NA	10–51
Solar membrane distillation [6,201]	0.5–29.75 l/m^2h	1.2–9079.5	0.5–8.1 (GOR)	NA	3–5
Forward osmosis [7,205,208]	1 m^3/h	1.0	NA	NA	NA
	NA	0.25–0.84	NA	NA	NA

NA – not available.

and (2) *operating cost*: cost of energy, maintenance and replacement cost. The energy cost and capital cost occupies nearly 81% of total water production cost of conventional RO units. The water production cost of MD unit will be lower than RO unit if waste heat is available. In case of thermal desalination units (MSF and MED), the cost of evaporator and condenser units contribute 50% of water production cost. The cost of water production from VC units are higher and can be made equivalent to MED or MSF by integrating VC with MED or MSF units [230,231]. Brackish water of salinity around 2000 ppm can be treated at a cost lower than RO units by solar PV powered ED units [232]. The energy cost of the desalination units can be reduced by integrating desalination units with power plants or with renewable energy sources [233]. The water production cost of solar powered desalination units is shown in Fig. 27.

4.4. Desalination and environment

Desalination plants play an important role in satisfying the fresh water demands of huge population around the globe but these technologies also have some negative impacts on environment. The negative impacts are mainly due to (1) leakage of sea water intake pipeline causing damage to aquifers, (2) brine and pre-treatment chemical disposal affecting marine ecosystem, (3) huge energy demands causing increased green house gas emissions. High temperature and high dense brine disposal affects corals and grass prairies of sea bed which are habitat to fishes and invertebrates [234]. The reduction in green house gases can be achieved by integrating desalination units with renewable energy and by using energy recovery devices as in case of RO and multi effect systems. Impacts arising due to disposal of brine can be reduced by discharging brine in hydrodynamic turbulent conditions and by using the brine for aquaculture and irrigation (salt resistant crop cultivation) by reducing its salinity [235]. The steps to be followed to reduce the impact of desalination on environment [236] is shown in Fig. 28.

A comprehensive performance analysis of all desalination technologies in terms of various performance parameters such as specific energy consumption, performance ratio, efficiency and recovery ratio is illustrated in Table 11. It could be seen from Table 11 that the energy consumption of membrane process is lower than other processes. Forward osmosis process is found be a more promising membrane desalination technique with minimal energy consumption followed by electrodialysis and reverse osmosis. The performance of thermal systems is found to be increased by increasing the number of effects (i.e. utilization of latent heat of condensation) and by cogeneration and it could be justified from the efficiency of solar chimney (both distilled water and power are produced) and multi effect desalination units (latent heat of condensation is utilized). The energy consumption of solar still is found to be larger due to loss of heat of condensation to the ambient.

4.5. General comments on solar operated desalination units

- Solar stills are cheap but occupies large area and are suitable only for small scale water production.
- Combined power and potable water production with solar chimney integrated is attractive but it could be possible only if large amount of waste lands or coastal regions are available.
- MSF, MED and VC systems are more matured technologies and can be easily coupled with solar energy for large scale water production but their long term operating nature when integrated with solar energy systems has not been reported.
- Natural vacuum solar desalination system can be integrated with tall buildings and mountains in remote areas.

- Adsorption desalination which produces both potable water and chilling effect is found to be more suitable for areas (food processing and dairy processing) where both refrigeration and potable water are required. Integration of the system with solar is possible and more on field tests are required to prove its long term performance.
- Theoretically freeze desalination requires less energy than other desalination systems but are more costly and their studies integrated with solar energy is much limited.
- For large capacity plants solar based humidification–dehumidification requires large number of stages for efficient operation which increases cost of the system hence this system is suitable for low capacity decentralized mode of operation.
- RO plants are much developed and could be easily coupled with PV panels. But to make the system more attractive much research must be dedicated to the development of long life membranes which would reduce the maintenance cost and water production cost.
- Solar organic Rankine cycle powered RO systems are more efficient than solar powered MED systems and are also suitable for large scale stand alone operation. However, safety related issues must be studied.
- MD and FO desalination systems can be operated by waste heat or solar thermal energy and can be used in combination with other desalination technologies to treat the discarded brine. Development of efficient membranes and draw solutions for FO is still a big challenge.
- Use of corrosion free alloy materials can increase the life of desalination unit and can reduce the maintenance and water production cost.
- Rejected brine can be utilized for aquaculture and irrigation of salt tolerant crops after reducing their salinity by blending them with feed water.

5. Conclusion

Solar energy driven desalination units can cut off carbon emissions and can provide desalinated water in a sustainable way with minimal impacts on environment and are highly suitable for remote and rural areas where provision for power supply and fresh water pipe lines are not possible. Currently, solar based desalination units are treating only brackish or saline water hence more research is needed on treatment of waste water using these units thereby considerable exploitation of ground water can be stopped. Identification and development of novel corrosion free materials and long life membranes are needed for enhanced and reliable operation of these units. Brine disposal is a big problem in every desalination industry hence proper ways to extract minerals from brine and reuse of brine for aquaculture and irrigation needs to be practiced. Solar energy has the capability to make desalination industry greener and any development in solar thermal collectors and PV panels will be more beneficial to desalination industries.

Acknowledgments

The financial support provided by the Department of Science and Technology (DST, Government of India), New Delhi through the research project (Grant No: DST/TM/SERI/2k12/16(G)) is duly acknowledged.

References

[1] ⟨http://en.wikipedia.org/wiki/Water_distribution_on_Earth⟩ [last accessed 02.02.13].
[2] ⟨http://www.unwater.org/statistics_use.html⟩ [last accessed 02.02.13].
[3] ⟨http://hbfreshwater.com/desalination-101/desalination-worldwide⟩ [last accessed 02.02.13].
[4] Kalogirou S. Seawater desalination using renewable energy sources. Prog Energy Combust Sci 2005;31:242–81.
[5] Roberts DA, Johnston EL, Knott NA. Impacts of desalination plant discharges on the marine environment: a critical review of published studies. Water Res 2010;44:5117–28.
[6] Ali MT, Fath HES, Armstrong PR. A comprehensive techno-economical review of indirect solar desalination. Renew Sustain Energy Rev 2011;15:4187–99.
[7] Subramani A, Badruzzaman M, Oppenheimer J, Jacangelo JG. Energy minimization strategies and renewable energy utilization for desalination: a review. Water Res 2011;45:1907–20.
[8] Eltawil MA, Zhengming Z, Yuan L. A review of renewable technologies integrated with desalination systems. Renew Sustain Energy Rev 2009;13:2245–62.
[9] ⟨http://www.medrc.org/index.cfm⟩ [last accessed 02.02.13].
[10] Chaibi MT. An overview of solar desalination for domestic and agriculture water needs in remote arid areas. Desalination 2000;127:119–33.
[11] Garcia-Rodriguez L, Palmero-Marrero AI, Gomez-Camacho C. Comparison of solar thermal technologies for applications in seawater desalination. Desalination 2002;142:135–42.
[12] Qiblawey HM, Banat F. Solar thermal desalination technologies. Desalination 2008;220:633–44.
[13] Voropoulos K, Mathioulakis E, Belessiotis V. A hybrid solar desalination and water heating system. Desalination 2004;164:189–95.
[14] Dev R, Tiwari GN. Annual performance of evacuated tubular collector integrated solar still. Desalin Water Treat 2012;41:204–23.
[15] Omara ZM, Eltawil MA. Hybrid of solar dish concentrator, new boiler and simple solar collector for brackish water desalination. Desalination 2013;326:62–8.
[16] El-Sebaii AA, Aboul-Enein S, Ramadan MRI, Khallaf AM. Thermal performance of an active single basin solar still (ASBS) coupled to shallow solar pond (SSP). Desalination 2011;280:183–90.
[17] Eltawil MA, Zhengming Z. Wind turbine-inclined still collector integration with solar still for brackish water desalination. Desalination 2009;249(2):490–7.
[18] Al-Garni AZ. Effect of external reflectors on the productivity of solar still during winter. J Energy Eng 2013. http://dx.doi.org/10.1061/(ASCE)EY1943-7897.0000135.
[19] Abdel-Rehim ZS, Lashine A. A study of solar desalination still combined with air-conditioning system. ISRN Renew Energy 2012;2012:1–7.
[20] Arunkumar T, Denkenberger D, Ahsan A, Jayaprakash R. The augmentation of distillate yield by using concentrator coupled solar still with phase change material. Desalination 2013;314:189–92.
[21] Tiwari GN, Singh SK, Bhatnagar VP. Analytical thermal modeling of multi-basin solar still. Energy Convers Manag 1993;34(12):1261–6.
[22] Patel SG, Bhatnagar S, Vardia J, Ameta SC. Use of photocatalysts in solar desalination. Desalination 2006;189:287–91.
[23] Al-Abbasi MA, Al-Karaghouli AA, Minasian AN. Photochemically assisted solar desalination of saline water. Desalination 1992;86:317–24.
[24] Jones JA, Lackey LW, Lindsay KE. Effects of wind and choice of cover material on the yield of a passive solar still. Desalin Water Treat 2014;52:48–56.
[25] Phadatare MK, Verma SK. Effect of cover materials on heat and mass transfer coefficients in a plastic still. Desalin Water Treat 2009;2:254–9.
[26] Sellami MH, Bouguettaia H, Bechki D, Zeroual M, Kachi S, Boughali S, Bouchekima B, Mahcene H. Effect of absorber coating on the performance of a solar still in the Ouargla (Algeria). Desalination and Water Treatment 2013;51:6490–7.
[27] Aybar HS, Assefi H. Simulation of a solar still to investigate water depth and glass angle. Desalin Water Treat 2009;7:35–40.
[28] Kabeel AE, Hamed AM, El-Agouz SA. Cost analysis of different solar still configurations. Energy 2010;35:2901–8.
[29] Tiwari GN, Yadav YP, Eames PC, Nortan B. Solar distillation systems: the state of the art in design development and performance analysis. Renew Energy 1994;5(Part I):509–16.
[30] Manikandan V, Shanmugasundaram K, Shanmugam S, Janarthanana B, Chandrasekaran J. Wick type solar stills: a review. Renew Sustain Energy Rev 2013;20:322–35.
[31] Setoodeh N, Rahimi R, Ameri A. Modeling and determination of heat transfer coefficient in a basin solar still using CFD. Desalination 2011;268:103–10.
[32] Khalifa AJN, Hamood AM. Performance correlations for basin type solar stills. Desalination 2009;249:24–8.
[33] Parekh S, Farid MM, Selman JR, Al-Halaj S. Solar desalination with a humidification–dehumidification technique – a comprehensive technical review. Desalination 2004;160:167–86.
[34] Narayan GP, Sharqawy MH, Summers EK, Lienhard JH, Zubair SM, Antar MA. The potential of solar-driven humidification–dehumidification desalination for small-scale decentralized water production. Renew Sustain Energy Rev 2010;14:1187–201.
[35] Hou S, Ye S, Zhang H. Performance optimization of solar humidification–dehumidification desalination process using Pinch technology. Desalination 2005;183:143–9.
[36] Hou S. Two-stage solar multi-effect humidification dehumidification desalination process plotted from pinch analysis. Desalination 2008;222:572–8.

[37] Farzad S, Behzadmehr A. Analysis of a solar desalination unit with humidification–dehumidification cycle using DoE method. Desalination 2011;278:70–6.
[38] Yamali C, Solmus I. A solar desalination system using humidification–dehumidification process: experimental study and comparison with the theoretical results. Desalination 2008;220:538–51.
[39] Zamen M, Amidpour M, Soufari SM. Cost optimization of a solar humidification–dehumidification desalination unit using mathematical programming. Desalination 2009;239:92–9.
[40] Hou S, Zeng D, Ye S, Zhang H. Exergy analysis of the solar multi-effect humidification–dehumidification desalination process. Desalination 2007;203:403–9.
[41] Al-Hallaj S, Parekh S, Farid MM, Selman JR. Solar desalination with humidification-dehumidification cycle: review of economics. Desalination 2006;195:169–86.
[42] Farid M, Al-Hajaj AW. Solar desalination with a humidification–dehumidification cycle. Desalination 1996;106:427–9.
[43] Nawayseh NK, Farid MM, Omar AA, Al-Hallaj SM, Tamimi AR. A simulation study to improve the performance of a solar humidification–dehumidification desalination unit constructed in Jordan. Desalination 1997;109:277–84.
[44] Al-Hallaj S, Farid MM, Tamimi AR. Solar desalination with a humidification–dehumidification cycle: performance of the unit. Desalination 1998;120: 273–80.
[45] Dai YJ, Zhang HF. Experimental investigation of a solar desalination unit with humidification and dehumidification. Desalination 2000;130:169–75.
[46] Dai YJ, Wang RZ, Zhang HF. Parametric analysis to improve the performance of a solar desalination unit with humidification and dehumidification. Desalination 2002;142:107–18.
[47] Garg HP, Adhikari RS, Kumar R. Experimental design and computer simulation of multi-effect humidification (MEH)–dehumidification solar distillation. Desalination 2002;153:81–6.
[48] Fath HES, Ghazy A. Solar desalination using humidification–dehumidification technology. Desalination 2002;142:119–33.
[49] Fath HES, El-Sherbiny SM, Ghazy A. Transient analysis of a new humidification-dehumidification solar still. Desalination 2003;155:187–203.
[50] Goosen MFA, Sablani SS, Paton C, Perret J, Al-Nuaimi A, Haffar I, et al. Solar energy desalination for arid coastal regions: development of a humidification–dehumidification seawater green house. Sol Energy 2003;75:413–9.
[51] Nafey AS, Fath HES, El-Helaby SO, Soliman A. Solar desalination using humidification–dehumidification processes. Part II. An experimental investigation. Energy Convers Manag 2004;45:1263–77.
[52] Chafik E. Design of plants for solar desalination using the multi-stage heating/humidifying technique. Desalination 2004;168:55–71.
[53] Houcine I, Amara MB, Guizani A, Maalej M. Pilot plant testing of a new solar desalination process by a multiple-effect-humidification technique. Desalination 2006;196:105–24.
[54] Orfi J, Galanis N, Laplante M. Air humidification–dehumidification for a water desalination system using solar energy. Desalination 2007;203:471–81.
[55] Yuan G, Zhang H. Mathematical modelling of a closed circulation solar desalination unit with humidification–dehumidification. Desalination 2007;205:156–62.
[56] Zhani K, Bacha HB. Experimental investigation of a new solar desalination prototype using the humidification–dehumidification principle. Renew Energy 2010;35:2610–7.
[57] Mohamed AMI, El-Minshawy NA. Theoretical investigation of solar humidification–dehumidification desalination system using parabolic trough concentrators. Energy Conserv Manag 2011;52:3112–9.
[58] Yuan G, Wang Z, Li H, Li X. Experimental study of a solar desalination system based on humidification–dehumidification process. Desalination 2011;277:92–8.
[59] Wang Jun-hong, Gao Nai-yun, Deng Y, Li Yong-li. Solar power-driven humidification–dehumidification (HDH) process for desalination of brackish water. Desalination 2012;305:17–23.
[60] Alnaimat F, Klausner JF. Solar diffusion driven desalination for decentralized water production. Desalination 2012;289:35–44.
[61] A.M.A. Dayem. Experimental and numerical performance of a multi-effect condensation–evaporation solar water distillation system. Energy 2006;31: 2710–27.
[62] Al-Enezi G, Ettouney H, Fawzy N. Low temperature humidification–dehumidification–desalination process. Energy Convers Manag 2006;47:470–84.
[63] Zhani K. Solar desalination based on multiple effect humidification process: thermal performance and experimental validation. Renew Sustain Energy Rev 2013;24:406–17.
[64] El-Agouz SA, Abugderah M. Experimental analysis of humidification process by air passing through seawater. Energy Convers Manag 2008;49:3698–703.
[65] El-Agouz SA. Desalination based on humidification–dehumidification by air bubbles passing through brackish water. Chem Eng J 2010;165:413–9.
[66] El-Agouz SA. A new process of desalination by air passing through seawater based on humidification–dehumidification process. Energy 2010;35: 5108–14.
[67] Sangi R. Performance evaluation of solar chimney power plants in Iran. Renew Sustain Energy Rev 2012;16:704–10.
[68] Cao F, Li H, Zhang Y, Zhao L. Numerical simulation and comparison of conventional and sloped solar chimney power plants: the case of Lanzhou. Sci World J 2013:1–8. http://dx.doi.org/10.1155/2013/852864.
[69] Lu Zuo, Zheng Y, Li Z, Sha Y. Solar chimneys integrated with sea water desalination. Desalination 2011;276:207–13.
[70] Lu Zuo, Yuan Y, Li Z, Zheng Y. Experimental research on solar chimneys integrated with seawater desalination under practical weather conditions. Desalination 2012;298:22–33.
[71] Zhou X, Bo Xiao, Liu W, Guo X, Yang J, Fan J. Comparison of classical solar chimney power system and combined solar chimney system for power generation and seawater desalination. Desalination 2010;250:249–56.
[72] Manjarrez R, Galvan M. Solar multistage flash evaporation (SMSF) as a solar energy application on desalination processes. Description of one demonstration project. Desalination 1979;31:545–54.
[73] Kriesi R. Design and operation experience with solar powered multistage desalination plants. Desalination 1981;39:109–16.
[74] Szacsvay T, Hofer-Noser P, Posnansky M. Technical and economical aspects of small-scale solar pond-powered seawater desalination systems. Desalination 1999;122:185–93.
[75] Singh D, Sharma SK. Performance ratio, area economy and economic return for an integrated solar energy/multi-stage flash desalination plant. Desalination 1989;73:191–5.
[76] Moustafa SMA, Jarrar DI, El-Mansy HI. Performance of a self-regulating solar multistage flash desalination system. Sol Energy 1985;35(4):333–40.
[77] Hanafi A. Design and performance of solar MSF desalination systems. Desalination 1991;82:175–85.
[78] Safi MJ. Performance of a flash desalination unit intended to be coupled to a solar pond. Renew Energy 1998;14:339–43.
[79] Hou S, Zhang Z, Huang Z, Xie A. Performance optimization of solar multi-stage flash desalination process using pinch technology. Desalination 2008;220:524–30.
[80] Mezher T, Fath H, Abbas Z, Khaled A. Techno-economic assessment and environmental impacts of desalination technologies. Desalination 2011;266:263–73.
[81] Ettouney H, El-Dessouky H, Al-Juwayhel F. Performance of the once-through multistage flash desalination process. Proc Inst Mech Eng Part A: J Power Energy 2002:229–41. http://dx.doi.org/10.1243/095765002320183559.
[82] Baig H, Antar MA, Zubair SM. Performance evaluation of a once-through multi-stage distillation system: impact of brine heater fouling. Energy Convers Manag 2011;52:1414–25.
[83] Alhazmy MM. Feed water cooler to increase evaporation range in MSF plants. Energy 2009;34:7–13.
[84] Alhazmy MM. Multi stage desalination plant with brine-feed mixing and cooling. Energy 2011;36:5225–32.
[85] Al-Weshahi MA, Anderson A, Tian G. Exergy efficiency enhancement of MSF desalination by heat recovery from hot distillate water stages. Appl Therm Eng 2013;53:226–33.
[86] Garcia-Rodriguez L, Gomez-Camacho C. Conditions for economical benefits of the use of solar energy in multi-stage flash distillation. Desalination 1999;125:133–8.
[87] Lu H, Walton JC, Swift AHP. Desalination coupled with salinity-gradient solar ponds. Desalination 2001;136:13–23.
[88] Suri RK, Al-Marafie AMR, Al-Homoud AA, Maheshwari GP. Cost-effectiveness of solar water production. Desalination 1989;71:165–75.
[89] Tsilingiris PT. The analysis and performance of large-scale stand-alone solar desalination plants. Desalination 1995;103:249–55.
[90] Alarcon-Padilla DC, Garcia-Rodriguez L. Application of absorption heat pumps to multi-effect distillation: a case study of solar desalination. Desalination 2007;212:294–302.
[91] Alarcon-Padilla DC, Blanco-Galvez J, Garcia-Rodriguez L, Gernjak W, Malato-Rodriguez S. First experimental results of a new hybrid solar/gas multi-effect distillation system: the AQUASOL project. Desalination 2008;220:619–25.
[92] Alarcon-Padilla DC, Garcia-Rodriguez L, Blanco-Galvez J. Design recommendations for a multi-effect distillation plant connected to a double-effect adsorption heat pump: a solar desalination case study. Desalination 2010;262:11–4.
[93] Jiang J, He Tian, Cui M, Liu L. Proof-of-concept study of an integrated solar desalination system. Renew Energy 2009;34:2798–802.
[94] Palenzuela P, Zaragoza G, Alarcon-Padilla DC, Blanco J. Evaluation of cooling technologies of concentrated solar power plants and their combination with desalination in the Mediterranean area. Appl Therm Eng 2011;60(2): 1514–21.
[95] Sharaf MA, Nafey AS, Garcia-Rodriguez L. Exergy and thermo-economic analyses of a combined solar organic cycle with multi effect distillation (MED) desalination process. Desalination 2011;272:135–47.
[96] Li C, Goswami DY, Shapiro A, Stefanakos EK, Demirkaya G. A new combined power and desalination system driven by low grade heat for concentrated brine. Energy 2012;46:582–95.
[97] Zhao D, Xue J, Li S, Sun H, Zhang Qing-Dong. Theoretical analyses of thermal and economical aspects of multi-effect distillation–desalination dealing with high-salinity wastewater. Desalination 2011;273:292–8.
[98] Hong-Jin Joo, Hee-Youl Kwak. Performance evaluation of multi-effect distiller for optimized solar thermal desalination. Appl Therm Eng 2013;61:491–9.
[99] Helal AM, Al-Malek SA. Design of a solar-assisted mechanical vapor compression (MVC) desalination unit for remote areas in the UAE. Desalination 2006;197:273–300.

[100] Zejli D, Ouammi A, Sacile R, Dagdougui H, Elmidaoui A. An optimization model for a mechanical vapor compression desalination plant driven by a Wind/PV hybrid system. Appl Energy 2011;88:4042–54.
[101] Sharaf MA, Nafey AS, Garcia-Rodriguez L. Thermo-economic analysis of solar thermal power cycles assisted MED–VC (multi effect distillation–vapor compression) desalination processes. Energy 2011;36:2753–64.
[102] Zhang L, Zheng H, Wu Y. Experimental study on a horizontal tube falling film evaporation and closed circulation solar desalination system. Renew Energy 2003;28:1187–99.
[103] Hongfei Z, He Kaiyan, Yang Yijun, Ziqian C, Hui Li. Study on a multi-effect regeneration and integral-type solar desalination unit with falling film evaporation and condensation processes. Sol Energy 2006;80:1189–98.
[104] Reddy KS, Kumar KR, O'Donovan TS, Mallick TK. Performance analysis of an evacuated multi-stage solar water desalination system. Desalination 2012;288:80–92.
[105] Nafey AS, Mohamed MA, El-Helaby SO, Sharaf MA. Theoretical and experimental study of a small unit for solar desalination using flashing process. Energy Convers Manag 2007;48:528–38.
[106] Wessley GJJ, Mathews PK. Investigations on solar desalination based on vacuum evaporation for small scale applications. Procedia Eng 2012;38:2413–9.
[107] Shatat MIM, Mahkamov K. Determination of rational design parameters of a multi-stage solar water desalination still use transient mathematical modelling. Renew Energy 2010;35:52–61.
[108] Xiong J, Xie G, Zheng H. Experimental and numerical study on a new multi-effect solar still with enhanced condensation surface. Energy Convers Manag 2013;73:176–85.
[109] Maroo SC, Goswami DY. Theoretical analysis of a single-stage and two-stage solar driven flash desalination system based on passive vacuum generation. Desalination 2009;249:635–46.
[110] Al-Karabsheh S, Goswami DY. Analysis of an innovative water desalination system using low-grade solar heat. Desalination 2003;156:323–32.
[111] Gude VG, Nirmalakandan N, Deng S, Maganti A. Low temperature desalination using solar collectors augmented by thermal energy storage. Appl Energy 2012;91(1):466–74.
[112] Gude VG, Nirmalakandan N. Combined desalination and solar-assisted air-conditioning system. Energy Convers Manag 2008;49:3326–30.
[113] Gude VG, Nirmalakhandan N, Deng S, Maganti A. Feasibility study of a new two-stage low temperature desalination process. Energy Convers Manag 2012;56:192–8.
[114] Ayhan T, Al Madani H. Feasibility study of renewable energy powered seawater desalination technology using natural vacuum technique. Renew Energy 2010;35:506–14.
[115] Zhao K, Liu Y. Theoretical study on multi-effect distillation system driven by tidal energy. Desalination 2009;249:566–70.
[116] Rane MV, Padiya YS. Heat pump operated freeze concentration system with tubular heat exchanger for seawater desalination. Energy Sustain Dev 2011;15:184–91.
[117] Rice W, DSC. Chau. Freeze distillation using hydraulic refrigerant compressors. Desalination 1997;109:157–64.
[118] Madani AA. Zero-discharge direct-contact freezing/solar evaporator desalination complex. Desalination 1992;85:179–95.
[119] Lloyd AI. An integral design for desalination plant using the secondary refrigeration freeze process. Desalination 1977;21:137–46.
[120] Gu W, Lin YB, Xu YJ, Chen WB, Tao J, Yuan S. Gravity-induced sea ice desalination under low temperature. Cold Reg Sci Technol 2012;86:133–41.
[121] Attia AAA. New proposed system for freeze water desalination using auto reversed R-22 vapor compression heat pump. Desalination 2010;254:179–84.
[122] Wang P, Chung Tai-Shung. A conceptual demonstration of freeze desalination–membrane distillation (FD–MD) hybrid desalination process utilizing liquefied natural gas (LNG) cold energy. Water Res 2012;46:4037–52.
[123] El-Nashar AM. Solar desalination using the vacuum freezing ejector absorption (VFEA) process. Desalination 1984;49:293–319.
[124] Zahed AH, Bashir MD. A case study of a solar energy transfer and storage system in a freeze desalination project in Yanbu, Saudi Arabia. Sol Wind Technol 1990;7(4):441–6.
[125] Williams PM, Ahmad M, Connolly BS. Freeze desalination: an assessment of an ice maker machine for desalting brines. Desalination 2013;308:219–24.
[126] Wu JW, Biggs MJ, Hu EJ. Thermodynamic analysis of an adsorption-based desalination cycle. Chem Eng Res Des 2010;88:1541–7.
[127] Zejli D, Benchrifa R, Bennouna A, Bouhelal OK. A solar adsorption desalination device: first simulation results. Desalination 2004;168:127–35.
[128] Wu JW, Biggs MJ, Hu EJ. Thermodynamic cycles of adsorption desalination system. Appl Energy 2012;90:316–22.
[129] Wu JW, Biggs MJ, Pendelton P, Badalyan A, Hu EJ. Experimental implementation and validation of thermodynamic cycles of adsorption-based desalination. Appl Energy 2012;98:190–7.
[130] Wang X, Ng KC. Experimental investigation of an adsorption desalination plant using low-temperature waste heat. Appl Therm Eng 2005;25:2780–9.
[131] Thu K, Ng KC, Saha BB, Chakraborty A, Koyama S. Operational strategy of adsorption desalination systems. Int J Heat Mass Transf 2009;52:1811–6.
[132] Ng KC, Thu K, Saha BB, Chakraborty A. Study on a waste heat-driven adsorption cooling cum desalination cycle. Int J Refrig 2012;35:685–93.
[133] Thu K, Saha BB, Chakraborty A, Chun WG, Ng KC. Study on a advanced adsorption desalination cycle with evaporator-condenser heat recovery circuit. Int J Heat Mass Transf 2011;54:43–51.
[134] ⟨http://www.sidem-desalination.com/en/Process/MED/MED-MVC/⟩ [last accessed 04.02.13].
[135] ⟨http://www.veoliawaterst.com/multipleffectdistillation/en/features_and_benefits.htm⟩ [last accessed 04.02.13].
[136] Midilli A, Ayhan T. Natural vacuum distillation technique – Part I: theory and basics. Int J Energy Res 2004;28:355–71.
[137] Greenlee LF, Lawler DF, Freeman BD, Marrot B, Moulin P. Reverse osmosis desalination: water sources, technology, and today's challenges. Water Res 2009;43:2317–48.
[138] Abdallah S, Abu-Hilal M, Mohsen MS. Performance of a photovoltaic powered reverse osmosis system under local climatic conditions. Desalination 2005;183:95–104.
[139] Gocht W, Sommerfeld A, Rautenbach R, Melin TH, Eilers L, Neskakis A, et al. Decentralized desalination of brackish water by a directly coupled reverse osmosis photovoltaic system – a pilot plant study in Jordan. Renew Energy 1998;14(1–4):287–92.
[140] Petersen G, Fries S, Mohn J, Muller A. Wind and solar powered reverse osmosis desalination units – description of two demonstration projects. Desalination 1979;31:501–9.
[141] Boesch WW. World's first solar powered reverse osmosis desalination plant. Desalination 1982;41:233–7.
[142] Al-Qahtani H. Feasibility of utilizing solar energy to power reverse osmosis domestic unit to desalinate water in the state of Bahrain. In: Proceedings of the WREC; 1996. p. 500–4.
[143] Hrayshat ES. Brackish water desalination by a standalone reverse osmosis desalination unit powered by photovoltaic solar energy. Renew Energy 2008;33:1784–90.
[144] Colangelo A, Marano D, Spagna G, Sharma VK. Photovoltaic powered reverse osmosis sea-water desalination systems. Appl Energy 1999;64:289–305.
[145] Al-Suleimani Z, Nair VR. Desalination by solar-powered reverse osmosis in a remote area of the Sultanate of Oman. Appl Energy 2000;65:367–80.
[146] Herold D, Neskakis A. A small PV-driven reverse osmosis desalination plant on the island of Gran Canaria. Desalination 2001;137:285–92.
[147] Thomson M, Infield D. A photovoltaic-powered seawater reverse-osmosis system without batteries. Desalination 2002;153(1–3):1–8.
[148] Thomson M, Infield D. Laboratory demonstration of a photovoltaic-powered seawater reverse-osmosis system without batteries. Desalination 2005;183:105–11.
[149] Mohamed ESh, Papadakis G. Design, simulation and economic analysis of a stand-alone reverse osmosis desalination unit powered by wind turbines and photovoltaics. Desalination 2004;164:87–97.
[150] Cherif H, Belhadj J. Large-scale time evaluation for energy estimation of stand-alone hybrid photovoltaic–wind system feeding a reverse osmosis desalination unit. Energy 2011;36:6058–67.
[151] Khayet M, Essalhi M, Armenta-Deu C, Cojocaru C, Hilal N. Optimization of solar-powered reverse osmosis desalination pilot plant using response surface methodology. Desalination 2010;261:284–92.
[152] Peterson EL, Gray SR. Effectiveness of desalination powered by a tracking solar array to treat saline bore water. Desalination 2012;293:94–103.
[153] Soric A, Cesaro R, Perez P, Guiol E, Moulin P. Eausmose project by reverse osmosis and batteryless solar energy: design for a 1 m^3 per day delivery. Desalination 2012;301:67–74.
[154] Laborde HM, Franca KB, Neff H, AMN. Lima. Optimization strategy for a small-scale reverse osmosis water desalination system based on solar energy. Desalination 2001;133:1–12.
[155] Penate B, Garcia-Rodriguez L. Current trends and future prospects in the design of seawater reverse osmosis desalination technology. Desalination 2012;284:1–8.
[156] Delgado-Torres AM, Garcia-Rodriguez L. Status of solar thermal-driven reverse osmosis desalination. Desalination 2007;216:242–51.
[157] Voros NG, Kiranoudis CT, Maroulis ZB. Solar energy exploitation for reverse osmosis desalination plants. Desalination 1998;115:83–101.
[158] Salcedo R, Antipova E, Boer D, Jimenez L, Guillen-Gosalbez G. Multi-objective optimization of solar Rankine cycles coupled with reverse osmosis desalination considering economic and life cycle environmental concerns. Desalination 2012;286:358–71.
[159] Manolakos D, Papadakis G, Mohamed ES, Kyritsis S, Bouzianas K. Design of an autonomous low-temperature solar Rankine cycle system for reverse osmosis desalination. Desalination 2005;183:73–80.
[160] Manolakos D, Papadakis G, Kyritsis S, Bouzianas K. Experimental evaluation of an autonomous low-temperature solar Rankine cycle system for reverse osmosis desalination. Desalination 2007;203:366–74.
[161] Delgado-Torres AM, Garcia-Rodriguez L, Romero-Ternero VJ. Preliminary design of a solar thermal-powered seawater reverse osmosis system. Desalination 2007;216:292–305.
[162] Delgado-Torres AM, Garcia-Rodriguez L. Double cascade organic Rankine cycle for solar-driven reverse osmosis desalination. Desalination 2007;216:306–13.
[163] Bruno JC, Lopez-Villada J, Letelier E, Romera S, Coronos A. Modelling and optimization of solar organic Rankine cycle engines for reverse osmosis desalination. Appl Therm Eng 2008;28:2212–26.

[164] Nafey AS, Sharaf MA, Garcia-Rodriguez L. Thermo-economic analysis of a combined solar organic Rankine cycle-reverse osmosis desalination process with different energy recovery configuration. Desalination 2010;261:138–47.
[165] Delgado-Torres AM, Garcia-Rodriguez L. Preliminary design of seawater and brackish water reverse osmosis desalination systems driven by low-temperature solar organic Rankine cycles (ORC). Energy Convers Manag 2010;51:2913–20.
[166] Karellas S, Terzis K, Manolakos D. Investigation of an autonomous hybrid solar thermal ORC–PV RO desalination system. The Chalki island case. Renew Energy 2011;36:583–90.
[167] Nafey AS, Sharaf MA. Combined solar organic Rankine cycle with reverse osmosis desalination process: energy, exergy and cost evaluations. Renew Energy 2010;35:2571–80.
[168] Penate B, Garcia-Rodriguez L. Seawater reverse osmosis desalination by a solar organic Rankine cycle: design and technology assessment for medium capacity range. Desalination 2012;284:86–91.
[169] Davies PA. A solar-powered reverse osmosis system for high recovery of freshwater from saline groundwater. Desalination 2011;271:72–9.
[170] A.A.A. Attia. Thermal analysis for system uses solar energy as a pressure source for reverse osmosis (RO) water desalination. Sol Energy 2012;86:2486–93.
[171] Charcosset C. A review of membrane processes and renewable energies for desalination. Desalination 2009;245:214–31.
[172] H.M.N. AlMadani. Water desalination by solar powered electrodialysis process. Renew Energy 2003;28:1915–24.
[173] Korngold E, Aronov L, Daltrophe N. Electrodialysis of brine solutions discharged from an RO plant. Desalination 2009;242:215–27.
[174] Lundstrom JE. Water desalting by solar powered electrodialysis. Desalination 1979;31:469–88.
[175] Kuroda O, Takahash S, Wakamatsu Itoh S, Kubota S, Kikuchi K, Eguchi Y, et al. An electrodialysis sea water desalination system powered by photovoltaic cells. Desalination 1987;65:161–9.
[176] Mahabala R, Adiga MR, Adhikary SK, Narayanan PK, Harkare WP, Gomkale SD, et al. Performance analysis of photovoltaic electrodialysis desalination plant at Tanote in Thar Desert. Desalination 1987;67:59–66.
[177] Ishimaru N. Solar photovoltaic desalination of brackish water in remote areas by electrodialysis. Desalination 1994;98:485–93.
[178] Oritz JM, Exposito E, Gallud F, Garcia-Garcia V, Montiel V, Aldaz A. Photovoltaic electrodialysis system for brackish water desalination: modeling of global process. J Membr Sci 2006;274:138–49.
[179] Oritz JM, Exposito E, Gallud F, Garcia-Garcia V, Montiel V, Aldaz A. Desalination of underground brackish waters using an electrodialysis system powered directly by photovoltaic energy. Sol Energy Mater Sol Cells 2008;92:1677–88.
[180] Qtaishat MR, Banat F. Desalination by solar powered membrane distillation systems. Desalination 2012;308(2):186–97.
[181] Alkhudhiri A, Darwish N, Hilal N. Membrane distillation: a comprehensive review. Desalination 2012;287:2–18.
[182] Hogan PA, Sudjito, Fane AG, Morrison GL. Desalination by solar heated membrane distillation. Desalination 1991;81:81–90.
[183] Saffarini RB, Summers EK, Arafat HA, Lienhard VJH. Economic evaluation of stand-alone solar powered membrane distillation systems. Desalination 2012;299:55–62.
[184] Summers EK, Arafat HA, Lienhard VJH. Energy efficiency comparison of single-stage membrane distillation (MD) desalination cycles in different configurations. Desalination 2012;290:54–66.
[185] Chang H, Lyu Shao-Gang, Tsai Chih-Ming, Chen Yih-Hang, Ceng Tung-Wen, Ying-Hsiu Chou. Experimental and simulation study of a solar thermal driven membrane distillation desalination process. Desalination 2012;286:400–11.
[186] Asadi RZ, Suja F, Tarikan F, Mashhoon F, Rahimi S, Jameh AA. Solar desalination of gas refinery waste water using membrane distillation process. Desalination 2012;291:56–64.
[187] Zwijnenberg HJ, Koops GH, Wessling M. Solar driven membrane pervaporation for desalination processes. Desalination 2005;250:235–46.
[188] Raluy RG, Schwantes R, Subiela VJ, Penate B, Melian G, Betancort JR. Operational experience of a solar membrane distillation demonstration plant in Pozolzquierdo – Gran Canaria Island (Spain). Desalination 2012;290:1–13.
[189] Kim Young-Deuk, Thu K, Ghaffour N, Ng KC. Performance investigation of a solar-assisted direct contact membrane distillation system. J Membr Sci 2013;427:345–64.
[190] Mericq Jean-Pierre, Laborie S, Cabassud C. Evaluation of systems coupling vacuum membrane distillation and solar energy for seawater distillation. Chem Eng J 2011;166:596–606.
[191] Banat F, Jwaeid N, Rommel M, Koschikowski J, Wieghaus M. Performance evaluation of the large SMADES autonomous desalination solar-driven membrane distillation plant in Aqaba, Jordan. Desalination 2007;217:17–28.
[192] Banat F, Jwaeid N, Rommel M, Koschikowski J, Wieghaus M. Desalination by a compact SMADES autonomous solar-powered membrane distillation unit. Desalination 2007;217:29–37.
[193] Banat F, Jwaied N. Economic evaluation of desalination by small-scale autonomous solar-powered membrane distillation units. Desalination 2008;220:566–73.
[194] Banat F, Jwaied N. Exergy analysis of desalination by solar-powered membrane distillation units. Desalination 2008;230:27–40.
[195] Wang X, Zhang L, Yang H, Chen H. Feasibility research of potable water production via solar-heated hollow fiber membrane distillation system. Desalination 2009;247:403–11.
[196] Banat F, Jumah R, Garaibeh M. Exploitation of solar energy collected by solar stills for desalination by membrane distillation. Renew Energy 2002;25(2):293–305.
[197] Manna AK, Sen M, Martin AR, Pal P. Removal of arsenic from contaminated ground water by solar-driven membrane distillation. Environ Pollut 2010;158:805–11.
[198] Chen Tsung-Ching, Ho. Chii-Dong. Immediate assisted solar direct contact membrane distillation in saline water desalination. J Membr Sci 2010;358:122–30.
[199] Guillen-Burrieza E, Blanco J, Zaragoza G, Diego-cesar A, Palenzuela P, Ibarra M, et al. Experimental analysis of an air gap membrane distillation solar desalination pilot system. J Membr Sci 2011;379(1–2):386–96.
[200] Guillen-Burrieza E, Zaragoza G, Miralles-Cuevas S, Blanco J. Experimental evaluation of two pilot-scale membrane distillation modules used for solar desalination. J Membr Sci 2012;409–410:264–75.
[201] Khayet M. Solar desalination by membrane distillation: dispersion in energy consumption analysis and water production costs (a review). Desalination 2012;308(2):89–101.
[202] Saffarini RB, Summers EK, Arafat HA, Lienhard VJH. Technical evaluation of stand-alone solar powered membrane distillation systems. Desalination 2012;286:332–41.
[203] Ong CL, Escher W, Paredes S, Khalil ASG, Michel B. A novel concept of energy reuse from high concentration photovoltaic thermal (HCPVT) system for desalination. Desalination 2012;295:70–81.
[204] Ding Z, Liu L, El-Bourawi MS, Ma R. Analysis of a solar-powered membrane distillation system. Desalination 2005;172:27–40.
[205] Cath TZ, Childress AE, Elimelech M. Forward osmosis: principles, applications and recent developments. J Membr Sci 2006;281(1–2):70–87.
[206] Chung Tai-Shung, Li X, Ong RC, Ge Q, Wang H, Han G. Emerging forward osmosis (FO) technologies and challenges ahead for clean water and clean energy applications. Curr Opin Chem Eng 2012;1:246–57.
[207] Butler E, Silva A, Horton K, Rom Z, Chwatko M, Havasov A, et al. Point of use water treatment with forward osmosis for emergency relief. Desalination 2013;312:23–30.
[208] Kravath RE, Davis JA. Desalination of sea water by direct osmosis. Desalination 1975;16:151–5.
[209] McCutcheon JR, McGinnis RL, Elimeleh M. A novel ammonia–carbondioxide forward (direct) osmosis desalination process. Desalination 2005;174:1–11.
[210] McCutcheon JR, McGinnis RL, Elimeleh M. Desalination by ammonia–carbondioxide forward osmosis: influence of draw and feed solution concentration on process performance. J Membr Sci 2006;278:114–23.
[211] ⟨http://www.greentechmedia.com/articles/read/guest-post-desalination-realization⟩ [last accessed 02.02.13].
[212] Zhao S, Zou L, Mulcahy D. Brackish water desalination by a hybrid forward osmosis–nanofiltration system using divalent draw solute. Desalination 2012;284:175–81.
[213] Phuntsho S, Vigneshwaran S, Kandasamy J, Hong S, Lee S, Shon HK. Influence of temperature and temperature difference in the difference in the performance of forward osmosis desalination process. J. Membr. Sci. 2012;415–416:734–44.
[214] Li D, Zhang X, Simon GP, Wang H. Forward osmosis desalination using polymer hydrogels as a draw agent: influence of draw agent, feed solution and membrane on process performance. Water Res 2013;47:209–15.
[215] Khaydarov RA, Khaydarov RR. Solar powered direct osmosis desalination. Desalination 2007;217(1-3):225–32.
[216] ⟨http://www.trevisystems.com/technology-2/types-of-water-purification/membrane-distillation/⟩ [last accessed 02.02.13].
[217] ⟨http://www.trevisystems.com/energy-comparison/⟩ [last accessed 02.02.13].
[218] ⟨http://www.trevisystems.com/technology-2/forward-osmosis/forward-osmosis-diagram-2/⟩ [last accessed 02.02.13].
[219] Oritz JM, Exposito E, Gallud F, Garcia-Garcia V, Montiel V, Aldaz A. Electrodialysis of brackish water powered by photovoltaic energy without batteries: direct connection behavior. Desalination 2007;208:89–100.
[220] Galvez JB, Garcia-Rodriguez L, Martin-Mateos I. Seawater desalination by an innovative solar-powered membrane distillation system: the MEDESOL project. Desalination 2009;246:567–76.
[221] Koschikowski J, Wieghaus M, Rommel M. Solar thermal-driven desalination plants based on membrane distillation. Desalination 2003;156:295–304.
[222] Oldfield JW, Todd B. Environmental aspects of corrosion in MSF and RO desalination plants. Desalination 1996;108:27–36.
[223] Sommariva C, Hogg H, Callister K. Fort-year design life: the next target material selection and operating conditions in thermal desalination plants. Desalination 2001;136:169–76.
[224] Salibi Z. Performance of reinforced thermosetting resin pipe systems in desalination applications: a long-term solution to corrosion-the Arabian Gulf example. Desalination 2001;138:379–84.
[225] El-Dahshan ME. Corrosion and scaling problems present in some desalination plants in Abu Dhabi. Desalination 2001;138:371–7.
[226] Potts DE, Ahlert RC, Wang SS. A critical review of fouling of reverse osmosis membranes. Desalination 1981;36:235–64.
[227] Lee S, Boo C, Elimelech M, Hong S. Comparison of fouling behaviour in forward osmosis (FO) and reverse osmosis (RO). J Membr Sci 2010;365:34–9.
[228] Gryta M. Fouling in direct contact membrane distillation process. J Membr Sci 2008;325:383–94.

[229] Zhao S, Zou L, Tang CY, Mulcahy D. Recent developments in forward osmosis: opportunities and challenges. J Membr Sci 2012;396:1–21.
[230] Kesieme UK, Milne N, Aral H, Cheng CY, Duke M. Economic analysis of desalination technologies in the context of carbon pricing, and opportunities for membrane distillation. Desalination 2013;323:66–74.
[231] Mezher T, Fath H, Abbas Z, Khaled A. Techno-economic assessment and environmental impacts of desalination technologies. Desalination 2011;266:263–73.
[232] Abraham T, Luthra A. Socio-economic & technical assessment of photovoltaic powered membrane desalination processes for India. Desalination 2011;268:238–48.
[233] Ali-Karaghouli A, Kazmerski LL. Energy consumption and water production cost of conventional and renewable-energy-powered desalination processes. Renew Sustain Energy Rev 2013;24:343–56.
[234] Sadhwani JJ, Veza JM, Santana C. Case studies on environmental impact of seawater desalination. Desalination 2005;185:1–8.
[235] Meerganz von Medeazza GL. Direct and socially-induced environmental impacts of desalination. Desalination 2005;185:57–70.
[236] Lattemann S, Hopner T. Environmental impact and impact assessment of seawater desalination. Desalination 2008;220:1–15.